



PUBLISHED FOR SISSA BY SPRINGER

RECEIVED: August 12, 2014

REVISED: May 16, 2015

ACCEPTED: July 15, 2015

PUBLISHED: August 5, 2015

# Deviation from bimaximal mixing and leptonic CP phases in $S_4$ family symmetry and generalized CP

**Cai-Chang Li and Gui-Jun Ding**

*Department of Modern Physics, University of Science and Technology of China,  
Hefei, Anhui 230026, China*

*E-mail:* [lcc0915@mail.ustc.edu.cn](mailto:lcc0915@mail.ustc.edu.cn), [dinggj@ustc.edu.cn](mailto:dinggj@ustc.edu.cn)

**ABSTRACT:** The lepton flavor mixing matrix having one row or one column in common with the bimaximal mixing up to permutations is still compatible with the present neutrino oscillation data. We provide a thorough exploration of generating such a mixing matrix from  $S_4$  family symmetry and generalized CP symmetry  $H_{CP}$ . Supposing that  $S_4 \rtimes H_{CP}$  is broken down to  $Z_2^{ST^2SU} \times H_{CP}^\nu$  in the neutrino sector and  $Z_4^{TST^2U} \rtimes H_{CP}^l$  in the charged lepton sector, one column of the PMNS matrix would be of the form  $(1/2, 1/\sqrt{2}, 1/2)^T$  up to permutations, both Dirac CP phase and Majorana CP phases are trivial to accommodate the observed lepton mixing angles. The phenomenological implications of the remnant symmetry  $K_4^{(TST^2, T^2U)} \times H_{CP}^\nu$  in the neutrino sector and  $Z_2^{SU} \times H_{CP}^l$  in the charged lepton sector are studied. One row of PMNS matrix is determined to be  $(1/2, 1/2, -i/\sqrt{2})$ , and all the three leptonic CP phases can only be trivial to fit the measured values of the mixing angles. Two models based on  $S_4$  family symmetry and generalized CP are constructed to implement these model independent predictions enforced by remnant symmetry. The correct mass hierarchy among the charged leptons is achieved. The vacuum alignment and higher order corrections are discussed.

**KEYWORDS:** Neutrino Physics, CP violation, Discrete and Finite Symmetries

**ARXIV EPRINT:** [1408.0785](https://arxiv.org/abs/1408.0785)

---

## Contents

<b>1</b>	<b>Introduction</b>	<b>1</b>
<b>2</b>	<b>Basic framework</b>	<b>3</b>
<b>3</b>	<b>Phenomenological analysis of deviation from bimaximal mixing</b>	<b>7</b>
<b>4</b>	<b>Lepton flavor mixing from remnant symmetries <math>K_4^{(TST^2, T^2U)} \times H_{\text{CP}}^\nu</math> in the neutrino sector and <math>Z_2^{SU} \times H_{\text{CP}}^l</math> in the charged lepton sector</b>	<b>11</b>
<b>5</b>	<b>Model predicting one column of BM mixing with <math>S_4</math> and generalized CP</b>	<b>17</b>
5.1	Vacuum alignment	20
5.2	The structure of the model	24
<b>6</b>	<b>Model predicting one row of BM mixing with <math>S_4</math> and generalized CP</b>	<b>27</b>
6.1	Vacuum alignment	27
6.2	Leading order results	30
6.3	Next-to-leading-order corrections	32
<b>7</b>	<b>Summary and conclusions</b>	<b>35</b>
<b>A</b>	<b>Group theory of <math>S_4</math> and Clebsch-Gordan coefficients</b>	<b>37</b>

---

## 1 Introduction

The neutrino flavor mixing and neutrino oscillation have been firmly established so far. The standard three flavor neutrino oscillation relates the flavor eigenstates of neutrinos to the mass eigenstates through the Pontecorvo-Maki-Nakagawa-Sakata (PMNS) mixing matrix. This matrix is a  $3 \times 3$  unitary matrix and can be parameterized by three mixing angles  $\theta_{12}, \theta_{13}, \theta_{23}$ , one Dirac type CP violating phase  $\delta_{\text{CP}}$  similar to the quark sector and two additional Majorana phases  $\alpha_{21}, \alpha_{31}$  if neutrinos are Majorana particles. Recently the last lepton mixing angle  $\theta_{13}$  has been precisely measured to be about  $9^\circ$  [1–10]. This discovery pushes neutrino oscillation experiments into a new era of precise determination of the lepton mixing angles and neutrino mass squared differences, and it also opens up new windows to probe leptonic CP violation. Although we still don't have convincing evidence for lepton CP violation, the current global fit to the neutrino oscillation data indicates nontrivial values of the Dirac type CP phase [11–13]. The present T2K data already exclude values of  $\delta_{\text{CP}}$  between  $0.14\pi \sim 0.87\pi$  at the 90% confidence level [14, 15]. Furthermore, several long-baseline neutrino oscillation experiments such as LBNE [16, 17], LBNO [18–22] and Hyper-Kamiokande [23, 24] are proposed to measure CP violation. Study of neutrino mixing including the CP violating phase would allow us to distinguish different flavor models.

In view of the fantastic experimental program of observing lepton CP violation and the fundamental role played by CP violation, it is crucial to be able to predict CP phases. The idea of combining flavor symmetry with generalized CP symmetry is a very interesting approach to predict both flavor mixing angles and CP phases from symmetry principle. The concept of generalized CP transformations has been put forward about thirty years ago. CP invariance at high energy scale and its subsequent breaking lead to nontrivial constraints on the fermion mass matrices [25–29]. It is somewhat tricky to include the generalized CP symmetry in the presence of a family symmetry. Generally the generalized CP transformation must be subject to the so-called consistency condition, which implies that the generalized CP transformation corresponds to an automorphism of the family symmetry group [30, 31]. Furthermore, it is shown that physical CP transformations always have to be class-inverting automorphisms of family symmetry group [32]. As a result, in some cases the conventional CP transformation  $\varphi \mapsto \varphi^*$  can not be consistently defined, but rather a non-trivial transformation in flavor space is needed. Here we would like to remind that the concrete form of the CP transformation matrix is basis dependent.

Generalized CP symmetry together with family symmetry can give us interesting phenomenological predictions. The simplest example is the so-called  $\mu - \tau$  reflection symmetry which is a combination of the canonical CP transformation and the  $\mu - \tau$  exchange symmetry. The invariance of the light neutrino mass matrix under  $\mu - \tau$  reflection in the charged lepton diagonal basis leads to maximal atmospheric mixing angle  $\theta_{23}$  and maximal Dirac CP phase  $\delta_{\text{CP}}$  with  $\delta_{\text{CP}} = \pm\pi/2$  [33–39]. The phenomenological implications of the generalized CP symmetry has been analyzed within the context of popular  $A_4$  [40],  $S_4$  [30, 41–44] and  $T'$  [45] family symmetries. By breaking the full symmetry down to  $Z_2 \times CP$  in the neutrino sector, the  $\text{TM}_1$  and  $\text{TM}_2$  mixing patterns in which the first and the second columns of the tri-bimaximal mixing is kept respectively, can be exactly produced. The Dirac CP phase  $\delta_{\text{CP}}$  is predicted to be conserved or maximally broken. Concrete models in which these symmetry breaking patterns are achieved dynamically have been proposed. Furthermore, the generalized CP has been extended to  $\Delta(48)$  [46, 47],  $\Delta(96)$  [48] and  $\Delta(6n^2)$  series [49–51] family symmetries as well. Some new mixing textures compatible with the experimental data are found, in particular CP phases can be neither vanishing nor maximal. A number of interesting models with definite predictions for CP phases have been constructed. There are other approaches to dealing with family symmetry and CP violation [52–62].

Besides the well-known tri-bimaximal mixing, the bimaximal (BM) mixing can also be naturally derived from the  $S_4$  family symmetry [63–65]. Since  $\theta_{13}$  is not so small as expected and  $\theta_{12}$  is not maximal, the BM pattern has been ruled out. However, the scheme with only one row or one column of the BM mixing preserved is still viable. In the present work, we shall assume  $S_4$  family symmetry and generalized CP symmetry which is then spontaneously broken down to  $Z_2 \times CP$  in the neutrino sector or the charged lepton sector. As a consequence, only one column or one row of the BM mixing is preserved and the PMNS matrix deviates from BM pattern. Moreover, the concrete forms of the deviation from the BM mixing are constrained by the remnant symmetry, the corresponding predictions for the mixing angles and CP phases are investigated in a model independent way. Furthermore two models realizing these scenarios are built.

The paper is organized as follows. In section 2, we present the basic concept of generalized CP symmetry and model independent approach of predicting lepton flavor mixing from remnant symmetry. The deviation from BM mixing induced by a rotation between two generation neutrinos or a rotation between two generation charged lepton fields is investigated in section 3, and the corresponding phenomenological predictions for the lepton mixing parameters are discussed. In section 4, the phenomenological implications of the symmetry breaking pattern of  $S_4 \rtimes H_{\text{CP}}$  into  $K_4^{(TST^2, T^2U)} \times H_{\text{CP}}^\nu$  in the neutrino sector and  $Z_2^{SU} \times H_{\text{CP}}^l$  in the charged lepton sector are studied in a model-independent way. The resulting PMNS matrix has a row of form  $(1/2, 1/2, -i/\sqrt{2})$ , and all the three leptonic CP phases are conserved to fit the measured values of the mixing angles. In section 5, we construct an  $S_4$  model with generalized CP symmetry, where the mixing pattern with one column  $(1/2, 1/\sqrt{2}, 1/2)^T$  and conserved CP found in ref. [30] are produced exactly at leading order. Agreement with experimental data can be achieved after subleading order contributions are considered. The model reproducing all aspects of the general results of section 4 is presented in section 6. Section 7 is devoted to our conclusion. The group theory of  $S_4$  and the Clebsch-Gordan coefficients in our basis are collected in appendix A.

## 2 Basic framework

We now consider a theory which is invariant under both family symmetry  $S_4$  and generalized CP at high energy scale. For a field multiplet  $\varphi(x)$  in a irreducible representation  $\mathbf{r}$  of  $S_4$ , it transforms under the action of  $S_4$  as

$$\varphi(x) \xrightarrow{g} \rho_{\mathbf{r}}(g)\varphi(x), \quad g \in S_4, \quad (2.1)$$

where  $\rho_{\mathbf{r}}(g)$  is the representation matrix for the element  $g$  in the representation  $\mathbf{r}$ . The generalized CP transformation on  $\varphi$  is defined as

$$\varphi(x) \xrightarrow{CP} X_{\mathbf{r}}\varphi^*(t, -\mathbf{x}), \quad (2.2)$$

where  $X_{\mathbf{r}}$  is the generalized CP transformation matrix, and it is a unitary matrix to keep the kinetic term invariant. Note that the obvious action of CP on the possible spinor indices has been suppressed in eq. (2.2). One subtle point that we should treat with care is that the family symmetry and the generalized CP must be compatible with each other. The following consistency condition has to be fulfilled [29–31],

$$X_{\mathbf{r}}\rho_{\mathbf{r}}^*(g)X_{\mathbf{r}}^{-1} = \rho_{\mathbf{r}}(g'), \quad g, g' \in S_4, \quad (2.3)$$

which maps one element  $g$  into another element  $g'$ . For the faithful representation  $\mathbf{r} = \mathbf{3}, \mathbf{3}'$ , the representation matrices of no two elements are identical. As a consequence, the mapping of  $g \rightarrow g'$  is bijective, and then the consistency equation of eq. (2.3) will define a unique mapping of the family symmetry group  $S_4$  to itself. Hence the generalized CP transformation  $X_{\mathbf{r}}$  corresponds an automorphism of  $S_4$  [31]. It has been shown that only the class-inverting automorphisms can lead to physical CP transformations [32]. For a given solution  $X_{\mathbf{r}}$  of eq. (2.3), we can easily check that  $\rho_{\mathbf{r}}(h)X_{\mathbf{r}}$  is also a solution for any  $h \in S_4$ . Since  $\rho_{\mathbf{r}}(h)X_{\mathbf{r}}$  maps one group element  $g$  into  $hg'h^{-1}$ ,<sup>1</sup> the effect of  $\rho_{\mathbf{r}}(h)$  is equivalent to an

<sup>1</sup>We have  $(\rho_{\mathbf{r}}(h)X_{\mathbf{r}})\rho_{\mathbf{r}}^*(g)(\rho_{\mathbf{r}}(h)X_{\mathbf{r}})^{-1} = \rho_{\mathbf{r}}(h)(X_{\mathbf{r}}\rho_{\mathbf{r}}^*(g)X_{\mathbf{r}}^{-1})\rho_{\mathbf{r}}^{-1}(h) = \rho_{\mathbf{r}}(h)\rho_{\mathbf{r}}(g')\rho_{\mathbf{r}}^{-1}(h) = \rho_{\mathbf{r}}(hg'h^{-1})$ .

inner automorphism  $\sigma_h : g' \rightarrow hg'h^{-1}$  for any  $h, g' \in S_4$ . Furthermore, since  $g'$  and  $hg'h^{-1}$  belong to the same conjugacy class, the automorphism  $g \rightarrow hg'h^{-1}$  induced by  $\rho_{\mathbf{r}}(h)X_{\mathbf{r}}$  is also class-inverting if the automorphism for  $X_{\mathbf{r}}$  is class-inverting. Generically this automorphism for  $\rho_{\mathbf{r}}(h)X_{\mathbf{r}}$  is not necessarily involuntary, but it can be. In other words,  $\rho_{\mathbf{r}}(h)X_{\mathbf{r}}$  is a physical one as well if  $X_{\mathbf{r}}$  is a physical CP transformation. Generally the element  $g$  is distinct from  $g'$  in eq. (2.3). Hence the mathematical structure of the full symmetry group comprising family symmetry  $S_4$  and generalized CP symmetry is in general a semi-direct product [30]. Consequently, the imposed symmetry at high energy scale is  $S_4 \rtimes H_{\text{CP}}$ .

Since the outer automorphism group of  $S_4$  is trivial [31, 51], all the automorphisms of  $S_4$  are inner automorphisms, and can be generated by group conjugation. As the inverse of each conjugacy class of  $S_4$  is equal to itself, all the inner automorphisms of  $S_4$  are class-inverting. Consequently the generalized CP transformation compatible with  $S_4$  family symmetry is defined by the inner automorphism of  $S_4$  through the consistency condition. Now we determine the explicit form of these CP transformation matrices in our working basis. We consider the representative inner automorphism  $\sigma_{TST^2} : (S, T, U) \rightarrow (S, ST, SU)$ . The corresponding generalized CP transformation denoted by  $X_{\mathbf{r}}^0$  should satisfy the following consistency equations:

$$\begin{aligned} X_{\mathbf{r}}^0 \rho_{\mathbf{r}}^*(S) (X_{\mathbf{r}}^0)^{-1} &= \rho_{\mathbf{r}}(\sigma_{TST^2}(S)) = \rho_{\mathbf{r}}(S), \\ X_{\mathbf{r}}^0 \rho_{\mathbf{r}}^*(T) (X_{\mathbf{r}}^0)^{-1} &= \rho_{\mathbf{r}}(\sigma_{TST^2}(T)) = \rho_{\mathbf{r}}(ST), \\ X_{\mathbf{r}}^0 \rho_{\mathbf{r}}^*(U) (X_{\mathbf{r}}^0)^{-1} &= \rho_{\mathbf{r}}(\sigma_{TST^2}(U)) = \rho_{\mathbf{r}}(SU). \end{aligned} \quad (2.4)$$

Given the representation matrices listed in table 4, we see that the following relations are satisfied for any irreducible representations  $\mathbf{r}$  of  $S_4$ ,

$$\rho_{\mathbf{r}}^*(S) = \rho_{\mathbf{r}}(S), \quad \rho_{\mathbf{r}}^*(T) = \rho_{\mathbf{r}}(ST), \quad \rho_{\mathbf{r}}^*(U) = \rho_{\mathbf{r}}(SU). \quad (2.5)$$

Therefore  $X_{\mathbf{r}}^0$  is determined to be a unity matrix up to an overall phase,

$$X_{\mathbf{r}}^0 = 1. \quad (2.6)$$

Including the remaining inner automorphisms, we obtain that the generalized CP transformations compatible with the  $S_4$  family symmetry are of the form

$$\rho_{\mathbf{r}}(h)X_{\mathbf{r}}^0 = \rho_{\mathbf{r}}(h), \quad h \in S_4, \quad (2.7)$$

where  $h$  can be any of the 24 group elements of  $S_4$ . In particular we see that the canonical CP transformation with  $\rho_{\mathbf{r}}(1) = X_{\mathbf{r}}^0 = 1$  is allowed. Therefore all coupling constants would be constrained to be real in a  $S_4$  model with imposed CP symmetry.

Being similar to the paradigm of family symmetry, the imposed symmetry is  $S_4 \rtimes H_{\text{CP}}$  at high energy in the present work, where  $H_{\text{CP}}$  is the CP transformation consistent with  $S_4$  family symmetry and its elements are given in eq. (2.7). Subsequently  $S_4 \rtimes H_{\text{CP}}$  is broken down to different residual symmetry subgroups  $G_{\nu} \times H_{\text{CP}}^{\nu}$  and  $G_l \times H_{\text{CP}}^l$  in the neutrino and the charged lepton sectors respectively. The misalignment between  $G_{\nu} \times H_{\text{CP}}^{\nu}$  and  $G_l \times H_{\text{CP}}^l$  leads to particular predictions for mixing angles and CP phases. The basic procedure of

predicting lepton flavor mixing from remnant symmetries in a model independent way has been stated clearly in refs. [30, 40, 41, 46–48]. In the following, we briefly review the most important points which will be exploited later. Without loss of generality, the three generations of left-handed lepton doublets are assigned to be a  $S_4$  triplet  $\mathbf{3}$ . The irreducible representation  $\mathbf{3}'$  is distinct from  $\mathbf{3}$  in the overall sign of the generator  $U$ , therefore the same results are obtained if the lepton doublet fields are embedded into  $\mathbf{3}'$  instead of  $\mathbf{3}$ . Firstly, invariance under the residual symmetries  $G_l$  and  $G_\nu$  implies

$$\begin{aligned}\rho_{\mathbf{3}}^\dagger(g_l)m_l^\dagger m_l \rho_{\mathbf{3}}(g_l) &= m_l^\dagger m_l, & g_l &\in G_l \\ \rho_{\mathbf{3}}^T(g_\nu)m_\nu \rho_{\mathbf{3}}(g_\nu) &= m_\nu, & g_\nu &\in G_\nu,\end{aligned}\quad (2.8)$$

where the charged lepton mass matrix  $m_l$  is given in the convention in which the right-handed (left-handed) fields are on the left-hand (right-hand) side of  $m_l$ . Furthermore, the neutrino and the charged lepton mass matrices are subject to the constraint of residual CP symmetry as follows,

$$\begin{aligned}X_{\nu\mathbf{3}}^T m_\nu X_{\nu\mathbf{3}} &= m_\nu^*, & X_{\nu\mathbf{3}} &\in H_{\text{CP}}^\nu, \\ X_{l\mathbf{3}}^\dagger m_l^\dagger m_l X_{l\mathbf{3}} &= (m_l^\dagger m_l)^*, & X_{l\mathbf{3}} &\in H_{\text{CP}}^l.\end{aligned}\quad (2.9)$$

From the residual CP invariant condition of eq. (2.9), we can straightforwardly derive [30, 36–38, 66, 67]

$$U_\nu^\dagger X_{\nu\mathbf{3}} U_\nu^* = \text{diag}(\pm 1, \pm 1, \pm 1), \quad U_l^\dagger X_{l\mathbf{3}} U_l^* = \text{diag}(e^{i\rho_1}, e^{i\rho_2}, e^{i\rho_3}), \quad (2.10)$$

where  $\rho_i (i = 1, 2, 3)$  is an arbitrary real phase,  $U_\nu$  and  $U_l$  are the unitary diagonalization matrices of  $m_\nu$  and  $m_l^\dagger m_l$  respectively with  $U_\nu^T m_\nu U_\nu = \text{diag}(m_1, m_2, m_3)$  and  $U_l^\dagger m_l^\dagger m_l U_l = \text{diag}(m_e^2, m_\mu^2, m_\tau^2)$ . As a result, the residual CP transformations  $X_{\nu\mathbf{3}}$  and  $X_{l\mathbf{3}}$  should be symmetric otherwise the neutrino or the charged lepton masses would be constrained to be partially degenerate which is not compatible with experimental data. Note that the conclusion that the remnant CP transformations in the neutrino sector have to be symmetric is also reached in ref. [30]. In the same manner, the residual flavor symmetry invariant condition of eq. (2.8) leads to [66, 67]

$$U_\nu^\dagger \rho_{\mathbf{3}}(g_\nu) U_\nu = \text{diag}(\pm 1, \pm 1, \pm 1), \quad U_l^\dagger \rho_{\mathbf{3}}(g_l) U_l = \text{diag}(e^{i\alpha_e}, e^{i\alpha_\mu}, e^{i\alpha_\tau}), \quad (2.11)$$

where  $\alpha_e$ ,  $\alpha_\mu$  and  $\alpha_\tau$  are real parameters. Combining the consistency equation of eq. (2.3), eq. (2.10) and eq. (2.11), we see that the remnant flavor and CP symmetries should satisfy the following restricted consistency conditions:

$$\begin{aligned}X_{\nu\mathbf{r}} \rho_{\mathbf{r}}^*(g_\nu) X_{\nu\mathbf{r}}^{-1} &= \rho_{\mathbf{r}}(g_\nu), & g_\nu &\in G_\nu, \\ X_{l\mathbf{r}} \rho_{\mathbf{r}}^*(g_l) X_{l\mathbf{r}}^{-1} &= \rho_{\mathbf{r}}(g_l^{-1}), & g_l &\in G_l,\end{aligned}\quad (2.12)$$

which implies that the residual flavor symmetry and residual CP symmetry in the neutrino sector should generically commute. This is the reason why the residual symmetry in the neutrino sector is assumed to be  $G_\nu \times H_{\text{CP}}^\nu$  instead of  $G_\nu \rtimes H_{\text{CP}}^\nu$ . Given a set of solutions

$X_{\nu\mathbf{r}}$  and  $X_{l\mathbf{r}}$ , we can straightforwardly check that the CP transformations  $\rho_{\mathbf{r}}(g_\nu)X_{\nu\mathbf{r}}$  and  $\rho_{\mathbf{r}}(g_l)X_{l\mathbf{r}}$  with  $g_\nu \in G_\nu$ ,  $g_l \in G_l$  are admissible as well, and they lead to the same constraints shown in eq. (2.9) on the lepton mass matrices as  $X_{\nu\mathbf{r}}$  and  $X_{l\mathbf{r}}$ .

We can obtain the most general form of  $m_\nu$  and  $m_l^\dagger m_l$  from the invariant requirements of eq. (2.8) and eq. (2.9), then diagonalize them, and finally we can determine the lepton mixing matrix  $U_{PMNS}$ . Last but not least, generally we have many possible choices for the residual symmetry subgroups. However, if the residual family symmetries are taken to be another pair of subgroups  $G'_\nu$  and  $G'_l$  which are conjugate to  $G_\nu$  and  $G_l$  under the same element  $h$  belonging to  $S_4$ ,

$$G'_\nu = hG_\nu h^{-1}, \quad G'_l = hG_l h^{-1}, \quad h \in S_4. \quad (2.13)$$

Solving the restricted consistency condition of eq. (2.12), we find that the residual CP symmetries  $H_{\text{CP}}^{\nu'}$  and  $H_{\text{CP}}^{l'}$  compatible with  $G'_\nu$  and  $G'_l$  are of the form

$$H_{\text{CP}}^{\nu'} = \rho_{\mathbf{r}}(h)H_{\text{CP}}^\nu \rho_{\mathbf{r}}^T(h), \quad H_{\text{CP}}^{l'} = \rho_{\mathbf{r}}(h)H_{\text{CP}}^l \rho_{\mathbf{r}}^T(h). \quad (2.14)$$

This means that the elements of  $H_{\text{CP}}^{\nu'}$  and  $H_{\text{CP}}^{l'}$  are given by  $\rho_{\mathbf{r}}(h)X_{\nu\mathbf{r}}\rho_{\mathbf{r}}^T(h)$  and  $\rho_{\mathbf{r}}(h)X_{l\mathbf{r}}\rho_{\mathbf{r}}^T(h)$  respectively with  $X_{\nu\mathbf{r}} \in H_{\text{CP}}^\nu$  and  $X_{l\mathbf{r}} \in H_{\text{CP}}^l$ . The neutrino and charged lepton mass matrices  $m'_\nu$  and  $m_l^{\dagger}m_l'$  invariant under  $G'_\nu \times H_{\text{CP}}^{\nu'}$  and  $G'_l \rtimes H_{\text{CP}}^{l'}$  respectively are determined to be

$$m'_\nu = \rho_{\mathbf{3}}^*(h)m_\nu \rho_{\mathbf{3}}^\dagger(h), \quad m_l^{\dagger}m_l' = \rho_{\mathbf{3}}(h)m_l^\dagger m_l \rho_{\mathbf{3}}^\dagger(h). \quad (2.15)$$

Obviously the lepton mixing matrix would be predicted to be of the same form as that in  $G_\nu$ ,  $G_l$  case. As a result, we only need to analyze few independent residual family symmetries not related by group conjugation and the compatible remnant CP. We assume that the light neutrinos are Majorana particles, and hence the remnant family symmetry  $G_\nu$  in the neutrino sector must be  $K_4$  or  $Z_2$  subgroups. The case that  $S_4 \rtimes H_{\text{CP}}$  is broken down to  $Z_2 \times H_{\text{CP}}^\nu$  in the neutrino sector and  $Z_3 \rtimes H_{\text{CP}}^l$  in the charged lepton sector has been comprehensively studied [30, 41, 44]. One column of the PMNS matrix is then determined to be proportional to  $(2, -1, -1)^T$  or  $(1, 1, 1)^T$ , i.e. the so-called  $\text{TM}_1$  and  $\text{TM}_2$  mixing patterns can be produced exactly. Besides the  $Z_3$  subgroup, the residual family symmetry  $G_l$  in the charged lepton sector can be  $Z_4$  or  $K_4$  subgroups of  $S_4$ .<sup>2</sup> For example, the choice  $G_l = Z_4^{TST^2U}$  (or  $G_l = K_4^{(S,U)}$ ) and  $G_\nu = K_4^{(TST^2, T^2U)}$  leads to BM mixing no matter whether the generalized CP is included or not. In order to be in accordance with experimental data, we degrade  $G_\nu$  from  $K_4$  to  $Z_2$  or  $G_l$  from  $Z_4(K_4)$  to  $Z_2$  such that only one column or one row of the BM mixing matrix is fixed. After the generalized CP transformation defined in eq. (2.7) is taken into account further, the resulting lepton mixing matrix  $U_{PMNS}$  is found to depend on only one free real parameter. In the following, we shall firstly investigate the phenomenological predictions of preserving one column or one row of BM mixing, which may originate from a  $2 \times 2$  rotation in the neutrino or the charged lepton sector. Furthermore, the  $S_4$  family symmetry together with the generalized

<sup>2</sup>Choosing  $G_l$  to be a non-abelian subgroup would lead to a degenerate mass spectrum.



CP is imposed onto the theory, and then lepton flavor mixings arising from the symmetry breaking into different residual subgroups in the neutrino and the charged lepton sectors are discussed in section 4 and section 5. We find that the PMNS matrix has one column or one row in common with BM mixing up to permutations, and moreover the CP phases are predicted to take definite values because of the constraint of generalized CP symmetry.

### 3 Phenomenological analysis of deviation from bimaximal mixing

In a particular phase convention, the BM mixing matrix  $U_{BM}$  (ignoring possible Majorana phases) is of the following form [68]

$$U_{BM} = \begin{pmatrix} \frac{1}{\sqrt{2}} & -\frac{1}{\sqrt{2}} & 0 \\ \frac{1}{2} & \frac{1}{2} & -\frac{1}{\sqrt{2}} \\ \frac{1}{2} & \frac{1}{2} & \frac{1}{\sqrt{2}} \end{pmatrix}, \quad (3.1)$$

which leads to the three lepton mixing angles

$$\theta_{12}^{BM} = \theta_{23}^{BM} = 45^\circ, \quad \theta_{13}^{BM} = 0^\circ. \quad (3.2)$$

Comparing with the latest global fitting results [11–13], we see that rather large corrections are needed to be compatible with the experimental data. In the following, we shall consider the minimal modifications for simplicity. The additional rotation of the 1-2, 1-3 or 2-3 generations of charged leptons or neutrinos in the BM basis would be considered. As a consequence, one column or one row of BM mixing would be retained. Similar deviation from tri-bimaximal mixing has been widely studied [69–74]. Notice that the Majorana CP violating phases are not constrained at all in this phenomenological approach, since they are indeterminant in the starting BM mixing. First of all, we discuss the case of an extra 1-2 rotation in the charged lepton sector. The PMNS mixing matrix is obtained by multiplying the BM matrix  $U_{BM}$  by a 1-2 rotation matrix in the left-hand side as follows:

$$U_{PMNS} = \begin{pmatrix} \cos \theta & -\sin \theta e^{-i\delta} & 0 \\ \sin \theta e^{i\delta} & \cos \theta & 0 \\ 0 & 0 & 1 \end{pmatrix} U_{BM}, \quad (3.3)$$

where  $\theta$  and  $\delta$  are real free parameters, and their values can be fitted by the experimental data. Then the three mixing angles read as

$$\sin^2 \theta_{13} = \frac{1}{2} \sin^2 \theta, \quad \sin^2 \theta_{12} = \frac{1}{2} + \frac{\sqrt{2} \sin 2\theta \cos \delta}{3 + \cos 2\theta}, \quad \sin^2 \theta_{23} = 1 - \frac{2}{3 + \cos 2\theta}. \quad (3.4)$$

We see that the atmospheric and reactor mixing angles are related with each other by

$$\sin^2 \theta_{23} = \frac{1}{2} - \frac{1}{2} \tan^2 \theta_{13}. \quad (3.5)$$

Hence  $\theta_{23}$  is constrained to lie in the first octant, i.e.  $\theta_{23} < \frac{\pi}{4}$ . The Jarlskog invariant  $J_{CP}$  is given by

$$J_{CP} = \frac{\sin 2\theta \sin \delta}{8\sqrt{2}}. \quad (3.6)$$



Then the Dirac CP phase  $\delta_{\text{CP}}$  in the standard parameterization [75] is

$$\sin \delta_{\text{CP}} = \frac{(3 + \cos 2\theta) \sin 2\theta \sin \delta}{|\sin 2\theta| \sqrt{(3 + \cos 2\theta)^2 - 8 \sin^2 2\theta \cos^2 \delta}}.$$

For the value of  $\delta = 0$ , the above mixing parameters are simplified into

$$\sin^2 \theta_{13} = \frac{1}{2} \sin^2 \theta, \quad \sin^2 \theta_{12} = \frac{1}{2} + \frac{\sqrt{2} \sin 2\theta}{3 + \cos 2\theta}, \quad \sin^2 \theta_{23} = \frac{2 \cos^2 \theta}{3 + \cos 2\theta}, \quad \sin \delta_{\text{CP}} = 0, \quad (3.7)$$

where the Dirac CP is conserved. Since the rotation of 2-3 generations of charged leptons gives a vanishing  $\theta_{13}$ , we turn to investigate an additional rotation of 1-3 generations. We can obtain the PMNS mixing matrix by multiplying the BM matrix by a 1-3 rotation matrix in the left-hand side as

$$U_{PMNS} = \begin{pmatrix} \cos \theta & 0 & -\sin \theta e^{-i\delta} \\ 0 & 1 & 0 \\ \sin \theta e^{i\delta} & 0 & \cos \theta \end{pmatrix} U_{BM}. \quad (3.8)$$

The lepton mixing angles can be straightforwardly extracted as follows,

$$\sin^2 \theta_{13} = \frac{1}{2} \sin^2 \theta, \quad \sin^2 \theta_{12} = \frac{1}{2} + \frac{\sqrt{2} \sin 2\theta \cos \delta}{3 + \cos 2\theta}, \quad \sin^2 \theta_{23} = \frac{2}{3 + \cos 2\theta}. \quad (3.9)$$

The atmospheric and reactor mixing angles are related by,

$$\sin^2 \theta_{23} = \frac{1}{2} + \frac{1}{2} \tan^2 \theta_{13}. \quad (3.10)$$

which implies  $\theta_{23} > \pi/4$  and  $\theta_{23}$  is in the second octant. The Jarlskog invariant reads as

$$J_{\text{CP}} = -\frac{\sin 2\theta \sin \delta}{8\sqrt{2}}, \quad (3.11)$$

and then the Dirac CP phase is given by

$$\sin \delta_{\text{CP}} = -\frac{(3 + \cos 2\theta) \sin 2\theta \sin \delta}{|\sin 2\theta| \sqrt{(3 + \cos 2\theta)^2 - 8 \sin^2 2\theta \cos^2 \delta}}. \quad (3.12)$$

We perform numerical analysis by scanning the free parameters  $\theta$  and  $\delta$  in the regions of  $-\pi < \theta \leq \pi$  and  $-\pi < \delta \leq \pi$ . The correlations and the possible allowed values of the mixing parameters are obtained, as shown in figure 1. We see that there is a strong correlation between  $\sin^2 \theta_{23}$  and  $\sin \theta_{13}$ , which is given in eq. (3.5) and eq. (3.10). Note that the allowed regions of the mixing parameters are rather large although only two free parameters  $\theta$  and  $\delta$  are involved. Furthermore, we take into account the current bounds for three neutrino mixing angles presented in ref. [12], then the values of the mixing parameters would shrink to quite small areas. It is remarkable that the Dirac CP phase  $\delta_{\text{CP}}$  is constrained to be in the range of  $\pm [2.52, \pi]$  and  $[-0.62, 0.62]$  for 1-2 and 1-3 rotations respectively. For comparison with the above phenomenological analysis, the theoretical predictions of the generalized CP symmetry discussed in section 4 are also shown in figure 1.

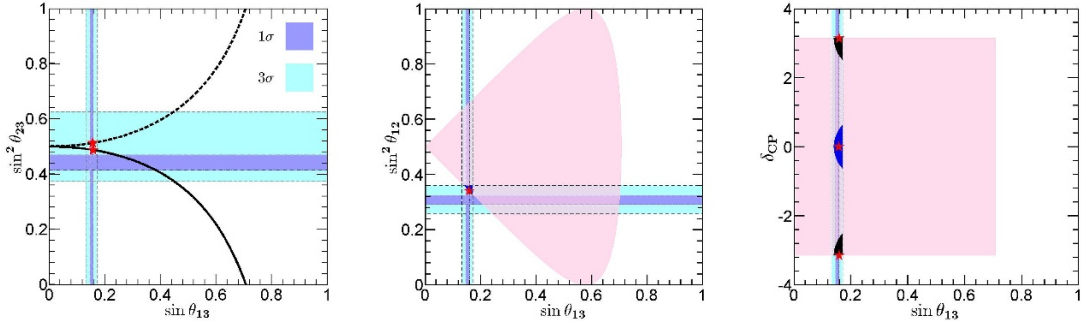


**Figure 1.** Correlations among mixing angles ( $\sin \theta_{13}, \sin^2 \theta_{12}, \sin^2 \theta_{23}$ ) and CP phase  $\delta_{\text{CP}}$  for additional rotations of 1-2 and 1-3 generations of charged leptons in the BM basis. In the first panel, the results of  $\sin^2 \theta_{23}$  vs.  $\sin \theta_{13}$  for 1-2 and 1-3 rotations are shown in solid line and dashed line respectively. The pink regions in the last two subfigures are the predictions for  $\sin^2 \theta_{12}$  and  $\delta_{\text{CP}}$  with respect to  $\sin \theta_{13}$  if both  $\theta$  and  $\delta$  vary in the range of  $-\pi$  to  $\pi$ . The black areas in the third panel denote the allowed region by the experimental data of three mixing angles for 1-2 rotation and the blue areas for 1-3 rotation. In the second subfigure, the allowed regions for 1-2 and 1-3 rotations coincide. The red stars represent the best fit values in  $S_4$  family symmetry combined with generalized CP.

Then we study the deviation from BM mixing induced by a rotation in the neutrino sector. Since the rotation of 1-2 generations leads to  $\theta_{13} = 0$ , we do not discuss this scenario. Firstly we consider the case that the neutrino mass matrix is rotated between 1-3 generations in the BM basis. The PMNS matrix is obtained by multiplying the BM matrix  $U_{\text{BM}}$  by a 1-3 rotation matrix in the right-hand side as follows:

$$U_{\text{PMNS}} = U_{\text{BM}} \begin{pmatrix} \cos \theta & 0 & \sin \theta e^{-i\delta} \\ 0 & 1 & 0 \\ -\sin \theta e^{i\delta} & 0 & \cos \theta \end{pmatrix}, \quad (3.13)$$

which gives rise to the solar mixing angle  $\sin^2 \theta_{12} = \frac{2}{3+\cos 2\theta} \geq \frac{1}{2}$ . This mixing pattern is obviously not compatible with the experimental data [11–13]. Next we consider the rotation of 2-3 generations of neutrinos. The PMNS matrix is given by

$$U_{\text{PMNS}} = U_{\text{BM}} \begin{pmatrix} 1 & 0 & 0 \\ 0 & \cos \theta & e^{-i\delta} \sin \theta \\ 0 & -e^{i\delta} \sin \theta & \cos \theta \end{pmatrix}. \quad (3.14)$$

The relation  $2 \cos^2 \theta_{12} \cos^2 \theta_{13} = 1$  is found to be fulfilled due to the fixed form of the first column. Using the  $3\sigma$  range  $1.76 \times 10^{-2} \leq \sin^2 \theta_{13} \leq 2.98 \times 10^{-2}$  as input, we obtain  $0.485 \leq \sin^2 \theta_{12} \leq 0.491$  which is outside of the experimentally preferred  $3\sigma$  range [11–13]. Consequently this case doesn't agree with the experimental data as well. In short summary, simple perturbative rotation to the BM mixing in the neutrino sector is not viable because the observed values of  $\theta_{12}$  and  $\theta_{13}$  can not be produced simultaneously. It is notable that agreement with the experimental data could be achieved if permutations of

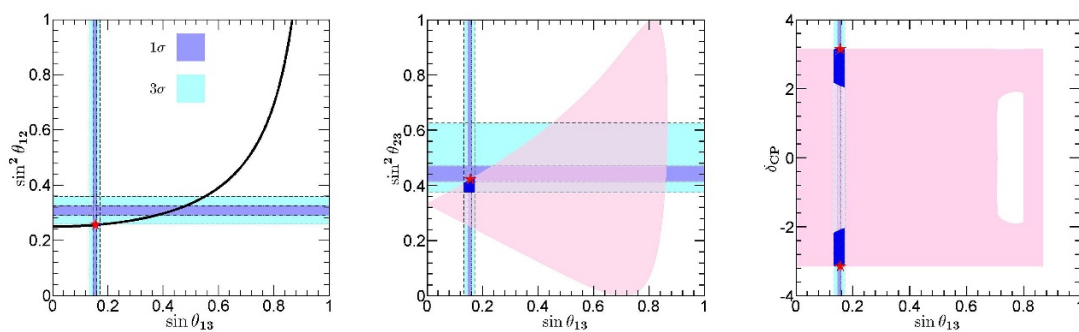


**Figure 2.** Correlations among mixing angles ( $\sin \theta_{13}, \sin^2 \theta_{12}, \sin^2 \theta_{23}$ ) and the Dirac CP phase  $\delta_{\text{CP}}$  for the perturbation from the neutrino sector with permutations of rows and columns. The pink areas denote the allowed parameter values when both  $\theta$  and  $\delta$  vary in the range of  $[-\pi, \pi]$ . The blue ones are allowed regions if both  $\theta_{13}$  and  $\theta_{23}$  are required to lie in the experimentally preferred  $3\sigma$  ranges [12]. The red stars represent the best fit values in generalized CP which will be discussed at the beginning of section 5.

rows and columns are allowed. If we perform both 2-3 rotation of neutrino and exchanges of rows and columns, the following PMNS matrix can be obtained

$$U_{PMNS} = \frac{1}{2} \begin{pmatrix} \sqrt{2} \cos \theta + \sin \theta e^{-i\delta} & 1 & \cos \theta - \sqrt{2} \sin \theta e^{i\delta} \\ -\sqrt{2} \sin \theta e^{-i\delta} & \sqrt{2} & -\sqrt{2} \cos \theta \\ -\sqrt{2} \cos \theta + \sin \theta e^{-i\delta} & 1 & \cos \theta + \sqrt{2} \sin \theta e^{i\delta} \end{pmatrix}. \quad (3.15)$$

The three mixing angles read as

$$\begin{aligned} \sin^2 \theta_{13} &= \frac{1}{8} (3 - \cos 2\theta - 2\sqrt{2} \sin 2\theta \cos \delta), \\ \sin^2 \theta_{12} &= \frac{2}{5 + \cos 2\theta + 2\sqrt{2} \sin 2\theta \cos \delta}, \\ \sin^2 \theta_{23} &= \frac{2 + 2 \cos 2\theta}{5 + \cos 2\theta + 2\sqrt{2} \sin 2\theta \cos \delta}. \end{aligned} \quad (3.16)$$

The following correlation is found

$$4 \sin^2 \theta_{12} \cos^2 \theta_{13} = 1. \quad (3.17)$$

For the fitted  $3\sigma$  range of  $\theta_{13}$ , the solar mixing angles is constrained to be in the interval of  $0.254 \leq \sin^2 \theta_{12} \leq 0.258$  which is rather close to its  $3\sigma$  lower limit 0.259 [12]. As a result, we suggest this mixing pattern is a good leading order approximation since accordance with experimental data should be easily achieved after subleading contributions are taken into account. The Jarlskog invariant  $J_{\text{CP}}$  is given by

$$J_{\text{CP}} = -\frac{\sin 2\theta \sin \delta}{8\sqrt{2}}, \quad (3.18)$$

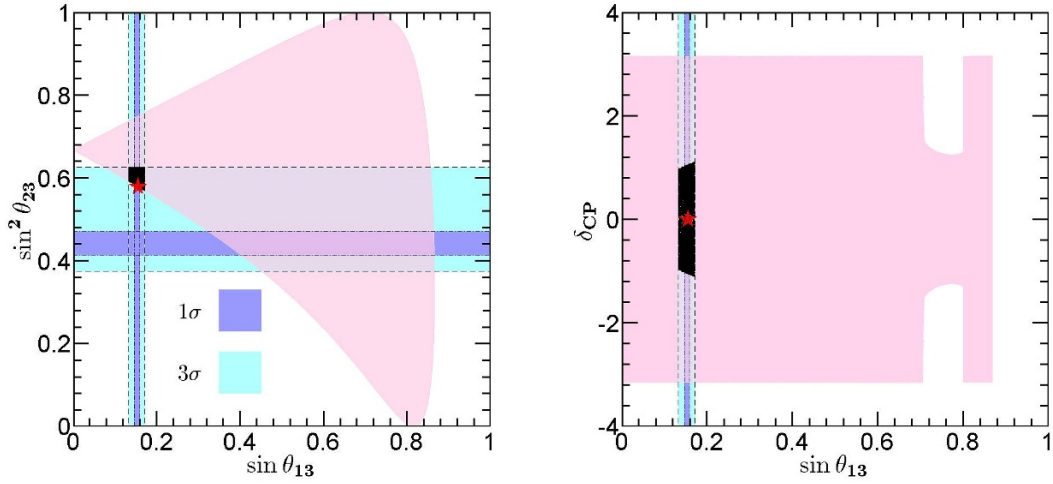


**Figure 3.** Correlations among  $\sin \theta_{13}$ ,  $\sin^2 \theta_{23}$  and Dirac CP phase  $\delta_{\text{CP}}$  for the lepton mixing obtained by exchanging the second and the third row of eq. (3.15). The result for  $\sin^2 \theta_{12}$  with respect to  $\sin \theta_{13}$  are not shown here since it is the same as the one in figure 2. The black areas denote the allowed regions after the measured  $3\sigma$  bounds of  $\theta_{13}$  and  $\theta_{23}$  are imposed.

The Dirac CP phase  $\delta_{\text{CP}}$  is determined to be

$$\sin \delta_{\text{CP}} = - \frac{(5 + \cos 2\theta + 2\sqrt{2} \sin 2\theta \cos \delta) \sin 2\theta \sin \delta}{|\cos \theta| \sqrt{2(3 + \cos 2\theta + 2\sqrt{2} \sin 2\theta \cos \delta) [(3 - \cos 2\theta)^2 - 8 \sin^2 2\theta \cos^2 \delta]}}. \quad (3.19)$$

Similar to perturbative rotation from the charged lepton sector discussed above, the numerical results are presented in figure 2, where we demand that  $\theta_{13}$  and  $\theta_{23}$  are in their  $3\sigma$  intervals [12] while  $\theta_{12}$  is fixed by the correlation of eq. (3.17) and it is slightly beyond the present  $3\sigma$  range. We see that  $\theta_{23}$  is constrained to be smaller than  $45^\circ$ , and  $\delta_{\text{CP}}$  is in the range of  $\pm [2.04, \pi]$ . The situation of  $\theta_{23}$  in the second octant can be accounted for by exchanging the second and the third rows in eq. (3.15). Then  $\theta_{23}$  would become  $\pi/2 - \theta_{23}$  and  $\delta_{\text{CP}}$  becomes  $\pi + \delta_{\text{CP}}$  while the predictions for  $\theta_{12}$  and  $\theta_{13}$  are the same as those in eq. (3.16). It is straightforward to get numerical results for this case, as shown in figure 3.  $\delta_{\text{CP}}$  is constrained to be in the range  $[-1.10, 1.10]$ . In the following, we shall show a lepton mixing matrix with one column or one row in common with BM mixing can be achieved from  $S_4$  family symmetry, and  $\delta_{\text{CP}}$  is predicted to take specific values 0 or  $\pi$  after generalized CP is imposed.

#### 4 Lepton flavor mixing from remnant symmetries $K_4^{(TST^2, T^2U)} \times H_{\text{CP}}^\nu$ in the neutrino sector and $Z_2^{SU} \times H_{\text{CP}}^l$ in the charged lepton sector

In this work, we shall extend the flavor symmetry to include additional CP symmetry. Analogous to the paradigm of flavor symmetry, lepton flavor mixing still arises from the mismatch between the remnant symmetries in the neutrino and the charged lepton sectors. The phenomenological implications of the breaking pattern of  $S_4$  and generalized CP into  $Z_2 \times CP$  in the neutrino sector and an abelian subgroup of  $S_4$  in the charged lepton

sector have been investigated in ref. [30]. In this section, we shall study another scenario that  $S_4$  is broken down to  $K_4$  and  $Z_2$  subgroups in the neutrino and the charged lepton sectors respectively. Including the generalized CP symmetry, the representative remnant symmetry considered here is  $K_4^{(TST^2, T^2U)} \times H_{\text{CP}}^\nu$  in the neutrino sector and  $Z_2^{SU} \times H_{\text{CP}}^l$  in the charged lepton sector. Other possible choices of remnant symmetry are related to this one by similarity transformations or lead to a vanishing reactor mixing angle. In this case, only one row (instead of one column) of the PMNS matrix can be fixed because of the residual  $Z_2^{SU}$  in the charged lepton sector. In this approach the remnant symmetries are assumed and we do not consider how the required vacuum alignment needed to achieve the remnant symmetries is dynamically realized, since the resulting lepton flavor mixing is independent of vacuum alignment mechanism although there are generally many possible symmetry breaking implementation schemes. Furthermore, we shall present dynamical models realizing the concerned symmetry breaking pattern in section 6.

Firstly we consider the neutrino sector. The full symmetry  $S_4 \rtimes H_{\text{CP}}$  is broken to  $K_4^{(TST^2, T^2U)} \times H_{\text{CP}}^\nu$ . In order to consistently formulate such a setup, the element  $X_{\nu\mathbf{r}}$  of  $H_{\text{CP}}^\nu$  must satisfy the following consistence conditions:

$$X_{\nu\mathbf{r}} \rho_{\mathbf{r}}^*(h) X_{\nu\mathbf{r}}^{-1} = \rho_{\mathbf{r}}(h), \quad \text{with } h \in K_4^{(TST^2, T^2U)}, \quad (4.1)$$

which follows from the consistency equation of eq. (2.12) for the remnant symmetries. We find that the residual CP transformation  $X_{\nu\mathbf{r}}$  can take 4 possible values,

$$H_{\text{CP}}^\nu = \{\rho_{\mathbf{r}}(1), \rho_{\mathbf{r}}(TST^2), \rho_{\mathbf{r}}(T^2U), \rho_{\mathbf{r}}(ST^2SU)\}. \quad (4.2)$$

The light neutrino mass matrix  $m_\nu$  is constrained by the residual family symmetry  $K_4^{(TST^2, T^2U)}$  and the residual CP symmetry  $H_{\text{CP}}^\nu$  as

$$\rho_{\mathbf{3}}^T(h) m_\nu \rho_{\mathbf{3}}(h) = m_\nu, \quad h \in K_4^{(TST^2, T^2U)}, \quad (4.3)$$

$$X_{\nu\mathbf{3}}^T m_\nu X_{\nu\mathbf{3}} = m_\nu^*, \quad X_{\nu\mathbf{3}} \in H_{\text{CP}}^\nu. \quad (4.4)$$

Eq. (4.3) constrains the light neutrino mass matrix to be of the form

$$m_\nu = a \begin{pmatrix} 0 & 0 & 1 \\ 0 & 1 & 0 \\ 1 & 0 & 0 \end{pmatrix} + b \begin{pmatrix} 3 & 0 & -1 \\ 0 & 2 & 0 \\ -1 & 0 & 3 \end{pmatrix} + c \begin{pmatrix} 0 & 1 & 0 \\ 1 & 0 & 1 \\ 0 & 1 & 0 \end{pmatrix}, \quad (4.5)$$

which can be diagonalized by a unitary matrix  $U_\nu$ , i.e.

$$U_\nu^T m_\nu U_\nu = \text{diag} \left( a + 2b - \sqrt{2}c, a + 2b + \sqrt{2}c, -a + 4b \right), \quad (4.6)$$

where

$$U_\nu = \frac{1}{2} \begin{pmatrix} 1 & 1 & -\sqrt{2} \\ -\sqrt{2} & \sqrt{2} & 0 \\ 1 & 1 & \sqrt{2} \end{pmatrix}. \quad (4.7)$$

Note that  $U_\nu$  is fixed up to column permutations since the order of the eigenvalues of  $m_\nu$  in eq. (4.6) is not determined. Furthermore, the residual CP symmetry invariant condition of eq. (4.4) implies that all the three parameters  $a$ ,  $b$  and  $c$  are real for  $X_{\nu\mathbf{r}} = \rho_{\mathbf{r}}(1), \rho_{\mathbf{r}}(TST^2), \rho_{\mathbf{r}}(T^2U), \rho_{\mathbf{r}}(ST^2SU)$ . Then the light neutrino masses are determined by three real parameters  $a$ ,  $b$  and  $c$ . As a consequence, either normal ordering (NO) or inverted ordering (IO) neutrino mass spectrum can be accommodated.

Now we turn to the charged lepton sector. The  $S_4$  flavor symmetry is broken down to  $G_l = Z_2^{SU}$ . The remnant CP symmetry  $H_{\text{CP}}^l$  has to be consistent with the remnant family symmetry  $Z_2^{SU}$ . That is to say, its element  $X_{l\mathbf{r}}$  should satisfy the consistency equation

$$X_{l\mathbf{r}}\rho_{\mathbf{r}}^*(SU)X_{l\mathbf{r}}^{-1} = \rho_{\mathbf{r}}(SU). \quad (4.8)$$

This restricted consistency equation can be derived from the general consistency condition of eq. (2.3) with  $g, g' \in Z_2^{SU}$ . For  $g = SU$ ,  $g'$  can only be  $SU$  (can not be identity element) since it is the unique element which has the same order as  $g = SU$ . This implies that the remnant CP symmetry  $H_{\text{CP}}^l$  is commutable with the remnant family symmetry  $Z_2^{SU}$ , and therefore the semidirect product between family and generalized CP symmetries will reduce to a direct product. As a consequence, the residual symmetry in the charged lepton sector would be  $Z_2^{SU} \times H_{\text{CP}}^l$  in this case. In fact, the reduction of the semidirect product structure to direct product holds true for a generic residual  $Z_2$  family symmetry [30]. It is easy to check that only four generalized CP transformations are acceptable,

$$H_{\text{CP}}^l = \{\rho_{\mathbf{r}}(TST^2), \rho_{\mathbf{r}}(TST^2U), \rho_{\mathbf{r}}(T^2ST), \rho_{\mathbf{r}}(T^2STU)\}. \quad (4.9)$$

We are able to construct the hermitian combination  $m_l^\dagger m_l$  of the charged lepton mass matrix from its invariance under the residual symmetry  $Z_2^{SU} \times H_{\text{CP}}^l$ ,

$$\begin{aligned} \rho_{\mathbf{3}}^\dagger(SU)m_l^\dagger m_l \rho_{\mathbf{3}}(SU) &= m_l^\dagger m_l, \\ X_{l\mathbf{3}}^\dagger m_l^\dagger m_l X_{l\mathbf{3}} &= \left(m_l^\dagger m_l\right)^*. \end{aligned} \quad (4.10)$$

Since  $X_{l\mathbf{r}}$  and  $\rho_{\mathbf{r}}(g_l)X_{l\mathbf{r}}$  with  $g_l \in Z_2^{SU}$  lead to the same constraints on the charged lepton mass matrix, as shown in section 2 and ref. [30]. Two distinct phenomenological predictions arise for the four possible generalized CP transformations in eq. (4.9). Firstly we focus on the case of  $X_{l\mathbf{r}} = \rho_{\mathbf{r}}(TST^2), \rho_{\mathbf{r}}(TST^2U)$ . The most general  $m_l^\dagger m_l$  satisfying eq. (4.10) is of the following form

$$m_l^\dagger m_l = \begin{pmatrix} \alpha & (1+i)\beta & i\epsilon \\ (1-i)\beta & \gamma & (1+i)\beta \\ -i\epsilon & (1-i)\beta & \alpha \end{pmatrix}, \quad (4.11)$$

where  $\alpha, \beta, \gamma$  and  $\epsilon$  are real. It can be diagonalized by the unitary transformation

$$U_l = \frac{1}{\sqrt{2}} \begin{pmatrix} e^{\frac{i\pi}{4}} \sin \theta & e^{\frac{i\pi}{4}} \cos \theta & e^{-\frac{i\pi}{4}} \\ -\sqrt{2} \cos \theta & \sqrt{2} \sin \theta & 0 \\ e^{-\frac{i\pi}{4}} \sin \theta & e^{-\frac{i\pi}{4}} \cos \theta & e^{\frac{i\pi}{4}} \end{pmatrix} \quad (4.12)$$

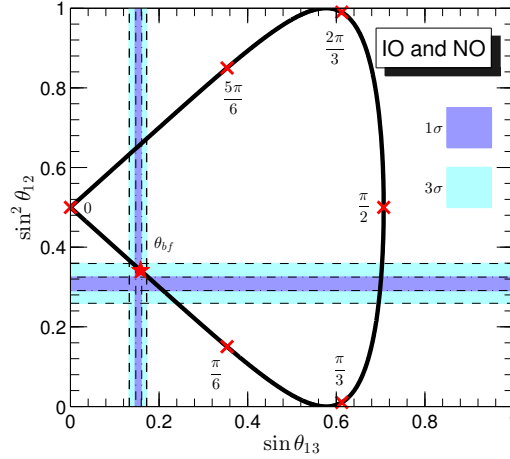


**Figure 4.** Correlations between  $\sin \theta_{13}$  and  $\sin^2 \theta_{12}$  for the mixing pattern of eq. (4.16). In this case, a residual symmetry  $Z_2 \times CP$  is preserved in the charged lepton sector. The best fitting value is marked with a red star, and the points for  $\theta = 0, \pi/6, \pi/3, \pi/2, 2\pi/3$  and  $5\pi/6$  are labelled with a cross to guide the eye. The shown  $1\sigma$  and  $3\sigma$  ranges for the mixing angles are taken from ref. [12].

up to rephasings and column permutations, and the angle  $\theta$  is specified by

$$\tan 2\theta = \frac{4\beta}{\alpha + \epsilon - \gamma} . \quad (4.13)$$

The charged lepton masses are

$$\begin{aligned} m_e^2 &= \frac{1}{2} \left[ \alpha + \epsilon + \gamma - \text{sign}((\alpha + \epsilon - \gamma) \cos(2\theta)) \sqrt{16\beta^2 + (\alpha + \epsilon - \gamma)^2} \right] , \\ m_\mu^2 &= \frac{1}{2} \left[ \alpha + \epsilon + \gamma + \text{sign}((\alpha + \epsilon - \gamma) \cos(2\theta)) \sqrt{16\beta^2 + (\alpha + \epsilon - \gamma)^2} \right] , \\ m_\tau^2 &= \alpha - \epsilon . \end{aligned} \quad (4.14)$$

Combining the unitary transformations  $U_\nu$  and  $U_l$  from neutrino and charged lepton sectors, we obtain the predictions for the PMNS matrix:

$$U_{PMNS} = U_l^\dagger U_\nu = \frac{1}{2} \begin{pmatrix} \sin \theta + \sqrt{2} \cos \theta & \sin \theta - \sqrt{2} \cos \theta & i\sqrt{2} \sin \theta \\ \cos \theta - \sqrt{2} \sin \theta & \cos \theta + \sqrt{2} \sin \theta & i\sqrt{2} \cos \theta \\ 1 & 1 & -i\sqrt{2} \end{pmatrix} , \quad (4.15)$$

The lepton mixing parameters can be straightforwardly extracted as follows

$$\begin{aligned} \sin \delta_{CP} &= \sin \alpha_{21} = \sin \alpha_{31} = 0, \\ \sin^2 \theta_{13} &= \frac{1}{2} \sin^2 \theta, \quad \sin^2 \theta_{12} = \frac{1}{2} - \frac{\sqrt{2} \sin 2\theta}{3 + \cos 2\theta}, \quad \sin^2 \theta_{23} = \frac{1 + \cos 2\theta}{3 + \cos 2\theta}, \end{aligned} \quad (4.16)$$

where the PDG convention for the lepton mixing angles and CP phases is adopted [75],  $\delta_{CP}$  is the Dirac CP phase,  $\alpha_{21}$  and  $\alpha_{31}$  stand for the Majorana CP phases. We see that



all CP phases are trivial, this is because that a common CP transformation  $X_{l\mathbf{r}} = X_{\nu\mathbf{r}} = \rho_{\mathbf{r}}(TST^2)$  is shared by the charged lepton and neutrino sectors. In contrast with the general phenomenological analysis of section 3, the CP phases are predicted to be of definite value 0 or  $\pi$  due to the imposed CP symmetry. Furthermore, the mixing angles are closely related with each other as follows,

$$\sin^2 \theta_{12} = \frac{1}{2} \pm \tan \theta_{13} \sqrt{1 - \tan^2 \theta_{13}}, \quad 2 \cos^2 \theta_{13} \cos^2 \theta_{23} = 1. \quad (4.17)$$

The measured values of reactor mixing angle  $\sin^2 \theta_{13} = 0.0234$  fixes the parameter  $\theta \simeq 12.494^\circ$ , and then the other two mixing angles are determined to be  $\sin^2 \theta_{12} \simeq 0.347$ ,  $\sin^2 \theta_{23} \simeq 0.488$  which are in the experimentally allowed regions. The correlations among the mixing angles are plotted in figure 4 and figure 5. We see that the predictions for the lepton mixing angles agree rather well with their measured values for certain values of the parameter  $\theta$ . The best fitting results of this mixing pattern for NO (IO) are:

$$\begin{aligned} \theta_{bf} &= 0.225(0.227), & \sin^2 \theta_{12}(\theta_{bf}) &= 0.342(0.341), & (4.18) \\ \sin^2 \theta_{13}(\theta_{bf}) &= 0.0250(0.0253), & \sin^2 \theta_{23}(\theta_{bf}) &= 0.487(0.487), & \chi_{\min}^2 = 6.938(4.288). \end{aligned}$$

Hence this mixing pattern can describe the experimental data very well, as the global minimum of the  $\chi^2$  is quite small: 4.288 for IO and 6.938 for NO spectrum. From eq. (4.17), we have  $\sin^2 \theta_{23} = 1 - 1/(2 \cos^2 \theta_{13}) < 1/2$ , namely  $\theta_{23}$  is in the first octant, as can be seen from figure 5. The present neutrino oscillation data can not tell us whether  $\theta_{23}$  is larger or smaller than  $45^\circ$ .  $\theta_{23}$  in the second octant can be achieved by exchanging the second and the third rows of the PMNS matrix in eq. (4.15). The observed values of the three mixing angles can also be accommodated. Results of the  $\chi^2$  analysis are as follows:

$$\begin{aligned} \theta_{bf} &= 0.224(0.227), & \sin^2 \theta_{12}(\theta_{bf}) &= 0.343(0.341), & (4.19) \\ \sin^2 \theta_{13}(\theta_{bf}) &= 0.0248(0.0253), & \sin^2 \theta_{23}(\theta_{bf}) &= 0.513(0.513), & \chi_{\min}^2 = 9.890(4.409) \end{aligned}$$

for NO (IO) mass spectrum.

It is notable that the Dirac CP  $\delta_{\text{CP}}$  is predicted to be conserved here. The present experiments have very low sensitivity to leptonic CP. T2K has recently reported a weak indication for  $\delta_{\text{CP}}$  around  $3\pi/2$  [14]. Analysis of the SuperKamiokande atmospheric neutrino data gives preferable range  $(1.2 \pm 0.5)\pi$  [78]. The global analysis of all oscillation data gives  $\delta_{\text{CP}} = 1.39_{-0.27}^{+0.38}\pi(1\sigma)$  for NO and  $\delta_{\text{CP}} = 1.31_{-0.33}^{+0.29}\pi(1\sigma)$  for IO and no restriction appears at  $3\sigma$  level [12]. Hence conserved CP with  $\delta_{\text{CP}} = 0, \pi$  can be accommodated by both present experimental data and global analysis. Future long baseline neutrino experiments LBNE [16, 17], LBNO [18–22] and Hyper-Kamiokande [23, 24] are designed to measure the Dirac phase. If the signal of leptonic CP violation is discovered, our proposal would be ruled out. In addition, the predictions for the atmospheric mixing angle  $\theta_{23}$  can be tested by future atmospheric neutrino oscillation experiments such as the India-based Neutrino Observatory.

Furthermore, the predictions for the conserved Dirac and Majorana CP phases in eq. (4.16) can be checked by the neutrinoless double beta ( $0\nu\beta\beta$ ) decay experiment which

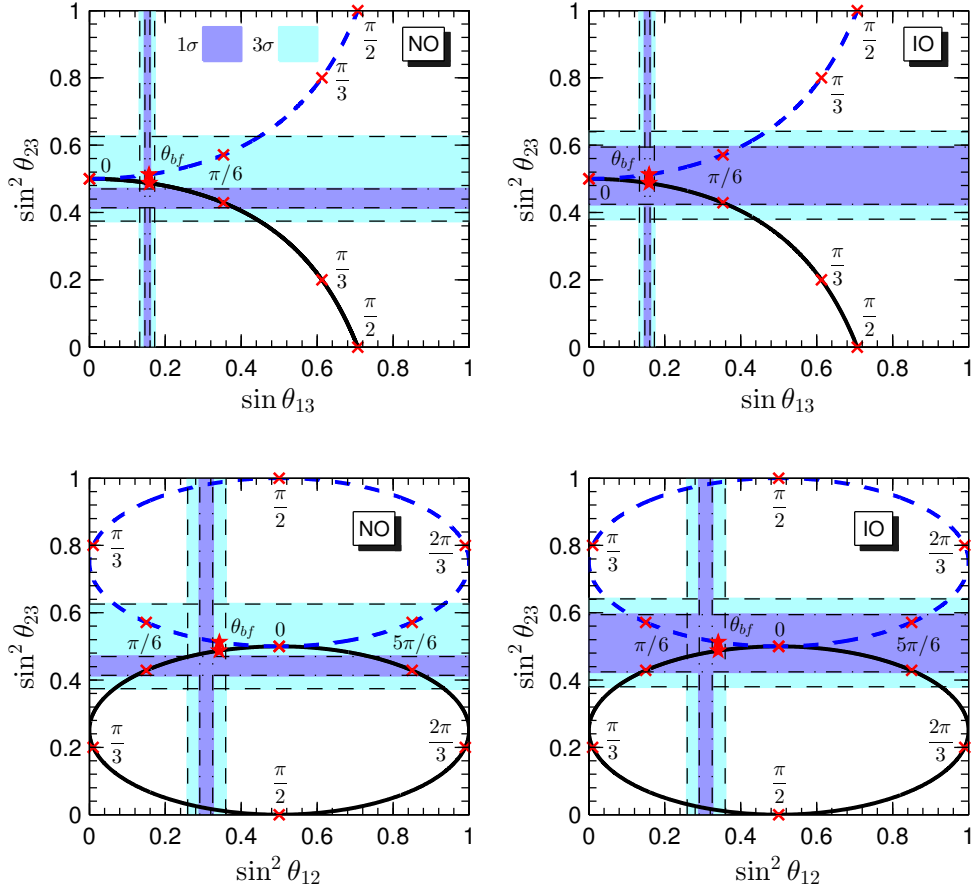


**Figure 5.**  $\sin^2 \theta_{23}$  with respect to  $\sin \theta_{13}$ ,  $\sin^2 \theta_{12}$  in the case of  $Z_2 \times CP$  preserved in the charged lepton sector. The solid lines and dashed lines represent the results for  $\theta_{23} < \pi/4$  and  $\theta_{23} > \pi/4$  respectively. The best fitting value is marked with a red star, and the points for  $\theta = 0, \pi/6, \pi/3, \pi/2, 2\pi/3$  and  $5\pi/6$  are labelled with a cross to guide the eye. The shown  $1\sigma$  and  $3\sigma$  ranges for the mixing angles are taken from ref. [12].

is an important probe for the Majorana nature of neutrino and lepton number violation. It is well-known that the  $0\nu\beta\beta$ -decay amplitude depends on the following effective Majorana mass:

$$|m_{ee}| = \left| (m_1 c_{12}^2 + m_2 s_{12}^2 e^{i\alpha_{21}}) c_{13}^2 + m_3 s_{13}^2 e^{i(\alpha_{31} - 2\delta_{CP})} \right|, \quad (4.20)$$

where  $c_{ij} \equiv \cos \theta_{ij}$  and  $s_{ij} \equiv \sin \theta_{ij}$ . The predictions for the effective mass are plotted in figure 6. We see that  $|m_{ee}|$  is determined to be around the  $3\sigma$  upper limit (0.049eV) or lower limit (0.013eV) for inverted hierarchy, which is within the reach of the forthcoming  $0\nu\beta\beta$  experiments. A large region of possible values of  $|m_{ee}|$  is allowed in case of NO, and  $|m_{ee}|$  could be rather small depending on the value of the lightest neutrino mass. Consequently this mixing pattern would be preferred if the  $|m_{ee}|$  is measured to be close to 0.049eV or 0.013eV in future. Note that the effective mass  $|m_{ee}|$  doesn't depend on  $\theta_{23}$ , and therefore it is invariant under the exchange of the 2nd and the 3rd rows of the PMNS matrix.

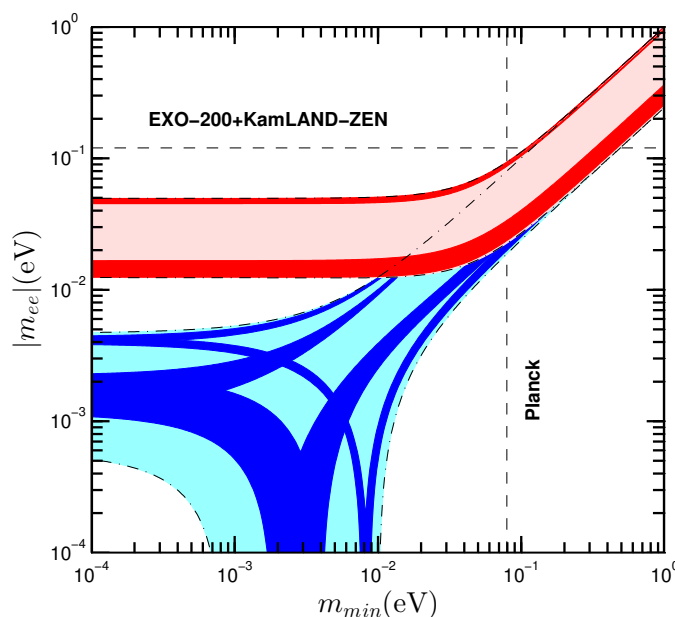


**Figure 6.** The allowed values of the effective mass  $|m_{ee}|$  with respect to the lightest neutrino mass in the case of  $Z_2 \times CP$  preserved in the charged lepton sector, where the light red and light blue bands denote the regions for the  $3\sigma$  ranges of the oscillation parameters in the inverted and normal neutrino mass spectrum respectively [12]. The red and blue regions are the predictions for inverted hierarchy and normal hierarchy with the PMNS matrix given in eq. (4.15). The upper bound  $|m_{ee}| < (0.120 - 0.250) \text{ eV}$  comes from the combination of the EXO-200 [82, 83] and KamLAND-ZEN experiments [84]. The upper limit on the mass of the lightest neutrino is derived from the latest Planck result  $m_1 + m_2 + m_3 < 0.230 \text{ eV}$  at 95% confidence level [80].

The phenomenological implications for the remaining two remnant CP transformations  $X_{lr} = \rho_r(T^2ST), \rho_r(T^2STU)$  can be studied in the same way. However, we find that the observed values of the three lepton mixing angles can not be fitted simultaneously. Hence this case will not be discussed in detail.

In short, the perturbative rotations to the BM mixing from the charged lepton sector, which is discussed in section 3, can be realized by breaking the  $S_4$  family symmetry to a  $Z_2$  subgroup in the charged lepton and to  $K_4$  in the neutrino sector. By further extending the  $S_4$  family symmetry to consistently include generalized CP symmetry, the phase  $\delta$  of the perturbative rotation can not take arbitrary value anymore. We have definite predictions for the leptonic CP phases: both Dirac CP phase and Majorana CP phases are trivial in order to fit the data of mixing angles.

## 5 Model predicting one column of BM mixing with $S_4$ and generalized CP

The scenario of the  $S_4$  flavor symmetry breaking to  $Z_2$  and  $Z_4$  subgroups in the neutrino and charged lepton sectors respectively with generalized CP symmetry has been investigated

in ref. [30]. In terms of the notation of present work, the representative residual symmetries can be chosen to be  $Z_2^{ST^2SU} \times H_{\text{CP}}^\nu$  in the neutrino sector and  $Z_4^{TST^2U} \rtimes H_{\text{CP}}^l$  in the charged lepton sector, where  $H_{\text{CP}}^\nu = \{\rho_{\mathbf{r}}(1), \rho_{\mathbf{r}}(ST^2SU)\}$  and  $H_{\text{CP}}^l = \{\rho_{\mathbf{r}}(1), \rho_{\mathbf{r}}(TST^2U), \rho_{\mathbf{r}}(S), \rho_{\mathbf{r}}(T^2STU)\}$ . Before presenting the model, we shall firstly review the lepton mixing arising from this breaking pattern. Note that the residual CP transformations  $H_{\text{CP}}^\nu = \{\rho_{\mathbf{r}}(T^2U), \rho_{\mathbf{r}}(TST^2)\}$  are also compatible with the remnant flavor symmetry  $Z_2^{ST^2SU}$ . However the measured values of the three mixing angles can not be accommodated simultaneously in that case. As the representation matrix of  $TST^2U$  is diagonal in all irreducible representations of  $S_4$ , the hermitian combination  $m_l^\dagger m_l$  is diagonal. Hence lepton flavor mixing completely arises from the neutrino sector. Straightforward calculations demonstrate that the neutrino mass matrix preserving  $Z_2^{ST^2SU} \times H_{\text{CP}}^\nu$  is of the following form:

$$m_\nu = \alpha \begin{pmatrix} 0 & 0 & 1 \\ 0 & 1 & 0 \\ 1 & 0 & 0 \end{pmatrix} + \beta \begin{pmatrix} -3 & 0 & 1 \\ 0 & -2 & 0 \\ 1 & 0 & -3 \end{pmatrix} + \gamma \begin{pmatrix} 0 & 1 & 0 \\ 1 & 0 & 1 \\ 0 & 1 & 0 \end{pmatrix} + \epsilon \begin{pmatrix} \sqrt{2} & -1 & 0 \\ -1 & 0 & 1 \\ 0 & 1 & -\sqrt{2} \end{pmatrix}, \quad (5.1)$$

where the all four parameters  $\alpha, \beta, \gamma$  and  $\epsilon$  are real. The lepton mixing matrix  $U_{PMNS}$ , which diagonalizes the neutrino mass matrix in eq. (5.1), is determined to be of the form

$$U_{PMNS} = \frac{1}{2} \begin{pmatrix} \sin \theta + \sqrt{2} \cos \theta & 1 & \cos \theta - \sqrt{2} \sin \theta \\ -\sqrt{2} \sin \theta & \sqrt{2} & -\sqrt{2} \cos \theta \\ \sin \theta - \sqrt{2} \cos \theta & 1 & \cos \theta + \sqrt{2} \sin \theta \end{pmatrix} K_\nu, \quad (5.2)$$

up to row and column permutations, where  $K_\nu$  is a unitary diagonal matrix with entries  $\pm 1$  or  $\pm i$  which renders the light neutrino masses positive. The rotation angle  $\theta$  is given by

$$\tan 2\theta = \frac{-4\epsilon}{2\alpha + 2\beta - \sqrt{2}\gamma}. \quad (5.3)$$

The light neutrino masses are

$$\begin{aligned} m_1 &= \frac{1}{2} \left| 6\beta + \sqrt{2}\gamma + \text{sign}((2\alpha + 2\beta - \sqrt{2}\gamma) \cos 2\theta) \sqrt{16\epsilon^2 + (2\alpha + 2\beta - \sqrt{2}\gamma)^2} \right|, \\ m_2 &= |\alpha - 2\beta + \sqrt{2}\gamma|, \\ m_3 &= \frac{1}{2} \left| 6\beta + \sqrt{2}\gamma - \text{sign}((2\alpha + 2\beta - \sqrt{2}\gamma) \cos 2\theta) \sqrt{16\epsilon^2 + (2\alpha + 2\beta - \sqrt{2}\gamma)^2} \right|. \end{aligned} \quad (5.4)$$

Notice that the mixing pattern with one column  $(1/2, 1/\sqrt{2}, 1/2)^T$  has been proposed in ref. [76, 77], where the scenario of only one  $Z_2$  symmetry imposed in the neutrino sector was analyzed in a general way. The lepton mixing angles and CP phases can be read out from eq. (5.2) as follow

$$\begin{aligned} \sin^2 \theta_{13} &= \frac{1}{8} (3 - \cos 2\theta - 2\sqrt{2} \sin 2\theta), & \sin^2 \theta_{12} &= \frac{2}{5 + \cos 2\theta + 2\sqrt{2} \sin 2\theta}, \\ \sin^2 \theta_{23} &= \frac{4 \cos^2 \theta}{5 + \cos 2\theta + 2\sqrt{2} \sin 2\theta}, & \sin \delta_{\text{CP}} = \sin \alpha_{21} = \sin \alpha_{31} &= 0, \end{aligned} \quad (5.5)$$

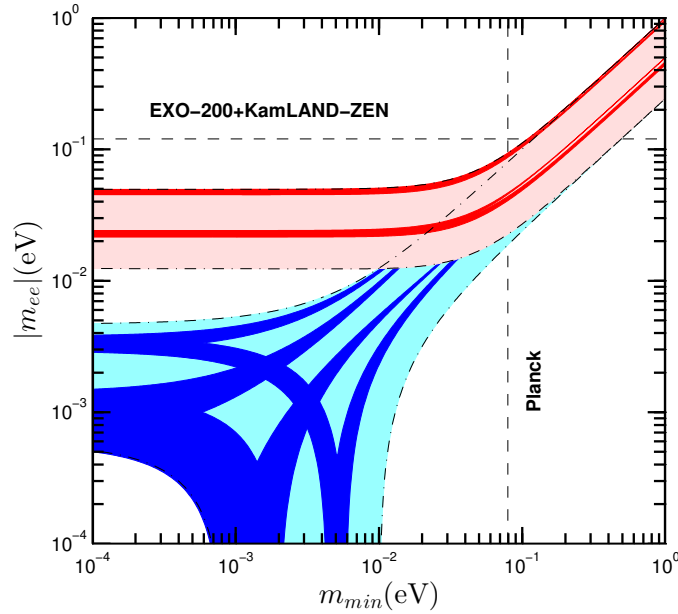


**Figure 7.** The allowed values of the effective mass  $|m_{ee}|$  in the case of  $Z_2 \times CP$  preserved in the neutrino sector, where the light red and light blue bands denote the regions for the  $3\sigma$  ranges of the oscillation parameters in the inverted and normal neutrino mass spectrum respectively [12]. The red and blue regions are the predictions for inverted hierarchy and normal hierarchy with the PMNS matrix given in eq. (5.2). The upper bound  $|m_{ee}| < (0.120 - 0.250)$  eV comes from the combination of the EXO-200 [82, 83] and KamLAND-ZEN experiments [84]. The upper limit on the mass of the lightest neutrino is derived from the latest Planck result  $m_1 + m_2 + m_3 < 0.230$  eV at 95% confidence level [80].

which match with the expressions of mixing parameters in ref. [30] after parameter redefinition  $\theta \rightarrow \pi/4 + \theta$ . We see that the three mixing angles are strongly correlated with each other

$$4 \cos^2 \theta_{13} \sin^2 \theta_{12} = 1, \quad \sin^2 \theta_{23} = \frac{1}{3} + \frac{\tan \theta_{13}}{9} \left( \tan \theta_{13} \pm 2\sqrt{6 - 2 \tan^2 \theta_{13}} \right). \quad (5.6)$$

The measured value of the reactor angle  $\sin^2 \theta_{13} = 0.0234$  [12] can be reproduced for  $\theta \simeq 25.091^\circ$ . With this value of  $\theta$ ,  $\sin^2 \theta_{12} \simeq 0.256$  and  $\sin^2 \theta_{23} \simeq 0.420$  follow from eq. (5.5). We see that  $\theta_{23}$  in the experimentally preferred regions can be achieved while  $\theta_{12}$  is predicted to be quite close to its  $3\sigma$  lower bound [12] due to the correlation with  $\theta_{13}$  shown in eq. (5.6). As has been emphasized in section 3, agreement with experimental data can be easily achieved after subleading corrections are included. A concrete model realization of this scenario will be presented in the following. In order to see quantitatively to which extent this mixing pattern can accommodate the present experimental data, we perform a conventional  $\chi^2$  analysis. The minimum of the  $\chi^2$  is  $\chi^2_{\min} = 9.865$  for NO and 10.454 for IO with

$$\begin{aligned} \theta_{bf} &= 0.436(0.434), & \sin^2 \theta_{12}(\theta_{bf}) &= 0.256(0.256), \\ \sin^2 \theta_{13}(\theta_{bf}) &= 0.0238(0.0244), & \sin^2 \theta_{23}(\theta_{bf}) &= 0.421(0.422), \end{aligned} \quad (5.7)$$

where the number before (in) the parenthesis denotes the best fitting value for NO (IO) spectrum. Obviously  $\theta_{23}$  in the first octant is favored, and  $\theta_{23}$  in the second octant can also be accommodated by interchanging the second and third rows of eq. (5.2). The resulting predictions for  $\theta_{13}$ ,  $\theta_{12}$  and CP phases remain the same as those given by eq. (5.5), while  $\theta_{23}$  becomes its complementary angle. The best fitting results are as follows:

$$\begin{aligned} \theta_{bf} &= 0.433(0.435), & \sin^2 \theta_{12}(\theta_{bf}) &= 0.256(0.256), \\ \sin^2 \theta_{13}(\theta_{bf}) &= 0.0246(0.0242), & \sin^2 \theta_{23}(\theta_{bf}) &= 0.578(0.579), & \chi^2_{\min} &= 27.807(10.086), \end{aligned} \quad (5.8)$$

for NO (IO) neutrino mass spectrum. Furthermore, the predictions for the effective mass  $|m_{ee}|$  is plotted in figure 7.  $|m_{ee}|$  is found to be around 0.049eV or 0.023eV for IO spectrum, which can be tested by forthcoming  $0\nu\beta\beta$  decay experiments. Nevertheless the allowed regions of  $|m_{ee}|$  are somewhat complex for NO spectrum, and the effective mass can be very small for certain values of the lightest neutrino mass. In concrete models where the mixing pattern in eq. (5.5) is produced at leading order,  $|m_{ee}|$  could lie outside of the red and blue areas of figure 7 after possible subleading order corrections are considered. Depending on the specific form of the corrections and how large they are, different predictions for  $|m_{ee}|$  can be obtained. Notice that the same mixing pattern of eq. (5.2) can also be derived from the symmetry breaking pattern of  $S_4 \rtimes H_{\text{CP}}$  into  $Z_2^{ST^2SU} \times H_{\text{CP}}^\nu$  in the neutrino sector and  $K_4^{(S,U)} \rtimes H_{\text{CP}}^l$  in the charged lepton sector [30].

In the following we shall construct a model based on  $S_4$  family symmetry and generalized CP symmetry  $H_{\text{CP}}$ . The auxiliary symmetry  $Z_3 \times Z_4$  is introduced to disentangle the flavon fields associated with the neutrino sector from those associated with the charged lepton sector and to eliminate unwanted dangerous operators. By a judicious choice of flavons, the above discussed symmetry breaking pattern of  $S_4 \rtimes H_{\text{CP}}$  into  $Z_2^{ST^2SU} \times H_{\text{CP}}^\nu$  and  $Z_4^{TST^2U} \rtimes H_{\text{CP}}^l$  is explicitly realized at leading order. As a result, the interesting mixing texture in eq. (5.2) is reproduced exactly in this model, and realistic  $\theta_{12}$  can be achieved after higher order corrections are included. This model is formulated in the context of supersymmetry. We assign the three generations of left-handed lepton doublets  $l$  and of right-handed neutrino  $\nu^c$  to  $S_4$  triplet **3**. The right-handed charged leptons  $e^c$ ,  $\mu^c$  and  $\tau^c$  are singlet states of  $S_4$ , and they transform as **1**, **1'** and **1** respectively. The matter fields, flavon fields, driving fields and their transformation properties under the family symmetry  $S_4 \times Z_3 \times Z_4 \times U(1)_R$  are summarized in table 1.

## 5.1 Vacuum alignment

The issue of vacuum alignment is handled with the help supersymmetric driving field mechanism [79]. This approach utilises a global  $U(1)_R$  continuous symmetry which contains the discrete  $R$ -parity as a subgroup. The flavon and Higgs fields are uncharged under  $U(1)_R$ , the matter fields carry  $R$  charge +1 and the driving fields  $\rho^0$ ,  $\varphi_T^0$ ,  $\eta^0$  and  $\varphi_S^0$  carry two units of  $R$  charge. Consequently all terms in the superpotential either contain two matter superfields or one driving field. The leading order (LO) driving superpotential  $w_d$  invariant under the family symmetry  $S_4 \times Z_3 \times Z_4$  is of the form

$$w_d = w_d^l + w_d^\nu, \quad (5.9)$$

Field	$l$	$\nu^c$	$e^c$	$\mu^c$	$\tau^c$	$h_{u,d}$	$\varphi_T$	$\phi$	$\xi$	$\eta$	$\varphi_S$	$\rho^0$	$\varphi_T^0$	$\eta^0$	$\varphi_S^0$
$S_4$	<b>3</b>	<b>3</b>	<b>1</b>	<b>1'</b>	<b>1</b>	<b>1</b>	<b>3</b>	<b>3'</b>	<b>1</b>	<b>2</b>	<b>3</b>	<b>2</b>	<b>3</b>	<b>2</b>	<b>3</b>
$Z_3$	$\omega_3$	1	$\omega_3^2$	$\omega_3^2$	$\omega_3^2$	1	1	1	$\omega_3^2$	$\omega_3^2$	$\omega_3^2$	1	1	$\omega_3^2$	$\omega_3^2$
$Z_4$	-1	1	-i	1	i	1	i	i	-1	-1	-1	-1	-1	1	1
$U(1)_R$	1	1	1	1	1	0	0	0	0	0	0	2	2	2	2

**Table 1.** The field contents and their classification under the family symmetry  $S_4 \times Z_3 \times Z_4$  and  $U(1)_R$ , where  $\omega_3 = e^{i2\pi/3}$ .

where  $w_d^l$  and  $w_d^\nu$  are responsible for the LO vacuum alignment of the charged lepton sector and neutrino sector respectively, and they can be expressed as

$$w_d^l = f_1(\rho^0(\varphi_T\varphi_T)\mathbf{2})\mathbf{1} + f_2(\rho^0(\varphi_T\phi)\mathbf{2})\mathbf{1} + f_3(\rho^0(\phi\phi)\mathbf{2})\mathbf{1} + f_4(\varphi_T^0(\varphi_T\varphi_T)\mathbf{3})\mathbf{1} \\ + f_5(\varphi_T^0(\varphi_T\phi)\mathbf{3})\mathbf{1} + f_6(\varphi_T^0(\phi\phi)\mathbf{3})\mathbf{1}, \quad (5.10)$$

$$w_d^\nu = g_1\xi(\eta^0\eta)\mathbf{1} + g_2(\eta^0(\eta\eta)\mathbf{2})\mathbf{1} + g_3(\eta^0(\varphi_S\varphi_S)\mathbf{2})\mathbf{1} + g_4\xi(\varphi_S^0\varphi_S)\mathbf{1} + g_5(\varphi_S^0(\eta\varphi_S)\mathbf{3})\mathbf{1} \\ + g_6(\varphi_S^0(\varphi_S\varphi_S)\mathbf{3})\mathbf{1}, \quad (5.11)$$

where the subscripts **1**, **2**, **3** etc stand for contractions into the corresponding  $S_4$  irreducible representations. Note that the terms proportional to  $f_4$ ,  $f_6$  and  $g_6$  give null contributions because of the antisymmetric contractions  $(\mathbf{3} \otimes \mathbf{3})\mathbf{3}$  and  $(\mathbf{3}' \otimes \mathbf{3}')\mathbf{3}$ . As we require the theory invariant under the generalized CP transformations defined in eq. (2.7), all couplings  $f_i$  and  $g_i$  would be real. The driving field is assumed to have vanishing vacuum expectation value (VEV). In the limit of unbroken supersymmetry, the vacuum configuration is fixed by the vanishing  $F$ -term of the driving field. For the vacuum alignment of the charged lepton sector, we have

$$\begin{aligned} \frac{\partial w_d^l}{\partial \rho_1^0} &= 2f_1(\varphi_{T_2}^2 - \varphi_{T_1}\varphi_{T_3}) + \sqrt{3}f_2(\varphi_{T_1}\phi_1 + \varphi_{T_3}\phi_3) + 2f_3(\phi_2^2 - \phi_1\phi_3) = 0, \\ \frac{\partial w_d^l}{\partial \rho_2^0} &= \sqrt{3}f_1(\varphi_{T_1}^2 + \varphi_{T_3}^2) + f_2(\varphi_{T_1}\phi_3 - 2\varphi_{T_2}\phi_2 + \varphi_{T_3}\phi_1) + \sqrt{3}f_3(\phi_1^2 + \phi_3^2) = 0, \\ \frac{\partial w_d^l}{\partial \varphi_{T_1}^0} &= f_5(\varphi_{T_1}\phi_2 + \varphi_{T_2}\phi_1) = 0, \\ \frac{\partial w_d^l}{\partial \varphi_{T_2}^0} &= f_5(\varphi_{T_1}\phi_1 - \varphi_{T_3}\phi_3) = 0, \\ \frac{\partial w_d^l}{\partial \varphi_{T_3}^0} &= -f_5(\varphi_{T_2}\phi_3 + \varphi_{T_3}\phi_2) = 0. \end{aligned} \quad (5.12)$$

The most general solution to these equations can be obtained by a straightforward calculation. We find two independent solutions up to symmetry transformations belonging to  $S_4$ . The first is

$$\langle \varphi_T \rangle = \begin{pmatrix} 1 \\ 0 \\ 0 \end{pmatrix} v_T, \quad \langle \phi \rangle = \begin{pmatrix} 0 \\ 0 \\ 1 \end{pmatrix} v_\phi, \quad v_\phi = -\frac{f_2 \pm \sqrt{f_2^2 - 12f_1f_3}}{2\sqrt{3}f_3} v_T. \quad (5.13)$$



This vacuum preserves the  $Z_4^{(D)}$  subgroup generated by  $iT^2STU$  defined as a simultaneous transformation of  $T^2STU \in S_4$  and  $i \in Z_4$ , although it breaks completely the  $S_4$  family symmetry. Indeed the generator  $iT^2STU$  is given by  $\pm \text{diag}(1, i, -1)$ , with the plus (minus) sign for the **3** (**3'**) representation. Moreover, the VEVs  $v_\phi$  and  $v_T$  are naturally of the same order of magnitude, since they are related through the couplings  $f_1$ ,  $f_2$  and  $f_3$  which are expected to have absolute values of order one. To reproduce the observed hierarchy among the charged lepton masses, we choose

$$\frac{v_\phi}{\Lambda} \sim \frac{v_T}{\Lambda} \sim \lambda^2, \quad (5.14)$$

where  $\lambda \simeq 0.23$  is the Cabibbo angle [75]. The second solution to eq. (5.12) is given by

$$\langle \varphi_T \rangle = \begin{pmatrix} 1 \\ 0 \\ i \end{pmatrix} v_T, \quad \langle \phi \rangle = \begin{pmatrix} i \\ 0 \\ 1 \end{pmatrix} v_\phi, \quad v_\phi = \frac{\sqrt{3}f_2 \pm \sqrt{3f_2^2 - 4f_1f_3}}{2f_3} v_T, \quad (5.15)$$

which preserves the  $Z_2^{SU}$  subgroup. The first vacuum in eq. (5.13) is required in our model. Since the two configurations of VEVs in eq. (5.13) and eq. (5.15) are degenerate in the supersymmetric limit, supersymmetry breaking effects are needed to discriminate the first one as the lowest minimum of the scalar potential. Here we consider the possibility of lifting the vacuum degeneracy by the soft supersymmetry breaking terms. The soft breaking terms involving  $\varphi_T$  and  $\phi$  can be written as

$$\mathcal{L}_{\text{soft}} = m_{\varphi_T}^2 |\varphi_T|^2 + m_\phi^2 |\phi|^2, \quad (5.16)$$

where the trilinear terms are forbidden by  $Z_4$ . We assume  $m_{\varphi_T, \phi}^2 < 0$  to stabilize the potential for both vacuum configurations. One can straightforwardly check that these soft terms take different values for the two alignments in eqs. (5.13), (5.15). With an appropriate choice of the soft parameters, it is possible to distinguish the two configurations and assure the desired one in eq. (5.13) as the setting with the lowest minimum. Now we turn to the  $F$ -term conditions of the neutrino sector,

$$\begin{aligned} \frac{\partial w_d^\nu}{\partial \eta_1^0} &= g_1 \xi \eta_1 + g_2 (\eta_2^2 - \eta_1^2) + 2g_3 (\varphi_{S_2}^2 - \varphi_{S_1} \varphi_{S_3}) = 0, \\ \frac{\partial w_d^\nu}{\partial \eta_2^0} &= g_1 \xi \eta_2 + 2g_2 \eta_1 \eta_2 + \sqrt{3} g_3 (\varphi_{S_1}^2 + \varphi_{S_3}^2) = 0, \\ \frac{\partial w_d^\nu}{\partial \varphi_{S_1}^0} &= g_4 \xi \varphi_{S_3} + g_5 (\sqrt{3} \eta_2 \varphi_{S_1} - \eta_1 \varphi_{S_3}) = 0, \\ \frac{\partial w_d^\nu}{\partial \varphi_{S_2}^0} &= g_4 \xi \varphi_{S_2} + 2g_5 \eta_1 \varphi_{S_2} = 0, \\ \frac{\partial w_d^\nu}{\partial \varphi_{S_3}^0} &= g_4 \xi \varphi_{S_1} + g_5 (\sqrt{3} \eta_2 \varphi_{S_3} - \eta_1 \varphi_{S_1}) = 0. \end{aligned} \quad (5.17)$$

It is then straightforward to work out the most general solutions to these equations. Disregarding the ambiguity caused by  $S_4$  family symmetry transformations we find two possible

non-trivial solutions. The first one is given by

$$\langle \xi \rangle = v_\xi, \quad \langle \eta \rangle = \begin{pmatrix} 1 \\ 0 \end{pmatrix} v_\eta, \quad \langle \varphi_S \rangle = \begin{pmatrix} 0 \\ 1 \\ 0 \end{pmatrix} v_S, \quad (5.18)$$

with

$$v_\eta = -\frac{g_4 v_\xi}{2g_5}, \quad v_S^2 = \frac{g_4(2g_1g_5 + g_2g_4)}{8g_3g_5^2} v_\xi^2, \quad (5.19)$$

where  $v_\xi$  is undetermined and generally complex. Given the representation matrices in appendix A, it is easy to check that this vacuum breaks the  $S_4$  family symmetry to  $Z_4^{T^2STU}$ . The second solution takes the form

$$\langle \xi \rangle = v_\xi, \quad \langle \eta \rangle = \begin{pmatrix} 1 \\ \sqrt{3} \end{pmatrix} v_\eta, \quad \langle \varphi_S \rangle = \begin{pmatrix} 1 \\ \sqrt{2} \\ 1 \end{pmatrix} v_S, \quad (5.20)$$

where

$$v_\eta = -\frac{g_4 v_\xi}{2g_5}, \quad v_S^2 = \frac{g_4(g_1g_5 - g_2g_4)}{4g_3g_5^2} v_\xi^2, \quad v_\xi \text{ undetermined}, \quad (5.21)$$

We see that the two VEVs  $v_\eta$  and  $v_\xi$  share the same phase modulo  $\pi$ , while the phase difference between  $v_S$  and  $v_\xi$  is  $0, \pi$  for  $g_3g_4(g_1g_5 - g_2g_4) > 0$  or  $\pm\pi/2$  for  $g_3g_4(g_1g_5 - g_2g_4) < 0$ . Since the phase of  $v_\xi$  can always be absorbed by lepton fields, we could take  $v_\xi$  to be real without loss of generality. Consequently  $v_\eta$  is real, and  $v_S$  is either real or pure imaginary depending on the combination  $g_3g_4(g_1g_5 - g_2g_4)$  being positive or negative. We find that the symmetry  $S_4 \times H_{\text{CP}}$  is broken to  $Z_2^{ST^2SU} \times H_{\text{CP}}^\nu$  by the VEVs of  $\xi$ ,  $\eta$  and  $\varphi_S$ , where the remnant CP symmetry  $H_{\text{CP}}^\nu = \{\rho_3(1), \rho_3(ST^2SU)\}$  for real  $v_S$  and  $H_{\text{CP}}^\nu = \{\rho_3(T^2U), \rho_3(TST^2)\}$  for pure imaginary  $v_S$ . Only the second solution in eq. (5.20) can allow us to derive the interesting mixing texture of eq. (5.2) discussed above. Some supersymmetry breaking effects are needed to select it as the lowest minimum of the scalar potential. We attempt to achieve this by considering the soft supersymmetry breaking terms for the flavons  $\xi$ ,  $\eta$  and  $\varphi_S$ , which is of the following form

$$\mathcal{L}_{\text{soft}} = m_\xi^2 |\xi|^2 + m_\eta^2 |\eta|^2 + m_{\varphi_S}^2 |\varphi_S|^2. \quad (5.22)$$

Note that the trilinear soft breaking term for  $\xi$ ,  $\eta$ ,  $\varphi_S$  is forbidden by the auxiliary  $Z_3 \times Z_4$  symmetry. For properly chosen values of the soft masses  $m_{\xi, \eta, \varphi_S}^2$ , the minimum of the potential for the second solution could be smaller than that for the first one, and therefore the required vacuum in eq. (5.20) would be picked out. Furthermore, the three VEVs  $v_\xi$ ,  $v_\eta$  and  $v_S$  are expected to be of the same order of magnitude without fine tuning among the parameters  $g_i (i = 1, 2, 3, 4, 5)$ . As usual, we shall take them to be of the same order as the VEVs of charged lepton sector flavons, i.e.

$$\frac{v_\xi}{\Lambda} \sim \frac{v_\eta}{\Lambda} \sim \frac{v_S}{\Lambda} \sim \lambda^2. \quad (5.23)$$

## 5.2 The structure of the model

The superpotential for the charged lepton masses is

$$w_l = \frac{y_\tau}{\Lambda} \tau^c (l \varphi_T)_1 h_d + \frac{y_{\mu 1}}{\Lambda^2} \mu^c (l(\varphi_T \varphi_T)_{\mathbf{3}'} )_1 h_d + \frac{y_{\mu 2}}{\Lambda^2} \mu^c (l(\varphi_T \phi)_{\mathbf{3}'} )_1 h_d + \frac{y_{\mu 3}}{\Lambda^2} \mu^c (l(\phi \phi)_{\mathbf{3}'} )_1 h_d + \sum_{i=1}^4 \frac{y_{e_i}}{\Lambda^3} e^c (l O_i)_1 h_d + \dots, \quad (5.24)$$

where

$$O = \{ \varphi_T \varphi_T \varphi_T, \varphi_T \varphi_T \phi, \varphi_T \phi \phi, \phi \phi \phi \}. \quad (5.25)$$

Notice that all possible  $S_4$  contractions should be considered. Dots stand for higher dimensional operators corrections which we will be discussed later. All the Yukawa couplings are real because of the generalized CP symmetry. Substituting the flavon VEVs in eq. (5.13), we find the charged lepton mass matrix is diagonal with

$$m_e = \left| y_e \frac{v_T^3}{\Lambda^3} \right| v_d, \quad m_\mu = \left| y_{\mu 1} \frac{v_T^2}{\Lambda^2} - y_{\mu 2} \frac{v_\phi v_T}{\Lambda^2} - y_{\mu 3} \frac{v_\phi^2}{\Lambda^2} \right| v_d, \quad m_\tau = \left| y_\tau \frac{v_T}{\Lambda} \right| v_d, \quad (5.26)$$

where  $v_d = \langle h_d \rangle$ ,  $y_e$  stands for the total result of all the different contributions of the  $y_{e_i}$  terms. For  $v_\phi \sim v_T \sim \lambda^2 \Lambda$ , the mass hierarchies of the charged lepton are obtained, i.e.

$$m_e : m_\mu : m_\tau \simeq \lambda^4 : \lambda^2 : 1. \quad (5.27)$$

As the representation matrix of the element  $T^2 STU$  is diagonal  $\rho_{\mathbf{3}}(T^2 STU) = \text{diag}(-i, 1, i)$ , we have  $\rho_{\mathbf{3}}^\dagger(T^2 STU) m_l^\dagger m_l \rho_{\mathbf{3}}(T^2 STU) = m_l^\dagger m_l$ . It is easy to check that the  $Z_4^{(D)}$  subgroup is preserved by the vacuum of  $\varphi_T$  and  $\phi$ , where  $Z_4^{(D)}$  is the diagonal subgroup generated by  $Z_4^{T^2 STU}$  and the auxiliary  $Z_4$  in usual way. Consequently the combination  $m_l^\dagger m_l$  is predicted to be diagonal due to this residual  $Z_4^{(D)}$  symmetry, and the lepton mixing arises from the neutrino sector.

The light neutrino masses are generated via type-I seesaw mechanism. The LO superpotential responsible for neutrino masses is

$$w_\nu = \frac{y_1}{\Lambda} \xi (\nu^c l)_1 h_u + \frac{y_2}{\Lambda} ((\nu^c l)_2 \eta)_1 h_u + \frac{y_3}{\Lambda} ((\nu^c l)_3 \varphi_S)_1 h_u + M (\nu^c \nu^c)_1, \quad (5.28)$$

where again all couplings are real due to the invariance under the generalized CP. The last term is the Majorana mass term for the right-handed neutrinos,

$$m_M = M \begin{pmatrix} 0 & 0 & 1 \\ 0 & 1 & 0 \\ 1 & 0 & 0 \end{pmatrix}. \quad (5.29)$$

Hence the three right-handed neutrinos have a degenerate mass  $M$ . With the vacuum alignment of  $\xi$ ,  $\eta$  and  $\varphi_S$  in eq. (5.20), we find the Dirac mass matrix is of the following form,

$$m_D = y_1 v_u \frac{v_\xi}{\Lambda} \begin{pmatrix} 0 & 0 & 1 \\ 0 & 1 & 0 \\ 1 & 0 & 0 \end{pmatrix} + y_2 v_u \frac{v_\eta}{\Lambda} \begin{pmatrix} 3 & 0 & -1 \\ 0 & 2 & 0 \\ -1 & 0 & 3 \end{pmatrix} + y_3 v_u \frac{v_S}{\Lambda} \begin{pmatrix} 0 & 1 & -\sqrt{2} \\ -1 & 0 & 1 \\ \sqrt{2} & -1 & 0 \end{pmatrix}. \quad (5.30)$$

The light neutrino mass matrix is given by the see-saw relation:  $m_\nu = -m_D^T m_M^{-1} m_D$ , we find that  $m_\nu$  is of the same form as the one shown in eq. (5.1) with

$$\alpha = \left(\frac{8}{3}y^2 - 8x^2 - 1\right)m_0, \quad \beta = \left(2x - 2x^2 + \frac{1}{3}y^2\right)m_0, \quad \gamma = -\sqrt{2}y^2m_0, \quad \epsilon = -6xy m_0, \quad (5.31)$$

where

$$x = \frac{y_2 v_\eta}{y_1 v_\xi}, \quad y = \frac{y_3 v_S}{y_1 v_\xi}, \quad m_0 = y_1^2 \frac{v_\xi^2}{\Lambda^2} \frac{v_u^2}{M}. \quad (5.32)$$

Note that the phase of  $v_\xi$  can be factorized out as an overall phase of  $m_\nu$  and therefore it can be absorbed by field redefinition. Accordingly eq. (5.21) implies that the VEVs  $v_\xi$  and  $v_\eta$  are real while  $v_S$  is real for  $g_3 g_4 (g_1 g_5 - g_2 g_4) > 0$  and pure imaginary for  $g_3 g_4 (g_1 g_5 - g_2 g_4) < 0$ .

In case of real  $v_S$ , all the four parameters  $\alpha$ ,  $\beta$ ,  $\gamma$  and  $\epsilon$  are real. The VEVs of the flavon  $\xi$ ,  $\eta$  and  $\varphi_S$  break the  $S_4$  family symmetry to  $Z_2^{ST^2SU}$  and break the generalized CP to  $H_{CP}^\nu = \{\rho_r(1), \rho_r(ST^2SU)\}$  in the neutrino sector. Hence the desired symmetry breaking pattern discussed at the beginning of this section is exactly reproduced here. The lepton flavor mixing matrix is of the form shown in eq. (5.2), and the predictions for light neutrino masses and mixing parameters are presented in eqs. (5.4), (5.5) with  $\tan 2\theta = -\frac{12xy}{1-2x+10x^2-4y^2}$ . Since the BM mixing has to undergo somewhat large corrections in order to be in accordance with experimental data,  $\tan 2\theta$  should be around 1.2, as shown in eqs. (5.7), (5.8). This required value of  $\theta$  can be naturally achieved in our model since both parameters  $x$  and  $y$  are of order one. On the other hand, if  $v_S$  is pure imaginary,  $\alpha$ ,  $\beta$  and  $\gamma$  are real while  $\epsilon$  is an imaginary parameter. The remnant symmetry in the neutrino sector would be  $Z_2^{ST^2SU} \times H_{CP}^\nu$  with  $H_{CP}^\nu = \{\rho_r(T^2U), \rho_r(TST^2)\}$ . However, the mixing pattern enforced by this residual symmetry can not fit the measured values of the mixing angles. Consequently we shall focus on the case of real  $v_S$  henceforth.

It is useful to study the constraints on the model imposed by the observed values of the mass-squared splitting  $\delta m^2 \equiv m_2^2 - m_1^2$ ,  $\Delta m^2 \equiv m_3^2 - (m_1^2 + m_2^2)/2$  and the reactor mixing angle  $\theta_{13}$ . As the light neutrino mass matrix effectively depends on three real (imaginary) parameters  $x$ ,  $y$  and  $m_0$ , their values can be completely fixed. Given the best fitting results  $\delta m^2 = 7.54 \times 10^{-5} \text{eV}^2$ ,  $\Delta m^2 = 2.43 \times 10^{-3} (-2.38 \times 10^{-3}) \text{eV}^2$  and  $\sin^2 \theta_{13} = 0.0234 (0.0240)$  for NO (IO) neutrino mass spectrum from ref. [12], the possible solutions for  $x$ ,  $y$  and the corresponding predictions for the light neutrino masses, the lepton mixing angles, CP phases and the effective mass  $|m_{ee}|$  of neutrinoless double-beta decay are collected in table 2. Note that there are other solutions predicting  $\theta_{23} = 30.137^\circ$  which is out of the  $3\sigma$  range [12], and consequently they are not included in table 2. It is remarkable that the absolute values of the light neutrino masses are fixed at leading order in the present model. We find that the light neutrino mass spectrum can be either NO or IO. Regarding the sum of the light neutrino masses, the latest Planck result is  $\sum m_\nu < 0.23 \text{eV}$  at 95% confidence level [80]. This bound is saturated for all the solutions except the second one which gives  $m_1 + m_2 + m_3 \simeq 0.238 \text{eV}$  close to the upper bound. Furthermore, the effective mass  $|m_{ee}|$  can take the values 12.650 meV, 33.044 meV, 22.821 meV and 48.936 meV in this model. The most stringent upper limit on  $|m_{ee}|$  from GERDA [81], EXO-200 [82, 83] and KamLAND-ZEN [84] is  $|m_{ee}| < (120 - 250) \text{meV}$ . Hence our predictions for  $|m_{ee}|$  are

$(x, y)$	$m_1$	$m_2$	$m_3$	$ m_{ee} $	$\alpha_{21}$	$\alpha_{31}$	$\delta_{\text{CP}}$	$\theta_{23}/^\circ$	$\theta_{12}/^\circ$	mass order
$(-0.109, -0.729)$	13.535	16.081	51.487	12.650	0	$\pi$	$\pi$	40.392	30.395	NO
$(0.855, -0.602)$	73.975	74.483	89.106	33.044	$\pi$					
$(-0.057, 0.468)$	48.529	49.300	3.569	22.821	$\pi$			40.459	30.405	IO
$(0.093, 0.606)$	50.284	51.028	13.644	48.936	0					

**Table 2.** The predictions for light neutrino masses  $m_i (i = 1, 2, 3)$ , the lepton flavor mixing parameters and the effective mass  $|m_{ee}|$  of the neutrinoless double-beta decay, where the unit of mass is meV.

compatible with present experimental measurements. Our model could be directly tested by future neutrinoless double-beta decay experiments such as nEXO which is expected to have the mass sensitivity of  $5 \sim 11$  meV [85].

Higher dimensional operators, suppressed by additional powers of the cutoff scale  $\Lambda$ , can be added to the leading terms studied above. As a result, the LO predictions would be modified. The subleading corrections to the driving superpotential are,

$$\Delta w_d^l = \frac{1}{\Lambda}(\rho^0 \Psi_\nu^3)_1 + \frac{1}{\Lambda}(\varphi_T^0 \Psi_\nu^3)_1, \quad \Delta w_d^\nu = \frac{1}{\Lambda^4}(\eta^0 \Psi_l^4 \Psi_\nu^2)_1 + \frac{1}{\Lambda^4}(\varphi_S^0 \Psi_l^4 \Psi_\nu^2)_1. \quad (5.33)$$

where  $\Psi_\nu = \{\xi, \eta, \varphi_S\}$ ,  $\Psi_l = \{\phi, \varphi_T\}$  and the couplings in front of each operators are omitted. Notice that there are generally several independent  $S_4$  contractions for each operator. The new VEV configuration is obtained by imposing the vanishing of the first derivative of  $w_d + \Delta w_d$  with respect to the driving fields  $\rho^0$ ,  $\varphi_T^0$ ,  $\eta^0$  and  $\varphi_S^0$ . To the first order in the  $1/\Lambda$  expansion, it is straightforward to find that the LO vacuum in eq. (5.13) and eq. (5.20) is modified into

$$\begin{aligned} \langle \varphi_T \rangle &= (v_T, \delta v_{T_2}, \delta v_{T_3}), & \langle \phi \rangle &= (\delta v_{\phi_1}, \delta v_{\phi_2}, v_\phi + \delta v_{\phi_3}), \\ \langle \eta \rangle &= (v_\eta + \delta v_{\eta_1}, \sqrt{3}v_\eta + \delta v_{\eta_2}), & \langle \varphi_S \rangle &= (v_S + \delta v_{S_1}, \sqrt{2}v_S + \delta v_{S_2}, v_S + \delta v_{S_3}). \end{aligned} \quad (5.34)$$

Note that all components of  $\langle \varphi_T \rangle$ ,  $\langle \phi \rangle$ ,  $\langle \eta \rangle$  and  $\langle \varphi_S \rangle$  acquire different corrections so that their alignments are tilted. Moreover, Since  $\Delta w_d^l$  and  $\Delta w_d^\nu$  are suppressed by  $1/\Lambda$  and  $1/\Lambda^4$  respectively, the shifts  $\delta v_{T_2}$ ,  $\delta v_{T_3}$ ,  $\delta v_{\phi_1}$ ,  $\delta v_{\phi_2}$  and  $\delta v_{\phi_3}$  are of relative order  $\lambda^2$  with respect to the LO results, while the deviations  $\delta v_{\eta_1}$ ,  $\delta v_{\eta_2}$ ,  $\delta v_{S_1}$ ,  $\delta v_{S_2}$  and  $\delta v_{S_3}$  in the neutrino sector are of relative order  $\lambda^8$ .

In the same fashion, the subleading terms of the Yukawa superpotential  $w_\nu$  and  $w_l$ , which are invariant under the family symmetry  $S_4 \times Z_3 \times Z_4$ , are of the following form:

$$\begin{aligned} \Delta w_l &= \frac{1}{\Lambda^5} \tau^c (l \Psi_l^5)_1 h_d + \frac{1}{\Lambda^3} \mu^c (l \Psi_\nu^3)_1 h_d + \frac{1}{\Lambda^4} e^c (l \Psi_l \Psi_\nu^3)_1 h_d, \\ \Delta w_\nu &= \frac{1}{\Lambda^5} (l \nu^c \Psi_l^4 \Psi_\nu)_1 h_u + \frac{1}{\Lambda^3} (\nu^c \nu^c \Psi_l^4)_1. \end{aligned} \quad (5.35)$$

The subleading corrections to the lepton mass and mixing matrices are obtained by inserting the corrected VEV alignment into the LO operators plus the contribution of the higher dimensional Yukawa operators evaluated with the unperturbed VEVs. It is easy

to check that the neutrino mass matrix receives a relative corrections of order  $\lambda^8$ . As a result, the subleading corrections to lepton mixing of the neutrino sector are suppressed by  $\langle \Phi_l \rangle^4 / \Lambda^4 \sim \lambda^8$  with respect to LO results and thus they can be ignored. In the charged lepton sector, all non-diagonal entries become non-vanishing after the inclusion of the subleading contributions. Eventually the corrected charged lepton mass matrix has the following structure,

$$m_l \sim \begin{pmatrix} m_e & \lambda^2 m_e & \lambda^2 m_e \\ \lambda^2 m_\mu & m_\mu & \lambda^2 m_\mu \\ \lambda^2 m_\tau & \lambda^2 m_\tau & m_\tau \end{pmatrix}. \quad (5.36)$$

We can estimate the higher order corrections to the LO predictions for the lepton mixing angles in eq. (5.5) as follows,

$$\delta \sin^2 \theta_{13} \sim \lambda^2, \quad \delta \sin^2 \theta_{12} \sim \lambda^2, \quad \delta \sin^2 \theta_{23} \sim \lambda^2. \quad (5.37)$$

Therefore the LO relation  $4 \cos^2 \theta_{13} \sin^2 \theta_{12} = 1$  is violated by small terms of order  $\lambda^2$  when the subleading contributions are included. As a consequence, the observed value of  $\theta_{12}$  can be achieved although a value of  $\theta_{12}$  close to the present  $3\sigma$  upper bound would be unnatural in our model.

## 6 Model predicting one row of BM mixing with $S_4$ and generalized CP

In this section, we shall present an explicit model realization for the mixing pattern investigated in section 4. The model is also based on  $S_4$  family symmetry and generalized CP, which is supplemented by  $Z_5 \times Z_6$ . The flavon fields and driving fields are properly arranged such that  $S_4 \rtimes H_{\text{CP}}$  is broken to  $K_4^{(TST^2, T^2U)} \times H_{\text{CP}}^\nu$  with  $H_{\text{CP}}^\nu = \{\rho_{\mathbf{r}}(1), \rho_{\mathbf{r}}(T^2U), \rho_{\mathbf{r}}(TST^2), \rho_{\mathbf{r}}(ST^2SU)\}$  in the neutrino sector at leading order, and the flavor symmetry preserved by the charged lepton mass matrix  $m_l^\dagger m_l$  is  $K_4^{(S,U)}$ . As a result, the lepton flavor mixing is predicted to be of the BM form at leading order. Furthermore, the next-to-leading-order (NLO) corrections break the remnant symmetry down to  $Z_2^{SU} \times H_{\text{CP}}^l$  in the charged lepton sector. Consequently the resulting PMNS matrix has one row of the form  $(1/2, 1/2, 1/\sqrt{2})$  which is exactly the third row of the BM mixing pattern, and agreement with experimental data can be achieved. As we shall show below, the general model independent results of section 4 can be naturally reproduced in this model. The involved fields and their transformation rules under the family symmetry are summarized in table 3. We start to explore the vacuum structure of the model in the following section.

### 6.1 Vacuum alignment

The most general flavon superpotential invariant under the symmetry of the model is

$$\begin{aligned} w_d = & M_\xi \xi^0 \xi + f_1 \xi^0 (\varphi_T \varphi_T)_{\mathbf{1}} + f_2 \rho^0 \xi^2 + f_3 \rho^0 (\eta \eta)_{\mathbf{1}} + f_4 \zeta^0 (\varphi_T \phi)_{\mathbf{1}'} + f_5 \xi (\eta^0 \eta)_{\mathbf{1}} \\ & + f_6 (\eta^0 (\varphi_T \phi)_{\mathbf{2}})_{\mathbf{1}} + f_7 (\varphi_T^0 (\varphi_T \phi)_{\mathbf{3}})_{\mathbf{1}} + M_\kappa^2 \kappa^0 + f_8 \kappa^0 (\phi \phi)_{\mathbf{1}} + g_1 \rho (\sigma^0 \sigma)_{\mathbf{1}} + g_2 (\sigma^0 (\sigma \sigma)_{\mathbf{2}})_{\mathbf{1}} \\ & + g_3 (\sigma^0 (\varphi_S \varphi_S)_{\mathbf{2}})_{\mathbf{1}} + g_4 \rho (\varphi_S^0 \varphi_S)_{\mathbf{1}} + g_5 (\varphi_S^0 (\sigma \varphi_S)_{\mathbf{3}'})_{\mathbf{1}} + g_6 (\varphi_S^0 (\varphi_S \varphi_S)_{\mathbf{3}'} )_{\mathbf{1}}, \end{aligned} \quad (6.1)$$

Field	$l$	$\nu^c$	$e^c$	$\mu^c$	$\tau^c$	$h_{u,d}$	$\xi$	$\eta$	$\varphi_T$	$\phi$	$\rho$	$\sigma$	$\varphi_S$	$\xi^0$	$\rho^0$	$\zeta^0$	$\eta^0$	$\varphi_T^0$	$\kappa^0$	$\sigma^0$	$\varphi_S^0$
$S_4$	<b>3</b>	<b>3</b>	<b>1'</b>	<b>1'</b>	<b>1</b>	<b>1</b>	<b>1</b>	<b>2</b>	<b>3</b>	<b>3'</b>	<b>1</b>	<b>2</b>	<b>3'</b>	<b>1</b>	<b>1</b>	<b>1'</b>	<b>2</b>	<b>3</b>	<b>1</b>	<b>2</b>	<b>3'</b>
$Z_5$	$\omega_5^3$	$\omega_5^2$	$\omega_5^2$	$\omega_5^2$	$\omega_5^2$	1	1	1	1	1	$\omega_5$	$\omega_5$	$\omega_5$	1	1	1	1	1	1	$\omega_5^3$	$\omega_5^3$
$Z_6$	1	1	$\omega_6^4$	$\omega_6^5$	$\omega_6^4$	1	$\omega_6^4$	$\omega_6$	$\omega_6^2$	$\omega_6^3$	1	1	1	$\omega_6^2$	$\omega_6^4$	$\omega_6$	$\omega_6$	$\omega_6$	1	1	1
$U(1)_R$	1	1	1	1	1	0	0	0	0	0	0	0	0	2	2	2	2	2	2	2	2

**Table 3.** The particle contents and their transformation properties under the family symmetry  $S_4 \times Z_5 \times Z_6$  and  $U(1)_R$ , where  $\omega_5 = e^{2i\pi/5}$  and  $\omega_6 = e^{2i\pi/6}$ .

where all couplings  $f_i$  and  $g_i$  are real due to the imposed generalized CP symmetry. In the charged lepton sector, the equations for the vanishing of the derivatives of  $w_d$  with respect to each component of the driving fields are as follows:

$$\begin{aligned}
 \frac{\partial w_d}{\partial \xi^0} &= M_\xi \xi + f_1(2\varphi_{T_1}\varphi_{T_3} + \varphi_{T_2}^2) = 0, \\
 \frac{\partial w_d}{\partial \rho^0} &= f_2\xi^2 + f_3(\eta_1^2 + \eta_2^2) = 0, \\
 \frac{\partial w_d}{\partial \zeta^0} &= f_4(\varphi_{T_1}\phi_3 + \varphi_{T_2}\phi_2 + \varphi_{T_3}\phi_1) = 0, \\
 \frac{\partial w_d}{\partial \eta_1^0} &= f_5\xi\eta_1 + \sqrt{3}f_6(\varphi_{T_1}\phi_1 + \varphi_{T_3}\phi_3) = 0, \\
 \frac{\partial w_d}{\partial \eta_2^0} &= f_5\xi\eta_2 + f_6(\varphi_{T_1}\phi_3 - 2\varphi_{T_2}\phi_2 + \varphi_{T_3}\phi_1) = 0, \\
 \frac{\partial w_d}{\partial \varphi_{T_1}^0} &= f_7(\varphi_{T_1}\phi_2 + \varphi_{T_2}\phi_1) = 0, \\
 \frac{\partial w_d}{\partial \varphi_{T_2}^0} &= f_7(\varphi_{T_1}\phi_1 - \varphi_{T_3}\phi_3) = 0, \\
 \frac{\partial w_d}{\partial \varphi_{T_3}^0} &= -f_7(\varphi_{T_2}\phi_3 + \varphi_{T_3}\phi_2) = 0, \\
 \frac{\partial \omega_d^l}{\partial \kappa^0} &= M_\kappa^2 + f_8(2\phi_1\phi_3 + \phi_2^2) = 0.
 \end{aligned} \tag{6.2}$$

By straightforward calculations, we find a unique alignment (up to  $S_4$  transformations):

$$\langle \xi \rangle = v_\xi, \quad \langle \eta \rangle = \begin{pmatrix} 1 \\ 0 \end{pmatrix} v_\eta, \quad \langle \varphi_T \rangle = \begin{pmatrix} 1+i \\ 0 \\ i-1 \end{pmatrix} v_T, \quad \langle \phi \rangle = \begin{pmatrix} i-1 \\ 0 \\ 1+i \end{pmatrix} v_\phi, \tag{6.3}$$

where the VEVs  $v_\xi$ ,  $v_\eta$ ,  $v_T$  and  $v_\phi$  are related by

$$v_\eta^2 = -\frac{f_2}{f_3}v_\xi^2, \quad v_T^2 = \frac{M_\xi v_\xi}{4f_1}, \quad v_\phi = \frac{f_5 v_\xi v_\eta}{4\sqrt{3}f_6 v_T}, \tag{6.4}$$

with

$$v_\xi^3 = -\frac{3f_3 f_6^2 M_\xi M_\kappa^2}{f_1 f_2 f_5^2 f_8}. \tag{6.5}$$



Hence the VEV  $v_\xi$  is fixed to be

$$v_\xi = - \left( \frac{3f_3 f_6^2 M_\xi M_\kappa^2}{f_1 f_2 f_5^2 f_8} \right)^{1/3}, \quad \left( \frac{3f_3 f_6^2 M_\xi M_\kappa^2}{f_1 f_2 f_5^2 f_8} \right)^{1/3} e^{i\pi/3}, \quad \text{or} \quad \left( \frac{3f_3 f_6^2 M_\xi M_\kappa^2}{f_1 f_2 f_5^2 f_8} \right)^{1/3} e^{5i\pi/3}. \quad (6.6)$$

In the present paper, we shall concentrate on the first solution, i.e. real  $v_\xi$ . The other two options of complex  $v_\xi$  would not be considered. Similar to previous cases, the soft supersymmetry breaking terms for the flavons  $\xi$ ,  $\eta$ ,  $\varphi_T$  and  $\phi$ , which are compatible with the imposed symmetry, are of the following form:

$$\begin{aligned} \mathcal{L}_{\text{soft}} = & m_\xi^2 |\xi|^2 + m_\eta^2 |\eta|^2 + m_{\varphi_T}^2 |\varphi_T|^2 + m_\phi^2 |\phi|^2 + \tilde{m}_\phi^2 (\phi\phi)_1 \\ & + \lambda_1 \xi (\eta\eta)_1 + \lambda_2 (\eta (\varphi_T \phi)_2)_1 + \lambda_3 \xi^3 + h.c., \end{aligned} \quad (6.7)$$

where the terms in the second line are the so-called trilinear terms. We expect that these soft breaking terms could discriminate the real  $v_\xi$  solution as the lowest minimum of the scalar potential. Accordingly the VEVs  $v_\eta$ ,  $v_T$  and  $v_\phi$  would be real or pure imaginary. If  $v_\eta$ ,  $v_T$  and  $v_\phi$  are all real parameters, this can be achieved for  $f_2 f_3 < 0$  and  $f_1 M_\xi v_\xi > 0$ , the residual CP symmetry preserved by the vacuum of eq. (6.3) is  $H_{\text{CP}}^l = \{\rho_{\mathbf{r}}(TST^2), \rho_{\mathbf{r}}(TST^2U)\}$ . If  $v_\eta$  is real and  $v_T$ ,  $v_\phi$  are pure imaginary, this can be realized for  $f_2 f_3 < 0$  and  $f_1 M_\xi v_\xi < 0$ , another two of the 24 generalized CP symmetries are preserved with  $H_{\text{CP}}^l = \{\rho_{\mathbf{r}}(T^2ST), \rho_{\mathbf{r}}(T^2STU)\}$ . On the other hand, the generalized CP symmetry  $H_{\text{CP}}^l$  will be completely broken for imaginary  $v_\eta$  no matter  $v_T$ ,  $v_\phi$  are real or imaginary. It is easy to check that the determined vacuum in eq. (6.3) breaks  $S_4$  family symmetry to  $Z_2^{SU}$  subgroup. Furthermore, since the different VEVs are related via dimensionless couplings in eq. (6.4), these VEVs are expected to have the same order of magnitude which we choose to be  $\lambda^2 \Lambda$ .

In the neutrino sector, the vacuum is determined by  $F$ -term conditions associated with the driving fields  $\sigma^0$  and  $\varphi_S^0$ ,

$$\begin{aligned} \frac{\partial w_d}{\partial \sigma_1^0} &= g_1 \rho \sigma_1 + g_2 (\sigma_2^2 - \sigma_1^2) + 2g_3 (\varphi_{S_2}^2 - \varphi_{S_1} \varphi_{S_3}) = 0, \\ \frac{\partial w_d}{\partial \sigma_2^0} &= g_1 \rho \sigma_2 + 2g_2 \sigma_1 \sigma_2 + \sqrt{3} g_3 (\varphi_{S_1}^2 + \varphi_{S_3}^2) = 0, \\ \frac{\partial w_d}{\partial \varphi_{S_1}^0} &= g_4 \rho \varphi_{S_3} + g_5 (\sqrt{3} \sigma_2 \varphi_{S_1} - \sigma_1 \varphi_{S_3}) + 2g_6 \varphi_{S_1} \varphi_{S_2} = 0, \\ \frac{\partial w_d}{\partial \varphi_{S_2}^0} &= g_4 \rho \varphi_{S_2} + 2g_5 \sigma_1 \varphi_{S_2} + g_6 (\varphi_{S_1}^2 - \varphi_{S_3}^2) = 0, \\ \frac{\partial w_d}{\partial \varphi_{S_3}^0} &= g_4 \rho \varphi_{S_1} + g_5 (\sqrt{3} \sigma_2 \varphi_{S_3} - \sigma_1 \varphi_{S_1}) - 2g_6 \varphi_{S_2} \varphi_{S_3} = 0. \end{aligned} \quad (6.8)$$

We find two classes of solutions for the vacuum: the first class comprises the vacua with vanishing VEV of one of  $\rho$ ,  $\sigma$  and  $\varphi_S$ , this type of solutions can be eliminated by adding soft breaking mass terms for the scalar fields with  $m_{\rho, \sigma, \varphi_S}^2 < 0$ , and all flavons acquire

non-zero VEVs for the second class with

$$\langle \rho \rangle = v_\rho, \quad \langle \sigma \rangle = \begin{pmatrix} 1 \\ \sqrt{3} \end{pmatrix} v_\sigma, \quad \langle \varphi_S \rangle = \begin{pmatrix} 1 \\ 0 \\ -1 \end{pmatrix} v_S, \quad (6.9)$$

where the VEVs obey the relations

$$v_\sigma = \frac{g_4 v_\rho}{4g_5}, \quad v_S = \frac{v_\rho}{4g_5} \sqrt{-\frac{g_4(2g_1g_5 + g_2g_4)}{g_3}}, \quad (6.10)$$

with  $v_\rho$  undetermined. The vacuum alignment in eq. (6.9) is invariant under the action of both the  $TST^2$  and  $T^2U$  elements of  $S_4$ , consequently it breaks the  $S_4$  family symmetry to Klein four  $K_4^{(TST^2, T^2U)}$  subgroup. Furthermore, since all couplings  $g_i$  are real, then eq. (6.10) implies that  $v_\sigma$  and  $v_\rho$  have the same phase up to  $\pi$ , and the phase difference between  $v_\rho$  and  $v_S$  is 0,  $\pi$  or  $\pm \frac{\pi}{2}$  determined by the sign of  $g_3g_4(2g_1g_5 + g_2g_4)$ . Similar to previous model, we expect a common order of magnitude for all the VEVs which is taken to be  $\lambda^2 \Lambda$ .

## 6.2 Leading order results

The charged lepton masses are described by the following superpotential

$$w_l = \frac{y_\tau}{\Lambda} \tau^c (l\varphi_T)_1 h_d + \frac{y_\mu}{\Lambda^2} \mu^c \xi (l\phi)_1 h_d + \dots, \quad (6.11)$$

where dots represent higher dimensional operators which we will consider later. After the electroweak and flavor symmetries breaking by the VEVs shown in eq. (6.3), we obtain a charged lepton mass matrix as follows

$$m_l = \begin{pmatrix} 0 & 0 & 0 \\ \frac{(1+i)y_\mu v_\xi v_\phi}{\Lambda^2} & 0 & \frac{(i-1)y_\mu v_\xi v_\phi}{\Lambda^2} \\ \frac{(i-1)y_\tau v_T}{\Lambda} & 0 & \frac{(1+i)y_\tau v_T}{\Lambda} \end{pmatrix} v_d. \quad (6.12)$$

As a consequence the unitary matrix  $U_l$ , which corresponds to the transformation of the charged leptons used to diagonalize  $m_l^\dagger m_l$ , is of the following form:

$$U_l = \frac{1}{\sqrt{2}} \begin{pmatrix} 0 & e^{\frac{i\pi}{4}} & e^{-\frac{i\pi}{4}} \\ -\sqrt{2} & 0 & 0 \\ 0 & e^{-\frac{i\pi}{4}} & e^{\frac{i\pi}{4}} \end{pmatrix}. \quad (6.13)$$

The charged lepton masses are given by,

$$m_e^2 = 0, \quad m_\mu^2 = 4y_\mu^2 \frac{|v_\xi v_\phi|^2}{\Lambda^4} v_d^2, \quad m_\tau^2 = 4y_\tau^2 \frac{|v_T|^2}{\Lambda^2} v_d^2. \quad (6.14)$$

Note that the correct mass hierarchy between muon and tau is generated for  $v_\xi/\Lambda \sim v_T/\Lambda \sim v_\phi/\Lambda \sim \lambda^2$ . The electron is massless at LO and its mass is generated by higher

dimensional operators, which will be studied in section 6.3. From the view of symmetry and its breaking, although the VEVs of  $\xi$ ,  $\eta$ ,  $\varphi_T$  and  $\phi$  leave  $Z_2^{SU}$  invariant, the remnant flavor symmetry of  $m_l^\dagger m_l$  is  $K_4^{(S,U)}$ . In other words, we have  $\rho_3^\dagger(S)m_l^\dagger m_l \rho_3(S) = m_l^\dagger m_l$  and  $\rho_3^\dagger(U)m_l^\dagger m_l \rho_3(U) = m_l^\dagger m_l$ . The enhancement of the remnant flavor symmetry from  $Z_2^{SU}$  to  $K_4^{(S,U)}$  is because that  $|v_T|^2$  and  $|v_\phi|^2$  instead of  $v_T$  and  $v_\phi$  are involved in  $m_l^\dagger m_l$ . Moreover, it is straightforward to check that the residual CP symmetry preserved by the combination  $m_l^\dagger m_l$  is  $H_{CP}^l = \{\rho_r(TST^2), \rho_r(TST^2U), \rho_r(T^2ST), \rho_r(T^2STU)\}$ .

Now we come to the neutrino sector. The LO superpotential of for the neutrino masses is

$$w_\nu = y(\nu^c l)_1 h_u + y_1 \rho(\nu^c \nu^c)_1 + y_2 ((\nu^c \nu^c)_2 \sigma)_1 + y_3 ((\nu^c \nu^c)_3 \varphi_S)_1, \quad (6.15)$$

where the first term is Dirac mass term and the last three are Majorana mass terms. The generalized CP symmetry constrains all the couplings to be real. The flavons  $\rho$ ,  $\sigma$  and  $\varphi_S$  get VEVs shown in eq. (6.9), and then the Dirac and right-handed Majorana neutrino mass matrices read as

$$m_D = y v_u \begin{pmatrix} 0 & 0 & 1 \\ 0 & 1 & 0 \\ 1 & 0 & 0 \end{pmatrix}, \quad m_M = y_1 v_\rho \begin{pmatrix} 0 & 0 & 1 \\ 0 & 1 & 0 \\ 1 & 0 & 0 \end{pmatrix} + y_2 v_\sigma \begin{pmatrix} 3 & 0 & -1 \\ 0 & 2 & 0 \\ -1 & 0 & 3 \end{pmatrix} + y_3 v_S \begin{pmatrix} 0 & 1 & 0 \\ 1 & 0 & 1 \\ 0 & 1 & 0 \end{pmatrix}. \quad (6.16)$$

The light neutrino mass matrix is given by the seesaw relation  $m_\nu = -m_D^T m_M^{-1} m_D$ , and we find  $m_\nu$  is of the same form as that in eq. (4.5) with

$$\begin{aligned} a &= \frac{[-3y_1^2 v_\rho^2 + 2(6y_2^2 v_\sigma^2 + y_3^2 v_S^2)] y^2 v_u^2}{3(y_1 v_\rho - 4y_2 v_\sigma) [(y_1 v_\rho + 2y_2 v_\sigma)^2 - 2y_3^2 v_S^2]}, \\ b &= \frac{[3y_2 v_\sigma (y_1 v_\rho + 2y_2 v_\sigma) - y_3^2 v_S^2] y^2 v_u^2}{3(y_1 v_\rho - 4y_2 v_\sigma) [(y_1 v_\rho + 2y_2 v_\sigma)^2 - 2y_3^2 v_S^2]}, \\ c &= \frac{y_3 y^2 v_S v_u^2}{(y_1 v_\rho + 2y_2 v_\sigma)^2 - 2y_3^2 v_S^2}. \end{aligned} \quad (6.17)$$

Hence  $m_\nu$  is exactly diagonalized by the unitary transformation  $U_\nu$  shown in eq. (4.7), and the resulting mass eigenvalues are  $a + 2b - \sqrt{2}c$ ,  $a + 2b + \sqrt{2}c$  and  $-a + 4b$ . As shown in eq. (6.15), here the VEVs of  $\rho$ ,  $\sigma$  and  $\varphi_S$  breaks both  $S_4$  family symmetry and generalized CP in the neutrino sector. From the vacuum alignment of section 6.1, we know that the remnant family symmetry is  $K_4^{(TST^2, T^2U)}$ . Since the phase of  $v_\rho$  can be factored out from  $m_\nu$ ,  $v_\rho$  can be taken to be real. As a consequence,  $v_\sigma$  is real and  $v_S$  can be real or purely imaginary. Since imaginary  $v_S$  leads to a partially degenerate neutrino mass spectrum,  $v_S$  will be considered as real hereafter, and this scenario can be achieved for  $g_3 g_4 (2g_1 g_5 + g_2 g_4) < 0$ . The residual CP symmetry would be  $H_{CP}^\nu = \{\rho_r(1), \rho_r(T^2U), \rho_r(TST^2), \rho_r(ST^2SU)\}$  which has been discussed in section 4. Then all the three parameters  $a$ ,  $b$  and  $c$  are real. The phenomenological constraints of  $\delta m^2 \equiv m_2^2 - m_1^2$  and  $\Delta m^2 \equiv m_3^2 - (m_1^2 + m_2^2)/2$  can be easily satisfied by properly choosing the values of  $a$ ,  $b$  and  $c$ . Either NO or IO neutrino mass spectrum is allowed.

In the end, combining the unitary transformation  $U_l$  and  $U_\nu$  from the charged lepton and the neutrino sectors, we obtain the lepton mixing matrix

$$U_{PMNS} = U_l^\dagger U_\nu = \frac{1}{2} \begin{pmatrix} \sqrt{2} & -\sqrt{2} & 0 \\ 1 & 1 & \sqrt{2}i \\ 1 & 1 & -\sqrt{2}i \end{pmatrix}. \quad (6.18)$$

Therefore the lepton flavor mixing is the BM pattern at LO. In the following section, we shall analyze the higher order corrections needed to modify the BM mixing in order to obtain an acceptable lepton mixing pattern.

### 6.3 Next-to-leading-order corrections

In brief, at leading order the model gives rise to a vanishing electron mass ( $m_e = 0$ ) and the BM mixing pattern leading to  $\theta_{13} = 0^\circ$  and  $\theta_{12} = \theta_{23} = 45^\circ$  which obviously don't match with the experimental measurements. Therefore the next-to-leading-order (NLO) corrections are crucial to achieve agreement with the present data. We will demonstrate in the following that a non-zero electron mass and realistic mass hierarchies among the charged lepton are obtained after the NLO contributions are included. In addition, the LO remnant symmetry  $K_4^{(S,U)}$  of  $m^\dagger m_l$  is further broken down to  $Z_2^{SU}$  such that the symmetry breaking patterns discussed in section 4 are realized and the resulting PMNS matrix is of the form of eq. (4.15). We first start with the corrections to the flavon superpotential  $w_d$  in eq. (6.1) which determines the vacuum alignment. The symmetry allowed NLO terms including the driving fields  $\xi^0$ ,  $\rho^0$ ,  $\zeta^0$ ,  $\eta^0$ ,  $\varphi_T^0$  and  $\kappa^0$  are

$$\begin{aligned} \Delta w_d^l = & f_9 \xi^0 \xi(\phi\phi)_1 / \Lambda + f_{10} \rho^0 \xi(\varphi_T \varphi_T)_1 / \Lambda + f_{11} \rho^0 (\varphi_T (\phi\phi)_3)_1 / \Lambda + f_{12} \zeta^0 (\eta(\varphi_T \varphi_T)_2)_1 / \Lambda \\ & + f_{13} (\eta^0 \eta)_1 (\varphi_T \varphi_T)_1 / \Lambda + f_{14} ((\eta^0 \eta)_2 (\varphi_T \varphi_T)_2)_1 / \Lambda + f_{15} ((\varphi_T^0 \eta)_3 (\eta\phi)_3)_1 / \Lambda \\ & + f_{16} ((\varphi_T^0 \eta)_{3'} (\eta\phi)_{3'})_1 / \Lambda + f_{17} ((\varphi_T^0 \eta)_3 (\varphi_T \varphi_T)_3)_1 / \Lambda + f_{18} ((\varphi_T^0 \eta)_{3'} (\varphi_T \varphi_T)_{3'})_1 / \Lambda \\ & + f_{19} \kappa^0 \xi^3 / \Lambda + f_{20} \kappa^0 \xi(\eta\eta)_1 / \Lambda + f_{21} \kappa^0 (\eta(\varphi_T \phi)_2)_1 / \Lambda + f_{22} \kappa^0 (\varphi_T (\varphi_T \varphi_T)_3)_1 / \Lambda. \end{aligned} \quad (6.19)$$

We see that they are suppressed by one of power of  $1/\Lambda$  with respect to the LO terms in eq. (6.1). The new vacuum configuration is obtained by searching for the zeros of the  $F$ -terms of  $w_d + \Delta w_d^l$  with respect to the driving fields  $\xi^0$ ,  $\rho^0$ ,  $\zeta^0$ ,  $\eta^0$ ,  $\varphi_T^0$  and  $\kappa^0$ . To the first order in  $1/\Lambda$  expansion, the LO vacuum alignment of the charged lepton sector is modified into

$$\begin{aligned} \langle \xi \rangle &= v_\xi + \delta v_\xi, & \langle \eta \rangle &= \begin{pmatrix} v_\eta + \delta v_{\eta_1} \\ \delta v_{\eta_2} \end{pmatrix}, \\ \langle \varphi_T \rangle &= \begin{pmatrix} (1+i)(v_T + \delta v_{T_1}) \\ \delta v_{T_2} \\ (i-1)(v_T + \delta v_{T_3}) \end{pmatrix}, & \langle \phi \rangle &= \begin{pmatrix} (i-1)(v_\phi + \delta v_{\phi_1}) \\ -i\delta v_{\phi_2} \\ (1+i)(v_\phi + \delta v_{\phi_3}) \end{pmatrix}. \end{aligned} \quad (6.20)$$

The shifts  $\delta v_\xi$ ,  $\delta v_{\eta_i}$ ,  $\delta v_{T_i}$  and  $\delta v_{\phi_i}$  are solved to be

$$\delta v_\xi = X \frac{M_\xi v_\xi}{\Lambda}, \quad \delta v_{\eta_1} = \left( X - \frac{f_{10}}{2f_1 f_2} \right) \frac{M_\xi v_\eta}{\Lambda}, \quad (6.21)$$

$$\begin{aligned}\delta v_{\eta_2} = \delta v_{T_2} = 0, \quad \delta v_{T_1} = \delta v_{T_3} &= \left( X - \frac{f_9 M_\kappa^2}{2f_8 M_\xi^2} \right) \frac{M_\xi v_T}{2\Lambda}, \\ \delta v_{\phi_1} = \delta v_{\phi_3} &= \frac{3f_6 [f_2(f_6 f_{20} - f_5 f_{21}) - f_3 f_6 f_{19}]}{2f_1 f_2 f_5^2 f_8} \frac{M_\xi v_\phi}{\Lambda}, \quad \delta v_{\phi_2} = -\frac{\sqrt{3}(f_{15} + f_{16})v_\eta^2 v_\phi}{f_7 v_T \Lambda},\end{aligned}$$

where  $X$  is a real parameter of order one with

$$X = \frac{[f_2 f_5 (2f_8(f_{13} + f_{14}) - 3f_6 f_{21}) + f_5^2 f_8 f_{10} + 3f_6^2(f_2 f_{20} - f_3 f_{19})] M_\xi^2 - f_1 f_2 f_5^2 f_9 M_\kappa^2}{3f_1 f_2 f_5^2 f_8 M_\xi^2}. \quad (6.22)$$

Notice that the shifts of the vacuum are suppressed by  $\lambda^2$  compared with the LO VEVs, and the structures of the LO vacuum of the flavons  $\eta$  and  $\varphi_T$  are unchanged by the NLO corrections. Because the NLO driving superpotential  $\Delta w_d^l$  only contain the charged lepton flavon fields  $\xi$ ,  $\eta$ ,  $\varphi_T$  and  $\phi$ , hence their VEVs still preserve the  $Z_2^{SU}$  subgroup even at NLO. Indeed the vacuum in eq. (6.20) is the most general form which is compatible with the residual family symmetry  $Z_2^{SU}$  in the charged lepton sector.

In the same way, the subleading corrections to the flavon superpotential of  $\rho$ ,  $\sigma$  and  $\varphi_S$  are of the form

$$\Delta w_d^\nu = (\sigma^0 \xi \varphi_T \Psi_\nu^2)_1 / \Lambda^2 + (\sigma^0 \phi^2 \Psi_\nu^2)_1 / \Lambda^2 + (\varphi_S^0 \xi \varphi_T \Psi_\nu^2)_1 / \Lambda^2 + (\varphi_S^0 \phi^2 \Psi_\nu^2)_1 / \Lambda^2. \quad (6.23)$$

where  $\Psi_\nu = \{\rho, \sigma, \varphi_S\}$  denotes the neutrino flavon fields, and the real coupling constant in front of each term has been omitted. The resulting contributions to the  $F$ -terms of the driving fields  $\sigma^0$  and  $\varphi_S^0$  are suppressed by  $\langle \xi \rangle \langle \varphi_T \rangle / \Lambda^2 \sim \langle \phi \rangle^2 / \Lambda \sim \lambda^4$  with respect to the LO terms in eq. (6.1). Hence they induce shifts in the VEVs of  $\rho$ ,  $\sigma$  and  $\varphi_S$  at relative order  $\lambda^4$ . After some straightforward algebra, the new VEVs can be written as

$$\langle \rho \rangle = v_\rho, \quad \langle \sigma \rangle = \begin{pmatrix} 1 + \epsilon_1 \lambda^4 \\ \sqrt{3} + \epsilon_2 \lambda^4 \end{pmatrix} v_\sigma, \quad \langle \varphi_S \rangle = \begin{pmatrix} 1 + \epsilon_3 \lambda^4 \\ \epsilon_4 \lambda^4 \\ -1 + \epsilon_5 \lambda^4 \end{pmatrix} v_S, \quad (6.24)$$

where  $v_\rho$  remains undetermined, and the coefficients  $\epsilon_i (i = 1, 2, \dots, 5)$  are unspecified constants with absolute value of order one. In the following we study the subleading corrections to the LO mass matrices from both the modified vacuum and higher dimensional operators in the Yukawa superpotential  $w_l$  and  $w_\nu$ .

In the neutrino sector, the subleading operators are obtained by adding to each term of  $w_\nu$  the factor of  $\xi \varphi_T$  or  $\phi^2$  in all possible ways, i.e.

$$\Delta w_\nu = (\nu^c l \xi \varphi_T)_1 h_u / \Lambda^2 + (\nu^c l \phi^2)_1 h_u / \Lambda^2 + (\nu^c \nu^c \xi \varphi_T \Psi_\nu)_1 / \Lambda^2 + (\nu^c \nu^c \phi^2 \Psi_\nu)_1 / \Lambda^2. \quad (6.25)$$

In addition to these corrections, we have to consider the ones from  $w_\nu$  in eq. (6.15) with the deviations of the VEVs at NLO, as shown in eq. (6.24). Eventually we find that the neutrino mass matrix is corrected by terms of relative order  $\lambda^4$  in every entry. As a result, the lepton mixing parameters acquire corrections of order  $\lambda^4$  which can be safely neglected.

The NLO operators contributing to the charged lepton masses are given by

$$\begin{aligned}
 \Delta w_l = & y_{e1} e^c \xi(l(\eta\phi)_{\mathbf{3}'} \mathbf{1})_{\mathbf{1}'} h_d / \Lambda^3 + y_{e2} e^c \xi(l(\varphi_T \varphi_T)_{\mathbf{3}'} \mathbf{1})_{\mathbf{1}'} h_d / \Lambda^3 + y_{e3} e^c ((l\varphi_T)_{\mathbf{2}} (\phi\phi)_{\mathbf{2}})_{\mathbf{1}'} h_d / \Lambda^3 \\
 & + y_{e4} e^c ((l\varphi_T)_{\mathbf{3}} (\phi\phi)_{\mathbf{3}'} \mathbf{1})_{\mathbf{1}'} h_d / \Lambda^3 + y_{e5} e^c ((l\varphi_T)_{\mathbf{3}'} (\phi\phi)_{\mathbf{3}} \mathbf{1})_{\mathbf{1}'} h_d / \Lambda^3 + y_{\mu 1} \mu^c \xi(l(\eta\varphi_T)_{\mathbf{3}'} \mathbf{1})_{\mathbf{1}'} h_d / \Lambda^3 \\
 & + y_{\mu 2} \mu^c ((l\eta)_{\mathbf{3}} (\phi\phi)_{\mathbf{3}'} \mathbf{1})_{\mathbf{1}'} h_d / \Lambda^3 + y_{\mu 3} \mu^c ((l\eta)_{\mathbf{3}'} (\phi\phi)_{\mathbf{3}} \mathbf{1})_{\mathbf{1}'} h_d / \Lambda^3 + y_{\mu 4} \mu^c (l\phi)_{\mathbf{1}'} (\varphi_T \varphi_T)_{\mathbf{1}} h_d / \Lambda^3 \\
 & + y_{\mu 5} \mu^c ((l\phi)_{\mathbf{2}} (\varphi_T \varphi_T)_{\mathbf{2}})_{\mathbf{1}'} h_d / \Lambda^3 + y_{\mu 6} \mu^c ((l\phi)_{\mathbf{3}} (\varphi_T \varphi_T)_{\mathbf{3}'} \mathbf{1})_{\mathbf{1}'} h_d / \Lambda^3 \\
 & + y_{\mu 7} \mu^c ((l\phi)_{\mathbf{3}'} (\varphi_T \varphi_T)_{\mathbf{3}} \mathbf{1})_{\mathbf{1}'} h_d / \Lambda^3 + y_{\tau 1} \tau^c \xi(l(\eta\phi)_{\mathbf{3}} \mathbf{1})_{\mathbf{1}'} h_d / \Lambda^3 + y_{\tau 2} \tau^c \xi(l(\varphi_T \varphi_T)_{\mathbf{3}} \mathbf{1})_{\mathbf{1}'} h_d / \Lambda^3 \\
 & + y_{\tau 3} \tau^c (l\varphi_T)_{\mathbf{1}} (\phi\phi)_{\mathbf{1}} h_d / \Lambda^3 + y_{\tau 4} \tau^c ((l\varphi_T)_{\mathbf{2}} (\phi\phi)_{\mathbf{2}})_{\mathbf{1}} h_d / \Lambda^3 \\
 & + y_{\tau 5} \tau^c ((l\varphi_T)_{\mathbf{3}} (\phi\phi)_{\mathbf{3}} \mathbf{1})_{\mathbf{1}} h_d / \Lambda^3 + y_{\tau 6} \tau^c ((l\varphi_T)_{\mathbf{3}'} (\phi\phi)_{\mathbf{3}'} \mathbf{1})_{\mathbf{1}} h_d / \Lambda^3.
 \end{aligned} \tag{6.26}$$

The charged lepton mass matrix is obtained by inserting the shifted vacuum alignment of eq. (6.20) into the LO operators plus the contribution of these higher dimensional operators evaluated with the LO VEVs of eq. (6.3). We find that the charged lepton mass matrix including NLO corrections takes the following form

$$m_l = \begin{pmatrix} -(1+i)a_1 v_T v_\phi^2 / \Lambda^3 & 4iy_{e2} v_\xi v_T^2 / \Lambda^3 & (1-i)a_1 v_T v_\phi^2 / \Lambda^3 \\ (1+i)y_\mu v_\xi v_\phi / \Lambda^2 & -ib_1 v_\xi v_\phi v_\eta^2 / (\Lambda^3 v_T) & (i-1)y_\mu v_\xi v_\phi / \Lambda^2 \\ (i-1)y_\tau v_T / \Lambda & 0 & (1+i)y_\tau v_T / \Lambda \end{pmatrix} v_d, \tag{6.27}$$

where  $y_\mu$  and  $y_\tau$  have been redefined to absorb the NLO contributions, and both  $a_1$  and  $b_1$  are real parameters with

$$\begin{aligned}
 a_1 &= 4(\sqrt{3}y_{e3} + y_{e4}) + y_{e1} \frac{v_\xi v_\eta}{v_T v_\phi} = 4(\sqrt{3}y_{e3} + y_{e4}) + 4\sqrt{3}y_{e1} \frac{f_6}{f_5}, \\
 b_1 &= \frac{v_T}{v_\xi v_\phi v_\eta^2} (y_\mu v_\xi \delta v_{\phi 2} \Lambda + 8y_{\mu 2} v_\eta v_\phi^2) = \frac{2y_{\mu 2} f_5}{\sqrt{3}f_6} - \frac{\sqrt{3}y_\mu (f_{15} + f_{16})}{f_7}.
 \end{aligned} \tag{6.28}$$

In order to diagonalize the charged lepton mass matrix  $m_l^\dagger m_l$ , it is helpful to apply the LO unitary transformation  $U_l$  in eq. (6.13) firstly, i.e.

$$U_l^\dagger m_l^\dagger m_l U_l = \begin{pmatrix} 16y_{e2}^2 \frac{|v_\xi|^2 |v_T|^4}{\Lambda^6} + b_1^2 \frac{|v_\xi|^2 |v_\phi|^2 |v_\eta|^4}{|v_T|^2 \Lambda^6} & 2b_1 y_\mu \frac{|v_\xi|^2 |v_\phi|^2 v_\eta^{*2}}{v_T \Lambda^5} + \mathcal{O}(\lambda^{12}) & 0 \\ 2b_1 y_\mu \frac{|v_\xi|^2 |v_\phi|^2 v_\eta^2}{v_T \Lambda^5} + \mathcal{O}(\lambda^{12}) & 4y_\mu^2 \frac{|v_\xi|^2 |v_\phi|^2}{\Lambda^4} + \mathcal{O}(\lambda^{12}) & 0 \\ 0 & 0 & 4y_\tau^2 \frac{|v_T|^2}{\Lambda^2} \end{pmatrix} v_d^2, \tag{6.29}$$

which can be easily diagonalized by a rotation in the (1, 2) sector. From eq. (6.4) and eq. (6.6), we see that  $v_\eta^2$  is real since  $v_\xi$  is chosen to be real, while the VEV  $v_T$  can be real or pure imaginary depending on the sign of the product  $f_2 f_3 f_8$ . In case of  $f_2 f_3 f_8 < 0$ ,  $v_T$  is real. The combination  $m_l^\dagger m_l$  is invariant under  $Z_2^{SU} \times H_{\text{CP}}^l$  with  $H_{\text{CP}}^l = \{\rho_{\mathbf{r}}(TST^2), \rho_{\mathbf{r}}(TST^2 U)\}$ . As a consequence, the scenario analyzed in section 4 is realized. Then the lepton mixing matrix is of the form

$$U_{PMNS} = \frac{1}{2} \begin{pmatrix} \sin \theta + \sqrt{2} \cos \theta & \sin \theta - \sqrt{2} \cos \theta & i\sqrt{2} \sin \theta \\ \cos \theta - \sqrt{2} \sin \theta & \cos \theta + \sqrt{2} \sin \theta & i\sqrt{2} \cos \theta \\ 1 & 1 & -i\sqrt{2} \end{pmatrix}, \tag{6.30}$$

where the parameter  $\theta$  is

$$\tan 2\theta \simeq -\frac{b_1}{y_\mu} \frac{v_\eta^2}{v_T \Lambda}. \quad (6.31)$$

The predictions for lepton mixing parameters are given in eq. (4.16). In this case both Dirac CP phase and Majorana CP phases are trivial, and very good agreement with the experimental data can be achieved for appropriate values of the parameter  $\theta$ , as shown in eq. (4.18) and eq. (4.19). In order to achieve the correct size of  $\theta \sim \lambda$ , an accidental enhancement of the combination  $\frac{b_1}{y_\mu} = \frac{2y_{\mu 2}f_5}{\sqrt{3}y_\mu f_6} - \frac{\sqrt{3}(f_{15}+f_{16})}{f_7}$  of order  $1/\lambda$  is required. If the two terms  $\frac{2y_{\mu 2}f_5}{\sqrt{3}y_\mu f_6}$  and  $\frac{\sqrt{3}(f_{15}+f_{16})}{f_7}$  are of opposite sign, then the two factors sum up and the required values can be easily explained. The charged lepton masses are determined to be

$$m_e \simeq 4 \left| y_{e2} \frac{v_\xi v_T^2}{\Lambda^3} \right| v_d, \quad m_\mu \simeq 2 \left| y_\mu \frac{v_\xi v_\phi}{\Lambda^2} \right| v_d, \quad m_\tau \simeq 2 \left| y_\tau \frac{v_T}{\Lambda} \right| v_d. \quad (6.32)$$

The electron mass is generated at NLO level, and realistic charged lepton mass hierarchy  $m_e : m_\mu : m_\tau \simeq \lambda^4 : \lambda^2 : 1$  is produced.

For the mixing pattern shown in eq. (6.30), the atmospheric mixing angle  $\theta_{23}$  fulfills

$$\sin^2 \theta_{23} = \frac{1 + \cos 2\theta}{3 + \cos 2\theta} = \frac{1}{1 + \sec^2 \theta} \leq \frac{1}{2}. \quad (6.33)$$

As a result,  $\theta_{23}$  deviates from maximal mixing and it lies in the first octant in this model.

Since the octant of  $\theta_{23}$  is not known so far, we would like to minimally modify this model to accommodate the situation of  $\theta_{23} > 45^\circ$ . The family symmetry is still  $S_4 \times Z_5 \times Z_6$ . For the assignment of the fields, only the right-handed charged leptons  $\mu^c$  and  $\tau^c$  are changed to be in  $(\mathbf{1}, \omega_5^2, \omega_6^3)$  and  $(\mathbf{1}', \omega_5^2, \omega_6^3)$  under  $S_4 \times Z_5 \times Z_6$ . Because both flavon fields and driving fields are kept intact, the vacuum is unchanged. Then the LO vacuum configuration is still given in eqs. (6.3) and (6.9), and the NLO VEVs are given by eqs. (6.20) and (6.24). After including the subleading contributions in the same manner described in previous paragraphs, we find that the PMNS matrix is related to the corresponding one of previous model by exchanging its second and third rows. As a consequence, the atmospheric angle  $\theta_{23}$  is in the second octant.

## 7 Summary and conclusions

Although the BM mixing pattern has already been ruled out by experiment data, the scheme of keeping one column or one row of BM mixing is viable. We perform a comprehensive analysis of how to naturally realize this scheme from  $S_4$  family symmetry and generalized CP symmetry in this paper. Furthermore, two models with  $S_4$  family symmetry and generalized CP are constructed to implement the model independent results enforced by remnant symmetry.

We firstly study the deviation from BM mixing which originates from a rotation between two generations of neutrinos or charged leptons. The phenomenological predictions for the lepton mixing angles and Dirac CP phase are discussed in detail. In this approach, all mixing parameters depend on two real parameters  $\theta$  and  $\delta$  while the Majorana CP



phases are indeterminate. For an additional rotation of 1-2 or 1-3 generations of charged leptons in the BM basis, good agreement with experiment data can be achieved, and the Dirac CP phase  $\delta_{\text{CP}}$  is constrained to be in the range of  $\pm [2.52, \pi]$  or  $[-0.62, 0.62]$  respectively, after the present  $3\sigma$  bounds of mixing angles from global data analysis are taken into account. For rotations in the neutrino sector, the measured values of the lepton mixing angles can not be accommodated. With the help of independent permutations of rows and columns of the PMNS matrix, interesting mixing patterns shown in eq. (3.15) is found. The Dirac CP phase is in the range of  $\pm [2.04, \pi]$  or  $[-1.10, 1.10]$ . Note that  $\delta_{\text{CP}}$  can vary within a quite wide range.

Since the BM mixing can be derived if we impose  $S_4$  family symmetry and spontaneously break it down to  $G_\nu = K_4^{(TST^2, T^2U)}$  in the neutrino sector and to  $G_l = Z_4^{TST^2U}$  or  $G_l = K_4^{(S,U)}$  in the charged lepton sector. It is easy to see that one column of the BM matrix would be retained if we degrade  $G_\nu$  from  $K_4$  to  $Z_2$  subgroup, and one row of the BM mixing would be preserved once  $G_l$  is degraded from  $K_4$  (or  $Z_4$ ) to  $Z_2$ . In order to have definite predictions for the leptonic CP violating phases, we extend the  $S_4$  family symmetry to include generalized CP symmetry. The phenomenological implications of the symmetry breaking of  $S_4 \rtimes H_{\text{CP}}$  into  $Z_2^{ST^2SU} \times H_{\text{CP}}^\nu$  in the neutrino sector and  $Z_4^{TST^2U} \rtimes H_{\text{CP}}^l$  in the charged lepton sector have been discussed by Feruglio et al. [30]. The resulting PMNS matrix is found to have one column of the form  $(1/2, 1/\sqrt{2}, 1/2)^T$  up to permutation of elements, and the Dirac CP phase  $\delta_{\text{CP}}$  as well as the Majorana CP phases are predicted to be conserved to account for the measured values of the mixing angles. In this work, the predictions for  $0\nu 2\beta$  decay are studied. The effective mass  $|m_{ee}|$  is predicted to be around 0.049 eV and 0.023 eV for inverted ordering spectrum. Hence this mixing pattern can be tested by future  $0\nu 2\beta$  experiments.

It is usually assumed the remnant symmetry in the neutrino sector is  $Z_2 \times CP$  in the context of family symmetry combined with generalized CP. In this work, we also consider another situation that  $Z_2 \times CP$  is preserved in the charged lepton sector instead of in the neutrino sector. The lepton flavor mixing arising from the remnant symmetry  $K_4^{(TST^2, T^2U)} \times H_{\text{CP}}^\nu$  in the neutrino sector and  $Z_2^{SU} \times H_{\text{CP}}^l$  in the charged lepton sector is explored in a model independent way. One row of PMNS matrix is determined to be  $(1/2, 1/2, -i/\sqrt{2})$ , and both Dirac CP and Majorana CP are fully conserved as well to fit the data on mixing angles. In this case, The effective mass  $|m_{ee}|$  is determined to be around the  $3\sigma$  upper or lower limit for inverted hierarchy. This prediction can also be tested by future  $0\nu 2\beta$  experiments. Furthermore, our above prediction for  $\delta_{\text{CP}}$  can be directly tested by forthcoming long baseline neutrino oscillation experiments LBNE, LBNO and Hyper-Kamiokande. If signal of leptonic CP violation is discovered, our proposal would be ruled out.

Inspired by the above fascinating results, we construct a model based on  $S_4 \rtimes H_{\text{CP}}$  which is spontaneously broken down to  $Z_2^{ST^2SU} \times H_{\text{CP}}^\nu$  in the neutrino sector and  $Z_4^{TST^2U} \rtimes H_{\text{CP}}^l$  in the charged lepton sector by the VEVs of flavons. The PMNS matrix is really found to be of the form predicted in ref. [30]. At leading order, the light neutrino mass matrix effectively contains only three real parameters which can be fixed by the measured values of the mass-squared difference  $\delta m^2 \equiv m_2^2 - m_1^2$  and  $\Delta m^2 \equiv m_3^2 - (m_1^2 + m_2^2)/2$  and the reactor

angle  $\theta_{13}$ . As a consequence, the light neutrino masses are completely determined. The predictions for the effective mass  $|m_{ee}|$  are safely below the present upper limit, and yet they are within the future sensitivity of planned neutrinoless double-beta decay experiments. Although  $\theta_{12}$  is slightly smaller than its  $3\sigma$  lower bound at leading order, agreement with experimental data can be achieved after subleading corrections are included.

Moreover, we present another model and its variant where the BM mixing is realized at LO. After the NLO corrections are included, the charged lepton mass hierarchy is obtained and the BM mixing is corrected by the effect of charged lepton diagonalization. One row of PMNS matrix is determined to be  $(1/2, 1/2, -i/\sqrt{2})$ , and all the general model independent predictions for lepton flavor mixing in section 4 are naturally reproduced. The Dirac CP phase  $\delta_{CP}$  is trivial 0 or  $\pi$  for  $f_2 f_3 f_8 < 0$ .

In the past years, family symmetry and generalized CP symmetry has been shown to be a very powerful and promising framework to predict lepton mixing angles and CP violating phases. It is intriguing to extend this approach to the quark sector to understand the established CP violation at  $B$ -factory and strong CP problem.

## Acknowledgments

This work is supported by the National Natural Science Foundation of China under Grant Nos. 11275188 and 11179007.

## A Group theory of $S_4$ and Clebsch-Gordan coefficients

$S_4$  is a symmetric group of degree four, and it is a good candidate for a family symmetry to realize the tri-bimaximal and BM mixing. Hence  $S_4$  has been widely studied in the literature. For the sake of being self-contained, in the following we shall present our convention for the  $S_4$  group, the working basis and the associated Clebsch-Gordan coefficients.  $S_4$  group can be generated by three generators  $S$ ,  $T$  and  $U$  obeying the relations [44]

$$S^2 = T^3 = U^2 = (ST)^3 = (SU)^2 = (TU)^2 = (STU)^4 = 1. \quad (\text{A.1})$$

Note that the chosen generators  $\tilde{S}$  and  $\tilde{T}$  of ref. [63] are related to our generators  $S$ ,  $T$  and  $U$  via  $\tilde{S} = ST^2SU$  and  $\tilde{T} = T^2STU$  or vice versa  $S = \tilde{T}^2$ ,  $T = \tilde{T}\tilde{S}$ ,  $U = \tilde{S}\tilde{T}^2\tilde{S}\tilde{T}$ . It is straightforward to check that the multiplication rules  $\tilde{T}^4 = \tilde{S}^2 = (\tilde{S}\tilde{T})^3 = (\tilde{T}\tilde{S})^3 = 1$  are satisfied. The 24 group elements can be divided into the five conjugacy classes as follows:

$$\begin{aligned} 1C_1 &= \{1\}, \\ 3C_2 &= \{S, TST^2, T^2ST\}, \\ 6C_2' &= \{U, TU, SU, T^2U, STSU, ST^2SU\}, \\ 8C_3 &= \{T, ST, TS, STS, T^2, ST^2, T^2S, ST^2S\}, \\ 6C_4 &= \{STU, TSU, T^2SU, ST^2U, TST^2U, T^2STU\}, \end{aligned} \quad (\text{A.2})$$

where  $kC_n$  denotes a conjugacy class with  $k$  elements and the subscript  $n$  is the order of its elements. Since the number of conjugacy class is equal to the number of irreducible

	$S$	$T$	$U$
$\mathbf{1}, \mathbf{1}'$	1	1	$\pm 1$
$\mathbf{2}$	$\begin{pmatrix} 1 & 0 \\ 0 & 1 \end{pmatrix}$	$\frac{1}{2} \begin{pmatrix} -1 & \sqrt{3} \\ -\sqrt{3} & -1 \end{pmatrix}$	$\begin{pmatrix} 1 & 0 \\ 0 & -1 \end{pmatrix}$
$\mathbf{3}, \mathbf{3}'$	$\begin{pmatrix} -1 & 0 & 0 \\ 0 & 1 & 0 \\ 0 & 0 & -1 \end{pmatrix}$	$\frac{1}{2} \begin{pmatrix} i & -\sqrt{2}i & -i \\ \sqrt{2} & 0 & \sqrt{2} \\ i & \sqrt{2}i & -i \end{pmatrix}$	$\mp \begin{pmatrix} 0 & 0 & -i \\ 0 & 1 & 0 \\ i & 0 & 0 \end{pmatrix}$

**Table 4.** The representation matrices of the generators  $S$ ,  $T$  and  $U$  for the five irreducible representations of  $S_4$  in our working basis.

representation,  $S_4$  has five irreducible representations: two singlet representations  $\mathbf{1}$  and  $\mathbf{1}'$ , one doublet representation  $\mathbf{2}$  and two triplet representations  $\mathbf{3}$  and  $\mathbf{3}'$ . Note that both  $\mathbf{3}$  and  $\mathbf{3}'$  are faithful representations of  $S_4$ . Our choice for the representation matrices of the generators  $S$ ,  $T$  and  $U$  are listed in table 4. For the three-dimensional representation  $\mathbf{3}$ , the representation matrices for the elements are as follows:

$$\begin{aligned}
 1C_1 : 1 &= \begin{pmatrix} 1 & 0 & 0 \\ 0 & 1 & 0 \\ 0 & 0 & 1 \end{pmatrix}, \\
 3C_2 : S &= \begin{pmatrix} -1 & 0 & 0 \\ 0 & 1 & 0 \\ 0 & 0 & -1 \end{pmatrix}, & TST^2 &= \begin{pmatrix} 0 & 0 & -1 \\ 0 & -1 & 0 \\ -1 & 0 & 0 \end{pmatrix}, & T^2ST &= \begin{pmatrix} 0 & 0 & 1 \\ 0 & -1 & 0 \\ 1 & 0 & 0 \end{pmatrix}, \\
 6C_2' : U &= \begin{pmatrix} 0 & 0 & i \\ 0 & -1 & 0 \\ -i & 0 & 0 \end{pmatrix}, & TU &= \frac{1}{2} \begin{pmatrix} -1 & \sqrt{2}i & -1 \\ -\sqrt{2}i & 0 & \sqrt{2}i \\ -1 & -\sqrt{2}i & -1 \end{pmatrix}, & SU &= \begin{pmatrix} 0 & 0 & -i \\ 0 & -1 & 0 \\ i & 0 & 0 \end{pmatrix}, \\
 T^2U &= \frac{1}{2} \begin{pmatrix} -1 & -\sqrt{2} & 1 \\ -\sqrt{2} & 0 & -\sqrt{2} \\ 1 & -\sqrt{2} & -1 \end{pmatrix}, & STSU &= \frac{1}{2} \begin{pmatrix} -1 & -\sqrt{2}i & -1 \\ \sqrt{2}i & 0 & -\sqrt{2}i \\ -1 & \sqrt{2}i & -1 \end{pmatrix}, \\
 ST^2SU &= \frac{1}{2} \begin{pmatrix} -1 & \sqrt{2} & 1 \\ \sqrt{2} & 0 & \sqrt{2} \\ 1 & \sqrt{2} & -1 \end{pmatrix}, \\
 8C_3 : T &= \frac{1}{2} \begin{pmatrix} i & -\sqrt{2}i & -i \\ \sqrt{2} & 0 & \sqrt{2} \\ i & \sqrt{2}i & -i \end{pmatrix}, & ST &= \frac{1}{2} \begin{pmatrix} -i & \sqrt{2}i & i \\ \sqrt{2} & 0 & \sqrt{2} \\ -i & -\sqrt{2}i & i \end{pmatrix}, & TS &= \frac{1}{2} \begin{pmatrix} -i & -\sqrt{2}i & i \\ -\sqrt{2} & 0 & -\sqrt{2} \\ -i & \sqrt{2}i & i \end{pmatrix}, \\
 STS &= \frac{1}{2} \begin{pmatrix} i & \sqrt{2}i & -i \\ -\sqrt{2} & 0 & -\sqrt{2} \\ i & -\sqrt{2}i & -i \end{pmatrix}, & T^2 &= \frac{1}{2} \begin{pmatrix} -i & \sqrt{2} & -i \\ \sqrt{2}i & 0 & -\sqrt{2}i \\ i & \sqrt{2} & i \end{pmatrix}, & ST^2 &= \frac{1}{2} \begin{pmatrix} i & -\sqrt{2} & i \\ \sqrt{2}i & 0 & -\sqrt{2}i \\ -i & -\sqrt{2} & -i \end{pmatrix},
 \end{aligned}$$

	$\chi_1$	$\chi_{1'}$	$\chi_2$	$\chi_3$	$\chi_{3'}$	Example
$1C_1$	1	1	2	3	3	1
$3C_2$	1	1	2	-1	-1	$S$
$6C'_2$	1	-1	0	-1	1	$U$
$8C_3$	1	1	-1	0	0	$T$
$6C_4$	1	-1	0	1	-1	$STU$

**Table 5.** Character table of  $S_4$ . We give an example of the elements for each class in the last column.

$$\begin{aligned}
 T^2S &= \frac{1}{2} \begin{pmatrix} i & \sqrt{2} & i \\ -\sqrt{2}i & 0 & \sqrt{2}i \\ -i & \sqrt{2} & -i \end{pmatrix}, & ST^2S &= \frac{1}{2} \begin{pmatrix} -i & -\sqrt{2} & -i \\ -\sqrt{2}i & 0 & \sqrt{2}i \\ i & -\sqrt{2} & i \end{pmatrix}, \\
 6C_4 : STU &= \frac{1}{2} \begin{pmatrix} 1 & -\sqrt{2}i & 1 \\ -\sqrt{2}i & 0 & \sqrt{2}i \\ 1 & \sqrt{2}i & 1 \end{pmatrix}, & TSU &= \frac{1}{2} \begin{pmatrix} 1 & \sqrt{2}i & 1 \\ \sqrt{2}i & 0 & -\sqrt{2}i \\ 1 & -\sqrt{2}i & 1 \end{pmatrix}, \\
 T^2SU &= \frac{1}{2} \begin{pmatrix} 1 & -\sqrt{2} & -1 \\ \sqrt{2} & 0 & \sqrt{2} \\ -1 & -\sqrt{2} & 1 \end{pmatrix}, & ST^2U &= \frac{1}{2} \begin{pmatrix} 1 & \sqrt{2} & -1 \\ -\sqrt{2} & 0 & -\sqrt{2} \\ -1 & \sqrt{2} & 1 \end{pmatrix}, & TST^2U &= \begin{pmatrix} i & 0 & 0 \\ 0 & 1 & 0 \\ 0 & 0 & -i \end{pmatrix}, \\
 T^2STU &= \begin{pmatrix} -i & 0 & 0 \\ 0 & 1 & 0 \\ 0 & 0 & i \end{pmatrix}.
 \end{aligned}$$

For the  $\mathbf{3}'$  representation, the matrices representing the elements of  $1C_1$ ,  $3C_2$  and  $8C_3$  are the same as those listed above for the representation  $\mathbf{3}$ , while they are the opposite for  $6C'_2$  and  $6C_4$ . The reason is that the generator  $U$  changes its sign in  $\mathbf{3}$  and  $\mathbf{3}'$  representations, the elements in  $1C_1$ ,  $3C_2$  and  $8C_3$  contain an even number of  $U$ , while those in  $6C'_2$  and  $6C_4$  contain an odd number of  $U$ . Character of an element is the trace of its representation matrix. The character table of  $S_4$  group can be easily obtained, as shown in table 5. The Kronecker products between various irreducible representations follow immediately:

$$\begin{aligned}
 \mathbf{1} \otimes R &= R \otimes \mathbf{1} = R, & \mathbf{1}' \otimes \mathbf{1}' &= \mathbf{1}, & \mathbf{1}' \otimes \mathbf{2} &= \mathbf{2}, & \mathbf{1}' \otimes \mathbf{3} &= \mathbf{3}', & \mathbf{1}' \otimes \mathbf{3}' &= \mathbf{3}, \\
 \mathbf{2} \otimes \mathbf{2} &= \mathbf{1} \oplus \mathbf{1}' \oplus \mathbf{2}, & \mathbf{2} \otimes \mathbf{3} &= \mathbf{2} \otimes \mathbf{3}' = \mathbf{3} \oplus \mathbf{3}', \\
 \mathbf{3} \otimes \mathbf{3} &= \mathbf{3}' \otimes \mathbf{3}' = \mathbf{1} \oplus \mathbf{2} \oplus \mathbf{3} \oplus \mathbf{3}', & \mathbf{3} \otimes \mathbf{3}' &= \mathbf{1}' \oplus \mathbf{2} \oplus \mathbf{3} \oplus \mathbf{3}'.
 \end{aligned} \tag{A.3}$$

where  $R$  denotes any  $S_4$  irreducible representation. In the following, we shall present the Clebsch-Gordan (CG) coefficients in our basis. we use  $\alpha_i$  to indicate the elements of the first representation of the product and  $\beta_i$  to indicate those of the second representation.

We first report the CG coefficients associated with the singlet representation  $\mathbf{1}'$ :

$$\begin{aligned}
 \mathbf{1}' \otimes \mathbf{1}' &= \mathbf{1} \sim \alpha\beta \\
 \mathbf{1}' \otimes \mathbf{2} &= \mathbf{2} \sim \begin{pmatrix} \alpha\beta_2 \\ -\alpha\beta_1 \end{pmatrix} \\
 \mathbf{1}' \otimes \mathbf{3} &= \mathbf{3}' \sim \begin{pmatrix} \alpha\beta_1 \\ \alpha\beta_2 \\ \alpha\beta_3 \end{pmatrix} \\
 \mathbf{1}' \otimes \mathbf{3}' &= \mathbf{3} \sim \begin{pmatrix} \alpha\beta_1 \\ \alpha\beta_2 \\ \alpha\beta_3 \end{pmatrix}
 \end{aligned} \tag{A.4}$$

The CG coefficients for the products involving the doublet representation  $\mathbf{2}$  are the following ones:

$$\begin{aligned}
 \mathbf{2} \otimes \mathbf{2} &= \mathbf{1} \oplus \mathbf{1}' \oplus \mathbf{2} & \text{with} & \begin{cases} \mathbf{1} \sim \alpha_1\beta_1 + \alpha_2\beta_2 \\ \mathbf{1}' \sim \alpha_1\beta_2 - \alpha_2\beta_1 \\ \mathbf{2} \sim \begin{pmatrix} \alpha_2\beta_2 - \alpha_1\beta_1 \\ \alpha_1\beta_2 + \alpha_2\beta_1 \end{pmatrix} \end{cases} \\
 \mathbf{2} \otimes \mathbf{3} &= \mathbf{3} \oplus \mathbf{3}' & \text{with} & \begin{cases} \mathbf{3} \sim \begin{pmatrix} \sqrt{3}\alpha_2\beta_3 - \alpha_1\beta_1 \\ 2\alpha_1\beta_2 \\ \sqrt{3}\alpha_2\beta_1 - \alpha_1\beta_3 \end{pmatrix} \\ \mathbf{3}' \sim \begin{pmatrix} \sqrt{3}\alpha_1\beta_3 + \alpha_2\beta_1 \\ -2\alpha_2\beta_2 \\ \sqrt{3}\alpha_1\beta_1 + \alpha_2\beta_3 \end{pmatrix} \end{cases} \\
 \mathbf{2} \otimes \mathbf{3}' &= \mathbf{3} \oplus \mathbf{3}' & \text{with} & \begin{cases} \mathbf{3} \sim \begin{pmatrix} \sqrt{3}\alpha_1\beta_3 + \alpha_2\beta_1 \\ -2\alpha_2\beta_2 \\ \sqrt{3}\alpha_1\beta_1 + \alpha_2\beta_3 \end{pmatrix} \\ \mathbf{3}' \sim \begin{pmatrix} \sqrt{3}\alpha_2\beta_3 - \alpha_1\beta_1 \\ 2\alpha_1\beta_2 \\ \sqrt{3}\alpha_2\beta_1 - \alpha_1\beta_3 \end{pmatrix} \end{cases}
 \end{aligned} \tag{A.5}$$

Finally the CG coefficients involving the three-dimensional representations  $\mathbf{3}$  and  $\mathbf{3}'$  are as follows:

$$\begin{aligned}
 \mathbf{3} \otimes \mathbf{3} = \mathbf{3}' \otimes \mathbf{3}' = \mathbf{1} \oplus \mathbf{2} \oplus \mathbf{3} \oplus \mathbf{3}' & \quad \text{with} \quad \left\{ \begin{array}{l} \mathbf{1} \sim \alpha_1\beta_3 + \alpha_2\beta_2 + \alpha_3\beta_1 \\ \mathbf{2} \sim \begin{pmatrix} 2\alpha_2\beta_2 - \alpha_1\beta_3 - \alpha_3\beta_1 \\ \sqrt{3}(\alpha_1\beta_1 + \alpha_3\beta_3) \end{pmatrix} \\ \mathbf{3} \sim \begin{pmatrix} \alpha_1\beta_2 - \alpha_2\beta_1 \\ \alpha_3\beta_1 - \alpha_1\beta_3 \\ \alpha_2\beta_3 - \alpha_3\beta_2 \end{pmatrix} \\ \mathbf{3}' \sim \begin{pmatrix} -\alpha_2\beta_3 - \alpha_3\beta_2 \\ \alpha_1\beta_1 - \alpha_3\beta_3 \\ \alpha_1\beta_2 + \alpha_2\beta_1 \end{pmatrix} \end{array} \right. \\
 \mathbf{3} \otimes \mathbf{3}' = \mathbf{1}' \oplus \mathbf{2} \oplus \mathbf{3} \oplus \mathbf{3}' & \quad \text{with} \quad \left\{ \begin{array}{l} \mathbf{1}' \sim \alpha_1\beta_3 + \alpha_2\beta_2 + \alpha_3\beta_1 \\ \mathbf{2} \sim \begin{pmatrix} \sqrt{3}(\alpha_1\beta_1 + \alpha_3\beta_3) \\ \alpha_1\beta_3 + \alpha_3\beta_1 - 2\alpha_2\beta_2 \end{pmatrix} \\ \mathbf{3} \sim \begin{pmatrix} -\alpha_2\beta_3 - \alpha_3\beta_2 \\ \alpha_1\beta_1 - \alpha_3\beta_3 \\ \alpha_1\beta_2 + \alpha_2\beta_1 \end{pmatrix} \\ \mathbf{3}' \sim \begin{pmatrix} \alpha_1\beta_2 - \alpha_2\beta_1 \\ \alpha_3\beta_1 - \alpha_1\beta_3 \\ \alpha_2\beta_3 - \alpha_3\beta_2 \end{pmatrix} \end{array} \right.
 \end{aligned} \tag{A.6}$$

Note that all the CG coefficients are real. The group structure of  $S_4$  has been studied comprehensively in ref. [86–90]. It has nine  $Z_2$  subgroups, four  $Z_3$  subgroups, three  $Z_4$  subgroups, four  $K_4 \cong Z_2 \times Z_2$  subgroups, four  $S_3$  subgroups, three  $D_4$  subgroups<sup>3</sup> and the alternating group  $A_4$  as a subgroup. In the present work, we focus on the Abelian subgroups as the remnant symmetry, which can be expressed in terms of the generators  $S$ ,  $T$  and  $U$  as follows:

---

<sup>3</sup>Here  $D_4$  is the symmetry group of the square, and its order is eight. Its mathematical definition is  $D_4 = \langle r, s | r^4 = s^2 = (rs)^2 = 1 \rangle$ .

- $Z_2$  subgroups

$$\begin{aligned}
 Z_2^{ST^2SU} &= \{1, ST^2SU\}, & Z_2^{TU} &= \{1, TU\}, & Z_2^{STSU} &= \{1, STSU\}, \\
 Z_2^{T^2U} &= \{1, T^2U\}, & Z_2^U &= \{1, U\}, & Z_2^{SU} &= \{1, SU\}, \\
 Z_2^S &= \{1, S\}, & Z_2^{T^2ST} &= \{1, T^2ST\}, & Z_2^{TST^2} &= \{1, TST^2\}.
 \end{aligned} \tag{A.7}$$

The former six  $Z_2$  subgroups are related to each other by group conjugation, and the latter three subgroups are conjugate to each other as well.

- $Z_3$  subgroups

$$\begin{aligned}
 Z_3^{ST} &= \{1, ST, T^2S\}, & Z_3^T &= \{1, T, T^2\}, \\
 Z_3^{STS} &= \{1, STS, ST^2S\}, & Z_3^{TS} &= \{1, TS, ST^2\}.
 \end{aligned} \tag{A.8}$$

All the above  $Z_3$  subgroups are conjugate to each other.

- $Z_4$  subgroups

$$\begin{aligned}
 Z_4^{TST^2U} &= \{1, TST^2U, S, T^2STU\}, & Z_4^{ST^2U} &= \{1, ST^2U, TST^2, T^2SU\}, \\
 Z_4^{TSU} &= \{1, TSU, T^2ST, STU\},
 \end{aligned} \tag{A.9}$$

which are related with each under group conjugation.

- $K_4$  subgroups

$$\begin{aligned}
 K_4^{(S, TST^2)} &\equiv Z_2^S \times Z_2^{TST^2} = \{1, S, TST^2, T^2ST\}, \\
 K_4^{(S, U)} &\equiv Z_2^S \times Z_2^U = \{1, S, U, SU\}, \\
 K_4^{(TST^2, T^2U)} &\equiv Z_2^{TST^2} \times Z_2^{T^2U} = \{1, TST^2, T^2U, ST^2SU\}, \\
 K_4^{(T^2ST, TU)} &\equiv Z_2^{T^2ST} \times Z_2^{TU} = \{1, T^2ST, TU, STSU\},
 \end{aligned} \tag{A.10}$$

where  $K_4^{(S, TST^2)}$  is a normal subgroup of  $S_4$ , and the other three  $K_4$  subgroups are conjugate to each other.

**Open Access.** This article is distributed under the terms of the Creative Commons Attribution License ([CC-BY 4.0](https://creativecommons.org/licenses/by/4.0/)), which permits any use, distribution and reproduction in any medium, provided the original author(s) and source are credited.

## References

- [1] T2K collaboration, K. Abe et al., *Indication of electron neutrino appearance from an accelerator-produced off-axis muon neutrino beam*, *Phys. Rev. Lett.* **107** (2011) 041801 [[arXiv:1106.2822](https://arxiv.org/abs/1106.2822)] [[INSPIRE](#)].
- [2] MINOS collaboration, P. Adamson et al., *Improved search for muon-neutrino to electron-neutrino oscillations in MINOS*, *Phys. Rev. Lett.* **107** (2011) 181802 [[arXiv:1108.0015](https://arxiv.org/abs/1108.0015)] [[INSPIRE](#)].

- [3] MINOS collaboration, P. Adamson et al., *Measurement of neutrino and antineutrino oscillations using beam and atmospheric data in MINOS*, *Phys. Rev. Lett.* **110** (2013) 251801 [[arXiv:1304.6335](#)] [[INSPIRE](#)].
- [4] DOUBLE CHOOZ collaboration, Y. Abe et al., *Indication for the disappearance of reactor electron antineutrinos in the Double CHOOZ experiment*, *Phys. Rev. Lett.* **108** (2012) 131801 [[arXiv:1112.6353](#)] [[INSPIRE](#)].
- [5] DOUBLE CHOOZ collaboration, Y. Abe et al., *Reactor electron antineutrino disappearance in the Double CHOOZ experiment*, *Phys. Rev. D* **86** (2012) 052008 [[arXiv:1207.6632](#)] [[INSPIRE](#)].
- [6] DOUBLE CHOOZ collaboration, Y. Abe et al., *Background-independent measurement of  $\theta_{13}$  in Double CHOOZ*, *Phys. Lett. B* **735** (2014) 51 [[arXiv:1401.5981](#)] [[INSPIRE](#)].
- [7] DOUBLE CHOOZ collaboration, Y. Abe et al., *Improved measurements of the neutrino mixing angle  $\theta_{13}$  with the Double CHOOZ detector*, *JHEP* **10** (2014) 086 [Erratum *ibid.* **02** (2015) 074] [[arXiv:1406.7763](#)] [[INSPIRE](#)].
- [8] DAYA BAY collaboration, F.P. An et al., *Observation of electron-antineutrino disappearance at Daya Bay*, *Phys. Rev. Lett.* **108** (2012) 171803 [[arXiv:1203.1669](#)] [[INSPIRE](#)].
- [9] DAYA BAY collaboration, F.P. An et al., *Improved measurement of electron antineutrino disappearance at Daya Bay*, *Chin. Phys. C* **37** (2013) 011001 [[arXiv:1210.6327](#)] [[INSPIRE](#)].
- [10] RENO collaboration, J.K. Ahn et al., *Observation of reactor electron antineutrino disappearance in the RENO experiment*, *Phys. Rev. Lett.* **108** (2012) 191802 [[arXiv:1204.0626](#)] [[INSPIRE](#)].
- [11] M.C. Gonzalez-Garcia, M. Maltoni, J. Salvado and T. Schwetz, *Global fit to three neutrino mixing: critical look at present precision*, *JHEP* **12** (2012) 123 [[arXiv:1209.3023](#)] [[INSPIRE](#)].
- [12] F. Capozzi, G.L. Fogli, E. Lisi, A. Marrone, D. Montanino and A. Palazzo, *Status of three-neutrino oscillation parameters, circa 2013*, *Phys. Rev. D* **89** (2014) 093018 [[arXiv:1312.2878](#)] [[INSPIRE](#)].
- [13] D.V. Forero, M. Tortola and J.W.F. Valle, *Neutrino oscillations refitted*, *Phys. Rev. D* **90** (2014) 093006 [[arXiv:1405.7540](#)] [[INSPIRE](#)].
- [14] T2K collaboration, K. Abe et al., *Observation of electron neutrino appearance in a muon neutrino beam*, *Phys. Rev. Lett.* **112** (2014) 061802 [[arXiv:1311.4750](#)] [[INSPIRE](#)].
- [15] T2K collaboration, K. Abe et al., *Precise measurement of the neutrino mixing parameter  $\theta_{23}$  from muon neutrino disappearance in an off-axis beam*, *Phys. Rev. Lett.* **112** (2014) 181801 [[arXiv:1403.1532](#)] [[INSPIRE](#)].
- [16] LBNE collaboration, C. Adams et al., *The Long-Baseline Neutrino Experiment: exploring fundamental symmetries of the universe*, [arXiv:1307.7335](#) [[INSPIRE](#)].
- [17] LBNE collaboration, M. Bass et al., *Baseline optimization for the measurement of CP-violation, mass hierarchy and  $\theta_{23}$  octant in a long-baseline neutrino oscillation experiment*, *Phys. Rev. D* **91** (2015) 052015 [[arXiv:1311.0212](#)] [[INSPIRE](#)].
- [18] D. Autiero et al., *Large underground, liquid based detectors for astro-particle physics in Europe: scientific case and prospects*, *JCAP* **11** (2007) 011 [[arXiv:0705.0116](#)] [[INSPIRE](#)].



- [19] A. Rubbia, *A CERN-based high-intensity high-energy proton source for long baseline neutrino oscillation experiments with next-generation large underground detectors for proton decay searches and neutrino physics and astrophysics*, [arXiv:1003.1921](#) [[INSPIRE](#)].
- [20] LAGUNA collaboration, D. Angus et al., *The LAGUNA design study: towards giant liquid based underground detectors for neutrino physics and astrophysics and proton decay searches*, [arXiv:1001.0077](#) [[INSPIRE](#)].
- [21] LAGUNA collaboration, A. Rubbia, *The LAGUNA design study: towards giant liquid based underground detectors for neutrino physics and astrophysics and proton decay searches*, *Acta Phys. Polon. B* **41** (2010) 1727 [[INSPIRE](#)].
- [22] LAGUNA-LBNO collaboration, S.K. Agarwalla et al., *The mass-hierarchy and CP-violation discovery reach of the LBNO long-baseline neutrino experiment*, *JHEP* **05** (2014) 094 [[arXiv:1312.6520](#)] [[INSPIRE](#)].
- [23] K. Abe et al., *Letter of intent: the Hyper-Kamiokande experiment — detector design and physics potential*, [arXiv:1109.3262](#) [[INSPIRE](#)].
- [24] HYPER-KAMIOKANDE WORKING GROUP collaboration, E. Kearns et al., *Hyper-Kamiokande physics opportunities*, [arXiv:1309.0184](#) [[INSPIRE](#)].
- [25] G. Ecker, W. Grimus and W. Konetschny, *Quark mass matrices in left-right symmetric gauge theories*, *Nucl. Phys. B* **191** (1981) 465 [[INSPIRE](#)].
- [26] G. Ecker, W. Grimus and H. Neufeld, *Spontaneous CP violation in left-right symmetric gauge theories*, *Nucl. Phys. B* **247** (1984) 70 [[INSPIRE](#)].
- [27] G. Ecker, W. Grimus and H. Neufeld, *A standard form for generalized CP transformations*, *J. Phys. A* **20** (1987) L807 [[INSPIRE](#)].
- [28] H. Neufeld, W. Grimus and G. Ecker, *Generalized CP invariance, neutral flavor conservation and the structure of the mixing matrix*, *Int. J. Mod. Phys. A* **3** (1988) 603 [[INSPIRE](#)].
- [29] W. Grimus and M.N. Rebelo, *Automorphisms in gauge theories and the definition of CP and P*, *Phys. Rept.* **281** (1997) 239 [[hep-ph/9506272](#)] [[INSPIRE](#)].
- [30] F. Feruglio, C. Hagedorn and R. Ziegler, *Lepton mixing parameters from discrete and CP symmetries*, *JHEP* **07** (2013) 027 [[arXiv:1211.5560](#)] [[INSPIRE](#)].
- [31] M. Holthausen, M. Lindner and M.A. Schmidt, *CP and discrete flavour symmetries*, *JHEP* **04** (2013) 122 [[arXiv:1211.6953](#)] [[INSPIRE](#)].
- [32] M.-C. Chen, M. Fallbacher, K.T. Mahanthappa, M. Ratz and A. Trautner, *CP violation from finite groups*, *Nucl. Phys. B* **883** (2014) 267 [[arXiv:1402.0507](#)] [[INSPIRE](#)].
- [33] P.F. Harrison and W.G. Scott, *Symmetries and generalizations of tri-bimaximal neutrino mixing*, *Phys. Lett. B* **535** (2002) 163 [[hep-ph/0203209](#)] [[INSPIRE](#)].
- [34] P.F. Harrison and W.G. Scott,  *$\mu$ - $\tau$  reflection symmetry in lepton mixing and neutrino oscillations*, *Phys. Lett. B* **547** (2002) 219 [[hep-ph/0210197](#)] [[INSPIRE](#)].
- [35] P.F. Harrison and W.G. Scott, *The simplest neutrino mass matrix*, *Phys. Lett. B* **594** (2004) 324 [[hep-ph/0403278](#)] [[INSPIRE](#)].
- [36] W. Grimus and L. Lavoura, *A nonstandard CP transformation leading to maximal atmospheric neutrino mixing*, *Phys. Lett. B* **579** (2004) 113 [[hep-ph/0305309](#)] [[INSPIRE](#)].
- [37] W. Grimus and L. Lavoura,  *$\mu$ - $\tau$  interchange symmetry and lepton mixing*, *Fortsch. Phys.* **61** (2013) 535 [[arXiv:1207.1678](#)] [[INSPIRE](#)].

- [38] P.M. Ferreira, W. Grimus, L. Lavoura and P.O. Ludl, *Maximal CP-violation in lepton mixing from a model with  $\Delta(27)$  flavour symmetry*, *JHEP* **09** (2012) 128 [[arXiv:1206.7072](#)] [[INSPIRE](#)].
- [39] Y. Farzan and A.Yu. Smirnov, *Leptonic CP-violation: zero, maximal or between the two extremes*, *JHEP* **01** (2007) 059 [[hep-ph/0610337](#)] [[INSPIRE](#)].
- [40] G.-J. Ding, S.F. King and A.J. Stuart, *Generalised CP and  $A_4$  family symmetry*, *JHEP* **12** (2013) 006 [[arXiv:1307.4212](#)] [[INSPIRE](#)].
- [41] G.-J. Ding, S.F. King, C. Luhn and A.J. Stuart, *Spontaneous CP-violation from vacuum alignment in  $S_4$  models of leptons*, *JHEP* **05** (2013) 084 [[arXiv:1303.6180](#)] [[INSPIRE](#)].
- [42] F. Feruglio, C. Hagedorn and R. Ziegler, *A realistic pattern of lepton mixing and masses from  $S_4$  and CP*, *Eur. Phys. J. C* **74** (2014) 2753 [[arXiv:1303.7178](#)] [[INSPIRE](#)].
- [43] C. Luhn, *Trimaximal  $TM_1$  neutrino mixing in  $S_4$  with spontaneous CP-violation*, *Nucl. Phys. B* **875** (2013) 80 [[arXiv:1306.2358](#)] [[INSPIRE](#)].
- [44] C.-C. Li and G.-J. Ding, *Generalised CP and trimaximal  $TM_1$  lepton mixing in  $S_4$  family symmetry*, *Nucl. Phys. B* **881** (2014) 206 [[arXiv:1312.4401](#)] [[INSPIRE](#)].
- [45] I. Girardi, A. Meroni, S.T. Petcov and M. Spinrath, *Generalised geometrical CP-violation in a  $T'$  lepton flavour model*, *JHEP* **02** (2014) 050 [[arXiv:1312.1966](#)] [[INSPIRE](#)].
- [46] G.-J. Ding and Y.-L. Zhou, *Predicting lepton flavor mixing from  $\Delta(48)$  and generalized CP symmetries*, *Chin. Phys. C* **39** (2015) 021001 [[arXiv:1312.5222](#)] [[INSPIRE](#)].
- [47] G.-J. Ding and Y.-L. Zhou, *Lepton mixing parameters from  $\Delta(48)$  family symmetry and generalised CP*, *JHEP* **06** (2014) 023 [[arXiv:1404.0592](#)] [[INSPIRE](#)].
- [48] G.-J. Ding and S.F. King, *Generalized CP and  $\Delta(96)$  family symmetry*, *Phys. Rev. D* **89** (2014) 093020 [[arXiv:1403.5846](#)] [[INSPIRE](#)].
- [49] S.F. King and T. Neder, *Lepton mixing predictions including Majorana phases from  $\Delta(6n^2)$  flavour symmetry and generalised CP*, *Phys. Lett. B* **736** (2014) 308 [[arXiv:1403.1758](#)] [[INSPIRE](#)].
- [50] C. Hagedorn, A. Meroni and E. Molinaro, *Lepton mixing from  $\Delta(3n^2)$  and  $\Delta(6n^2)$  and CP*, *Nucl. Phys. B* **891** (2015) 499 [[arXiv:1408.7118](#)] [[INSPIRE](#)].
- [51] G.-J. Ding, S.F. King and T. Neder, *Generalised CP and  $\Delta(6n^2)$  family symmetry in semi-direct models of leptons*, *JHEP* **12** (2014) 007 [[arXiv:1409.8005](#)] [[INSPIRE](#)].
- [52] G.C. Branco, J.M. Gerard and W. Grimus, *Geometrical T violation*, *Phys. Lett. B* **136** (1984) 383 [[INSPIRE](#)].
- [53] I. de Medeiros Varzielas and D. Emmanuel-Costa, *Geometrical CP-violation*, *Phys. Rev. D* **84** (2011) 117901 [[arXiv:1106.5477](#)] [[INSPIRE](#)].
- [54] I. de Medeiros Varzielas, D. Emmanuel-Costa and P. Leser, *Geometrical CP-violation from non-renormalisable scalar potentials*, *Phys. Lett. B* **716** (2012) 193 [[arXiv:1204.3633](#)] [[INSPIRE](#)].
- [55] I. de Medeiros Varzielas, *Geometrical CP-violation in multi-Higgs models*, *JHEP* **08** (2012) 055 [[arXiv:1205.3780](#)] [[INSPIRE](#)].
- [56] G. Bhattacharyya, I. de Medeiros Varzielas and P. Leser, *A common origin of fermion mixing and geometrical CP-violation and its test through Higgs physics at the LHC*, *Phys. Rev. Lett.* **109** (2012) 241603 [[arXiv:1210.0545](#)] [[INSPIRE](#)].

- [57] I.P. Ivanov and L. Lavoura, *Geometrical CP-violation in the N-Higgs-doublet model*, *Eur. Phys. J. C* **73** (2013) 2416 [[arXiv:1302.3656](#)] [[INSPIRE](#)].
- [58] I. de Medeiros Varzielas and D. Pidt, *Towards realistic models of quark masses with geometrical CP-violation*, *J. Phys. G* **41** (2014) 025004 [[arXiv:1307.0711](#)] [[INSPIRE](#)].
- [59] K.S. Babu and J. Kubo, *Dihedral families of quarks, leptons and Higgses*, *Phys. Rev. D* **71** (2005) 056006 [[hep-ph/0411226](#)] [[INSPIRE](#)].
- [60] K.S. Babu, K. Kawashima and J. Kubo, *Variations on the supersymmetric  $Q_6$  model of flavor*, *Phys. Rev. D* **83** (2011) 095008 [[arXiv:1103.1664](#)] [[INSPIRE](#)].
- [61] M.-C. Chen and K.T. Mahanthappa, *Group theoretical origin of CP-violation*, *Phys. Lett. B* **681** (2009) 444 [[arXiv:0904.1721](#)] [[INSPIRE](#)].
- [62] A. Meroni, S.T. Petcov and M. Spinrath, *A SUSY  $SU(5) \times T'$  unified model of flavour with large  $\theta_{13}$* , *Phys. Rev. D* **86** (2012) 113003 [[arXiv:1205.5241](#)] [[INSPIRE](#)].
- [63] G. Altarelli, F. Feruglio and L. Merlo, *Revisiting bimaximal neutrino mixing in a model with  $S_4$  discrete symmetry*, *JHEP* **05** (2009) 020 [[arXiv:0903.1940](#)] [[INSPIRE](#)].
- [64] D. Meloni, *Bimaximal mixing and large  $\theta_{13}$  in a SUSY  $SU(5)$  model based on  $S_4$* , *JHEP* **10** (2011) 010 [[arXiv:1107.0221](#)] [[INSPIRE](#)].
- [65] G.-J. Ding and Y.-L. Zhou, *Dirac neutrinos with  $S_4$  flavor symmetry in warped extra dimensions*, *Nucl. Phys. B* **876** (2013) 418 [[arXiv:1304.2645](#)] [[INSPIRE](#)].
- [66] P. Chen, C.-C. Li and G.-J. Ding, *Lepton flavor mixing and CP symmetry*, *Phys. Rev. D* **91** (2015) 033003 [[arXiv:1412.8352](#)] [[INSPIRE](#)].
- [67] L.L. Everett, T. Garon and A.J. Stuart, *A bottom-up approach to lepton flavor and CP symmetries*, *JHEP* **04** (2015) 069 [[arXiv:1501.04336](#)] [[INSPIRE](#)].
- [68] V.D. Barger, S. Pakvasa, T.J. Weiler and K. Whisnant, *Bimaximal mixing of three neutrinos*, *Phys. Lett. B* **437** (1998) 107 [[hep-ph/9806387](#)] [[INSPIRE](#)].
- [69] C.H. Albright and W. Rodejohann, *Comparing trimaximal mixing and its variants with deviations from tri-bimaximal mixing*, *Eur. Phys. J. C* **62** (2009) 599 [[arXiv:0812.0436](#)] [[INSPIRE](#)].
- [70] C.H. Albright, A. Dueck and W. Rodejohann, *Possible alternatives to tri-bimaximal mixing*, *Eur. Phys. J. C* **70** (2010) 1099 [[arXiv:1004.2798](#)] [[INSPIRE](#)].
- [71] X.-G. He and A. Zee, *Minimal modification to tri-bimaximal mixing*, *Phys. Rev. D* **84** (2011) 053004 [[arXiv:1106.4359](#)] [[INSPIRE](#)].
- [72] B. Wang, J. Tang and X.-Q. Li, *Study on perturbation schemes for achieving the real PMNS matrix from various symmetric textures*, *Phys. Rev. D* **88** (2013) 073003 [[arXiv:1303.1592](#)] [[INSPIRE](#)].
- [73] Y. Shimizu, M. Tanimoto and K. Yamamoto, *Predicting CP-violation in deviation from tri-bimaximal mixing of neutrinos*, *Mod. Phys. Lett. A* **30** (2015) 1550002 [[arXiv:1405.1521](#)] [[INSPIRE](#)].
- [74] S.T. Petcov, *Predicting the values of the leptonic CP-violation phases in theories with discrete flavour symmetries*, *Nucl. Phys. B* **892** (2015) 400 [[arXiv:1405.6006](#)] [[INSPIRE](#)].
- [75] PARTICLE DATA GROUP collaboration, J. Beringer et al., *Review of particle physics (RPP)*, *Phys. Rev. D* **86** (2012) 010001 [[INSPIRE](#)].

- [76] D. Hernandez and A. Yu. Smirnov, *Lepton mixing and discrete symmetries*, *Phys. Rev. D* **86** (2012) 053014 [[arXiv:1204.0445](#)] [[INSPIRE](#)].
- [77] D. Hernandez and A.Y. Smirnov, *Discrete symmetries and model-independent patterns of lepton mixing*, *Phys. Rev. D* **87** (2013) 053005 [[arXiv:1212.2149](#)] [[INSPIRE](#)].
- [78] SUPER-KAMIOKANDE collaboration, A. Himmel, *Recent results from Super-Kamiokande*, *AIP Conf. Proc.* **1604** (2014) 345 [[arXiv:1310.6677](#)] [[INSPIRE](#)].
- [79] G. Altarelli and F. Feruglio, *Tri-bimaximal neutrino mixing,  $A_4$  and the modular symmetry*, *Nucl. Phys. B* **741** (2006) 215 [[hep-ph/0512103](#)] [[INSPIRE](#)].
- [80] PLANCK collaboration, P.A.R. Ade et al., *Planck 2013 results. XVI. Cosmological parameters*, *Astron. Astrophys.* **571** (2014) A16 [[arXiv:1303.5076](#)] [[INSPIRE](#)].
- [81] GERDA collaboration, M. Agostini et al., *Results on neutrinoless double- $\beta$  decay of  $^{76}\text{Ge}$  from phase I of the GERDA experiment*, *Phys. Rev. Lett.* **111** (2013) 122503 [[arXiv:1307.4720](#)] [[INSPIRE](#)].
- [82] EXO collaboration, M. Auger et al., *Search for neutrinoless double-beta decay in  $^{136}\text{Xe}$  with EXO-200*, *Phys. Rev. Lett.* **109** (2012) 032505 [[arXiv:1205.5608](#)] [[INSPIRE](#)].
- [83] EXO-200 collaboration, J.B. Albert et al., *Search for Majorana neutrinos with the first two years of EXO-200 data*, *Nature* **510** (2014) 229 [[arXiv:1402.6956](#)] [[INSPIRE](#)].
- [84] KAMLAND-ZEN collaboration, A. Gando et al., *Limit on neutrinoless  $\beta\beta$  decay of  $^{136}\text{Xe}$  from the first phase of KamLAND-Zen and comparison with the positive claim in  $^{76}\text{Ge}$* , *Phys. Rev. Lett.* **110** (2013) 062502 [[arXiv:1211.3863](#)] [[INSPIRE](#)].
- [85] EXO collaboration, D. Tosi, *The search for neutrino-less double-beta decay: summary of current experiments*, [arXiv:1402.1170](#) [[INSPIRE](#)].
- [86] C. Hagedorn, M. Lindner and R.N. Mohapatra,  *$S_4$  flavor symmetry and fermion masses: towards a grand unified theory of flavor*, *JHEP* **06** (2006) 042 [[hep-ph/0602244](#)] [[INSPIRE](#)].
- [87] F. Bazzocchi, L. Merlo and S. Morisi, *Fermion masses and mixings in a  $S_4$ -based model*, *Nucl. Phys. B* **816** (2009) 204 [[arXiv:0901.2086](#)] [[INSPIRE](#)].
- [88] G. Altarelli, F. Feruglio and L. Merlo, *Revisiting bimaximal neutrino mixing in a model with  $S_4$  discrete symmetry*, *JHEP* **05** (2009) 020 [[arXiv:0903.1940](#)] [[INSPIRE](#)].
- [89] G.-J. Ding, *Fermion masses and flavor mixings in a model with  $S_4$  flavor symmetry*, *Nucl. Phys. B* **827** (2010) 82 [[arXiv:0909.2210](#)] [[INSPIRE](#)].
- [90] C. Hagedorn, S.F. King and C. Luhn, *A SUSY GUT of flavour with  $S_4 \times \text{SU}(5)$  to NLO*, *JHEP* **06** (2010) 048 [[arXiv:1003.4249](#)] [[INSPIRE](#)].